

(i.e., it has a “specific and substantial utility”) and the assertion would be considered credible by a person of skill in the art, a rejection based on lack of utility should not be imposed. *Id.*

Where one or more uses for an invention are set forth in the specification, a rejection for lack of utility should not be made or maintained unless an Examiner has reason to doubt the objective truth of the asserted utility. A reason to doubt an invention's asserted utility may be established when the written description suggests an inherently unbelievable undertaking or involves implausible scientific principles. *In re Cortright*, 49 USPQ2d 1464, 1466 (Fed. Cir. 1999). Further, a claimed invention need not accomplish every asserted utility. As long as the claimed invention meets at least one stated utility, the utility requirement is satisfied. *Stiftung v. Renishaw PLC*, 20 USPQ2d 1094, 1100 (Fed. Cir. 1991).

While acknowledging that the specification sets forth several utilities, such as screening of drugs and treatment or prevention of diseases, the Office Action indicates that the specification and art of record collectively fail to teach (1) what the TASK protein is, (2) how it functions, and (3) a specific and well established utility. With regard to the latter, the Office Action alleges that the specification does not teach a relationship between the claimed invention and any specific disease.

With reference to the assertion that the specification (1) fails to teach what the TASK protein is, it is respectfully pointed out that the primary structure of TASK is set forth in the amino acid sequence of SEQ. ID. NO: 4. Further, higher order structures are well characterized in the specification. For example, Fig. 1C shows the putative membrane topology of TASK, including the relative position of the four transmembrane segments and P domains. Figure 8 shows consensus sites for N-linked glycosylation (*) and phosphorylation by protein kinase C (n), protein kinase A (s) and tyrosine kinase (1) in TASK. The Examiner's

attention is also drawn to the section of the specification at page 16, line 20 through the end of page 17, entitled “Cloning and Primary Structure of TASK”, and the section beginning on page 23, line 20, entitled “Unique Structural Features of TWIK-1 and TASK Family of Potassium Transport Channels”. The specification therefore provides an extensive description characterizing the structure of TASK.

As to assertion (2), the function of TASK is also well described. The activity of TASK, including the biophysical properties of the currents induced by TASK are described in detail from page 19, line 13 through the end of page 21. Briefly, TASK is a K^+ channel exhibiting outward rectification at physiological K^+ concentrations, which activity can be approximated by the Goldman-Hodgkin-Katz current equation. (*See also*, page 24, lines 17-19.) This indicates that TASK lacks intrinsic voltage sensitivity and behaves like a K^+ -selective “hole” (page 24, lines 20-21), whose activity is not changed by activation of protein kinase A or C (page 25, lines 12-14). On the other hand, TASK is sensitive to extracellular pH in the physiological range between 6.5 and 7.8. (Fig. 13A, page 22, lines 11-12, page 25, lines 14-15.) The Hill coefficient of ~ 1.6 was found for the H^+ concentration dependence of the TASK current. (Page 25, line 16.) Further, regulation of the TASK channel is described in detail on page 22. Thus, the function of TASK is described in the specification in more than sufficient detail.

With reference to assertion (3), that the specification fails to set forth a specific and well-established utility, the Applicants respectfully contend that the specification sets forth several utilities for the invention (although only one is required), for example, at page 27, line 23 through page 29, line 17. None of the asserted utilities are “inherently unbelievable” so as to warrant a rejection under § 101. To the contrary, among the disclosed uses for TASK are

treatments of several diseases known to involve potassium channels, such as epilepsy, heart disease (including arrhythmias and vascular diseases) neurodegenerative diseases, especially those associated with ischemia or anoxia, endocrine diseases and muscle diseases. (Page 28, lines 8-11.)

The *Utility Examination Guidelines* explain that when a class of proteins is defined such that the members share a specific, substantial, and credible utility, the reasonable assignment of a new protein to the class of sufficiently conserved proteins would impute the same specific, substantial and credible utility to the assigned protein. 66(4) F.R. 1092, 1096, January 5, 2001. This is the case with TASK, because it is well known in the art that potassium channels are good targets for drug therapy to treat the diseases noted in the specification. Several articles describing the role of potassium channels are discussed in the Background section of the application. The role of these channels in the above-mentioned diseases is also well established in the art. *See, e.g.,* Monsuez, J. (1997) Cardiac potassium currents and channels Part I: Basic science aspects, *Int J Cardiol* 61:209-210; Yoshino, T. (1998) Protective Effect of the K⁺ Channel Opener KRN4884 on Peripheral Occlusive Arterial Disease in Rats, *Gen Pharmac* 31(1):59-62; Gordon, N (1997) Episodic ataxia and channelopathies, *Brain Dev* 20:9-13; Fujimura, N., *et al.* (1997) Contribution of ATP Sensitive Potassium Channels to Hypoxic Hyperpolarization in Rat Hippocampal CA1 Neurons In Vitro, *J Neurophysiol* 77(1):378-85.

In addition, it is well known that several of these diseases can be treated by targeting potassium channels with various drugs. For example, Monsuez, J. (1997) Cardiac potassium currents and channels Part II: Implications for clinical practice and therapy, *Int J Cardiol* 62:1-12 describes the blocking action of various drugs on known potassium channels to treat

arrhythmias (table 1) and the opening of potassium channels using channel activators (section 3) to treat, among other things, heart failure and hypertension. Other medical uses for targeting potassium channels are also well characterized in the art. Thus, one skilled in the art recognizes that potassium channels, as a class, represent an excellent target for drug therapies.

Based on the above, it should be understood that TASK, as a new potassium channel, has numerous uses as a target for drug therapy. A specific utility for TASK is the above-mentioned treatment of neurodegenerative diseases involving ischemia or anoxia. As of the accorded priority date of the application (August 4, 1998), it was known that hypoxia-induced hyperpolarization, which can protect neurons from ischemia through membrane stabilizing action, is mediated by an increase in potassium conductance. Fujimura, N., *supra*. Further, it was known that potassium channel activators can have positive effects on ischemic events in the mammalian brain. Takaba, H (1997) An ATP-sensitive potassium channel activator reduces infarct volume in focal cerebral ischemia in rats, *Am J Physiol* 273(2 Pt 2):R583-6. Significantly, it has been recognized that the ability of a neuron to function properly is dependent on the regulation of its transmembrane ionic gradients and resting potential, and that studying the effects of hypoxia in a variety of species may lead to clinical strategies to limit the impact of hypoxia on the human central nervous system. Corrionc, H., *et al.* (1999) Ionic Mechanisms Underlying Depolarizing Responses of an Identified Insect Motor Neuron to Short Periods of Hypoxia *J Neurophysiol* 81(1):307-18. As such, it is well established that potassium channels are suitable targets for drug therapies to treat the above-noted human diseases, and especially neurodegenerative diseases involving ischemia or anoxia. Thus, one skilled in the art would recognize that TASK, as a new member of the class of potassium channels, is a good target for drugs aimed to treat these diseases. In fact, in the short time

since this patent application was filed, it has already been recognized by others that TASK is such a target, supporting the assertions of utility made in the application as filed. “[S]ince TASK-1 appears to be a major determinant of cell input resistance and membrane potential, its specific inhibition by acute hypoxia is likely to be a major contributory factor in the overall response of neurons during infarction; as such, it represents a potentially important therapeutic target for treatment of conditions characterized by ischemia/hypoxia, such as stroke.” Plant, L. (2002) Hypoxic Depolarization of Cerebellar Granule Neurons by Specific Inhibition of TASK-1, *Stroke* 33(9):2324-8.¹ Other medicinal uses for TASK have also been found. *See, e.g.,* Warltier, D. (2001) “Anesthetic-sensitive 2P Domain K⁺ Channels” *Anesthesiology* 95:1013-21.

In light of the foregoing, it is respectfully requested that the rejection based on 35 U.S.C. § 101 be reconsidered and withdrawn. A copy of each article cited above is enclosed for the Examiner’s convenience.

Claim Rejections Under 35 U.S.C. §112, first paragraph

Applicants also acknowledge the Examiner’s rejections of claims 9-15 under 35 U.S.C. 112, first paragraph. This rejection follows from and is dependent upon the §101 rejection discussed above, stating, in essence, that one skilled in the art would not know how to use the invention because an appropriate utility has allegedly not been established. For the reasons set forth above, the application does, in fact, set forth sufficient utility. Thus, it is respectfully requested that the §112 rejection also be reconsidered and withdrawn.

¹ TASK, as used in the application, is now known in the literature as TASK-1. Reyes, et al. (1998) Cloning and Expression of a Novel pH-sensitive Two Pore Domain K⁺ Channel from Human Kidney, *J. Biol Chem* 273(47) 30863, 30864.)

Claim Rejections Under 35 U.S.C. §102

Applicants acknowledge the Examiner's rejections of claims 9-14 under 35 U.S.C. 102(a) as being anticipated by Leonaudakis *et al.* (J. Neuroscience 1998 Feb; 18(3):868-877). It is respectfully submitted that the Applicants invented the presently claimed subject matter before the publication of Leonaudakis. The Combined Declaration of Fabrice Duprat, Florian Lesage, Michel Fink and Michel Lazdunski Under 37 CFR §§ 1.131 and 1.132 is submitted herewith in support of this fact. The portion of the Combined Declaration sub-captioned "37 CFR § 1.131" establishes that the Applicants conceived and reduced to practice the invention prior to the publication of Leonaudakis. The Applicants also memorialized the actual reduction to practice and published same in the form of a peer-reviewed article (the Duprat article - see below) before the publication of Leonaudakis. In fact, Leonaudakis cites the Duprat article and indicates that the Duprat article was published earlier, incontrovertibly establishing the Applicants' invention of the presently claimed subject matter prior to the publication of Leonaudakis. Thus, Leonaudakis is not prior art under § 102(a), and the present rejection must be withdrawn.

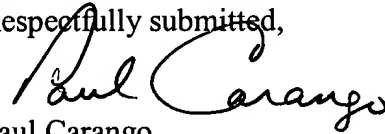
Applicants also acknowledge the Examiner's rejections of claims 9-15 under 35 U.S.C. § 102(a) as being anticipated by Duprat *et al.* (EMBO J 1997 September; 16(17): 5464-5471). The Combined Declaration of Fabrice Duprat, Florian Lesage, Michel Fink and Michel Lazdunski Under 37 CFR §§ 1.131 and 1.132 also establishes that the Duprat article represents the Applicants' own work. In addition to the Applicants, Roberto Reyes and Catherine Heurteaux are co-authors of the Duprat article. As set forth in the section of the Combined Declaration sub-captioned "37 CFR § 1.132", Roberto Reyes and Catherine Heurteaux acted under the direction and supervision of the Applicants, and made no inventive contribution to

the subject matter described in the Duprat article that is now claimed in the application. As such, the work described in the Duprat article is not “to another”, and is not prior art against the application. *In re Katz*, 215 USPQ 14, 18 (CCPA 1982).

For the reasons established above and supported by the accompanying Combined Declaration, it is respectfully requested that the rejections under 35 U.S.C. §102 be reconsidered and withdrawn.

In view of the foregoing, Applicants respectfully submit that the application is now in condition for allowance, which action is respectfully requested.

Respectfully submitted,

A handwritten signature in black ink, appearing to read "Paul Carango". The signature is fluid and cursive, with the first name "Paul" and last name "Carango" clearly distinguishable.

Paul Carango
Reg. No. 42,386
Attorney for Applicants

PC:SAN:pam:vb
(215)656-3320



IN THE UNITED STATES PATENT AND TRADEMARK OFFICE

Art Unit	: 3868	Customer No.: 35811
Examiner	: Christopher H. Yaen	
Serial No.	: 09/939,484	
Filed	: August 24, 2001	
Inventor	: Fabrice Duprat	Docket: 1201-CIP-DIV-00
	: Florian Lesage	
	: Michel Fink	Confirmation No.: 3868
	: Michel Lazdunski	
Title	: FAMILY OF MAMMALIAN POTASSIUM	
	: CHANNELS, THEIR CLONING AND THEIR	
	: USE, ESPECIALLY FOR THE SCREENING	
	: OF DRUGS	

**COMBINED DECLARATION OF FABRICE DUPRAT, FLORIAN LESAGE,
MICHEL FINK AND MICHEL LAZDUNSKI UNDER 37 CFR §§ 1.131 and 1.132**

Commissioner for Patents
P.O. Box 1450
Alexandria, VA 22313-1450

Dear Sir:

We, Fabrice Duprat, Florian Lesage, Michel Fink and Michel Lazdunski, hereby declare as follows:

1. We are the inventors of the subject matter claimed in U.S. Pat. App. No. 09/939,484 (hereinafter "the application").
2. We are familiar with the application, including the claims, and have reviewed the Office Action issued on April 20, 2004 with respect thereto. We have also reviewed the references cited in the Office Action as bases for rejection under 35 U.S.C. § 102(a), namely Duprat, F, *et al.* (1997) "TASK, a human background K⁺ channel to sense external pH variations near physiological pH" EMBO J.16:5464-5471 (hereinafter "the Duprat article"), and Leonoudakis, D, *et al.* (1998) "An Open Rectifier Potassium Channel with Two Pore Domains in Tandem Cloned from Rat Cerebellum" J. Neurosci 18(3):868-877 (hereinafter "Leonoudakis").

37 CFR § 1.132

3. We (Fabrice Duprat, Florian Lesage, Michel Fink and Michel Lazdunski) and Roberto Reyes and Catherine Heurteaux are co-authors of the Duprat article. Roberto Reyes and Catherine Heurteaux are not named as co-inventors of the application.

4. The subject matter described in the Duprat article, including that which is now claimed in the application, represents our work.
5. Roberto Reyes and Catherine Heurteaux acted, at all relevant times, under our direction and supervision.
6. Roberto Reyes and Catherine Heurteaux made no inventive contribution to the subject matter described in the Duprat article that is now claimed in the application.

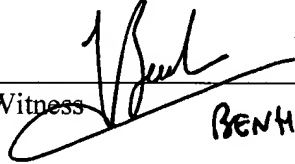
37 CFR § 1.131

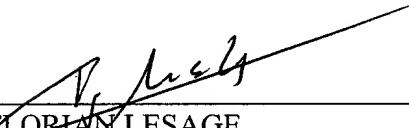
7. Leonoudakis was published on or about 1 February 1988. We invented the subject matter claimed in the application before the publication of Leonoudakis.
8. Leonoudakis cites to the Duprat article, and indicates that the Duprat article was published before Leonoudakis. (*See* Leonoudakis, pg. 868, last paragraph of the Introduction.)
9. The Duprat article represents objective evidence that we conceived and reduced to practice the ideas that are now claimed in the application, before the publication of Leonoudakis.
10. The sole independent claim in the application is directed to an isolated and purified protein of SEQ ID No: 4, or a functionally equivalent derivative having at least 85% identity to SEQ ID No: 4, and said functionally equivalent derivative having a potassium permeable channel comprising more than one P domain and three, four, five or more than six transmembrane segments.
11. The methods we used to identify, clone, isolate and purify SEQ ID No: 4 and the functionally equivalent mouse protein having 85% identity to SEQ ID No: 4 are described in the Materials and Methods section of the Duprat article, and the outcome of these experiments was presented in the Results section of the Duprat article. *See*, for example, the Duprat article on page 5465 in the first partial paragraph of column 2.
12. We, or individuals working under our direction and supervision, did, in fact, perform each of the steps reported in the Duprat article to successfully isolate and purify a protein of SEQ ID No: 4 and a functionally equivalent derivative having at least 85% identity to SEQ ID No: 4, where said functionally equivalent derivative had a potassium permeable channel comprising two P domains and four transmembrane segments, before the publication of Leonoudakis.

Each of us hereby declares that all statements made herein of my own knowledge are true and that all statements made on information and belief are believed to be true; and further that these statements were made with the knowledge that willful false statements and the like so made are punishable by fine or imprisonment, or both, under Section 1001 of Title 18 of the United States Code and that such willful false statements may jeopardize the validity of the application or any patent issued thereon.

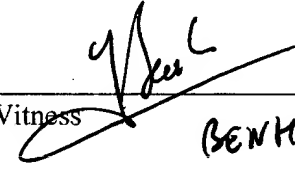

FABRICE DUPRAT

10.21.2004
Date

Witness  10.21.2004
BENHAMOU Juliette

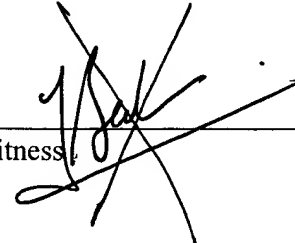

FLORIAN LESAGE

10 21 2004
Date

Witness  10.21.2004
BENHAMOU Juliette

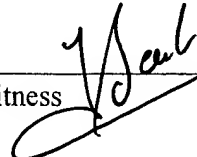

MICHEL FINK

10-27-2004.
Date

Witness  10-27-2004
ANSANAY Hervé


MICHEL LAZDUNSKI

10/21/2004
Date

Witness  10.21.2004
BENHAMOU Juliette



Review Article

Cardiac potassium currents and channels Part I: Basic science aspects

Jean-Jacques Monsuez*

Department of Internal Medicine, Hôpital Paul Brousse, 12 avenue Paul Vaillant Couturier 94804 Villejuif Cedex Paris, France

Received 15 January 1997; accepted 3 July 1997

1. Introduction

Recent advances in molecular biology and voltage-clamp techniques have resulted in dramatic improvements in our understanding of cardiac potassium channels and cardiac potassium currents. Potassium currents play a key-role in cardiac electrophysiology at resting membrane potential and during the action potential (AP) of cardiac cell in normal and ischemic myocardium.

An increasing number of cardiac K^+ currents have been recognized and are new targets for pharmacological intervention. There is also a growing body of evidence to show that cardiac K^+ currents are impaired in disease, especially in heart failure, cardiac hypertrophy and congenital long QT-syndrome.

This article is a comprehensive review of the role of K^+ currents from cardiac physiology to their clinical implications.

This first part is devoted to basic science and includes a review of:

- K^+ currents involved in maintaining the resting potential ($IRK1$, $Na-K$ pump, $IK_{(Na)}$, $IK_{(Ado, Ach)}$, I_f and $IK_{(ATP)}$),
- Repolarizing K^+ currents (IK_r and IK_s , I_{to1} , IK_{ur} , IK_p and $SR-K$),
- Regional differences in repolarization,

- Respective roles of K^+ currents during repolarization in normal and ischemic myocardium,
- Molecular structure of K^+ channels.

2. Resting potential

At resting potential (V_r), cardiac cell membranes are polarized, exhibiting positive charges outside and negative charges inside the cell. The resulting negative resting potential is maintained by the Na^+-K^+ pump which exchanges three intracellular Na^+ for two extracellular K^+ ions, and by the higher membrane permeability (conductance) for K^+ than for Na^+ ions. Due to the unbalanced gradients of these 2 ions across the membrane, the resting potential ($V_r = -80$ mV) is set close to the equilibrium (or reversal) potential for potassium ($E_K = -94$ mV). Thus, at resting potential, the driving force for K^+ loss is low ($V_r - E_K = 6$ mV) and potassium channels conduct only little current despite a relatively high conductance (gK^+) for potassium.

2.1. $IRK1$ or IK_i current

This potassium current, also known as the inward rectifier potassium current $IRK1$ or IK_i , maintains the resting membrane potential near the equilibrium potential for K^+ .

*Tel.: +33 1 45593038; Fax: +33 1 45593788

At negative membrane potentials above its reversal potential (-94 mV), $IRK1$ passes an outward K^+ current with a significant conductance. This outward current drops to very low levels at voltage positive to -40 mV. This inward rectification occurs because $IRK1$ channels close when the membrane potential reaches positive voltages (Fig. 1). In other words, $IRK1$ shuts off during cell depolarization. The characteristics and kinetic properties of the human atrial and ventricular IK_1 channels have been reported [1]. Both atrial and ventricular myocytes exhibit weak inward rectification, but the averaged current–voltage plots of atrial and ventricular IK_1 differ slightly as a prominent negative slope region at potential between -40 and $+20$ mV is only seen in ventricular myocytes (Fig. 1).

Inward rectification was initially thought to result from the blockade of the outward K^+ current by intracellular magnesium (Mg^{++}), since, in its absence, IK_1 demonstrated a linear current–voltage relationship [2]. More recently, inward rectification

has been shown to be generated not by Mg^{++} block, but by cytoplasmic polyamines, the most potent of which is the tetravalent polyamine spermine. This intrinsic modulation may have important implications since cardiac hypertrophy is associated with increased excitability and elevated polyamine levels [3]. As the spermine block determines the trigger threshold for depolarizing currents, this compound may partly control cardiac excitability [4].

Recognition of the role played by intracytoplasmic polyamines may also have pharmacological implications since future drugs that can lower polyamine levels will decrease K^+ conduction only around the resting potential (i.e. stabilize it), without shortening the action potential duration (and, in turn, the refractory period).

Conversely, at membrane potentials more negative than -94 mV, $IRK1$ reverts to an inward current. The large inward conductance at membrane potentials below the equilibrium potential for potassium prevents excessive hyperpolarization potentially gener-

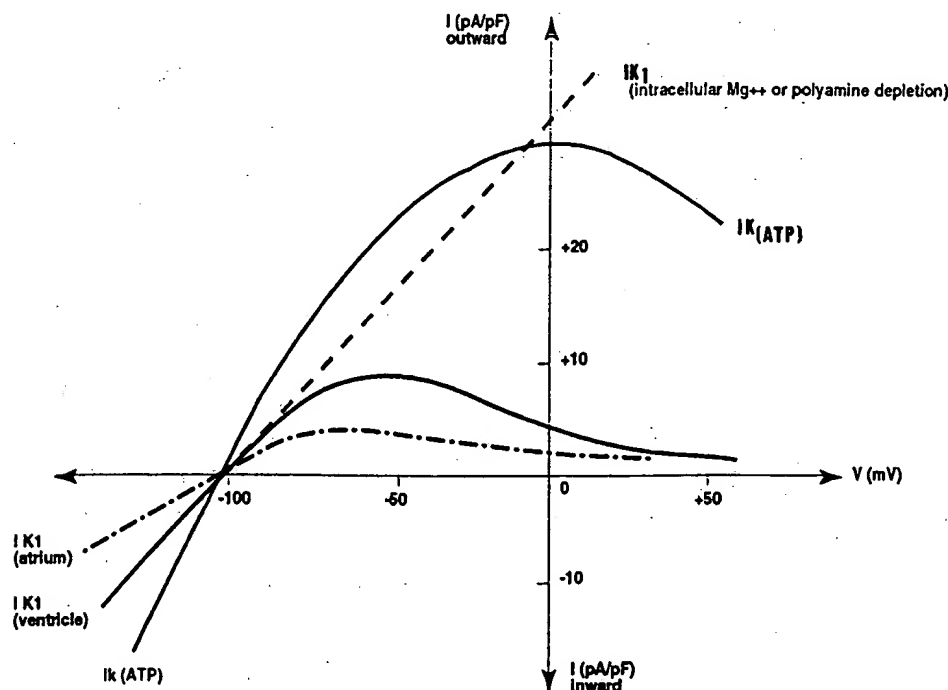


Fig. 1. Current–voltage plot of the inwardly rectifying potassium currents IK_1 and $IK_{(ATP)}$. In the absence of intracellular Mg^{++} , the inward rectification was previously reported to disappear and IK_1 to show linear current–voltage relationship [2]. The changes of channel properties underlying the strong inward rectification of IK_1 are in fact largely determined by intracellular polyamines (spermine) levels [4]. At voltages negative to -80 mV, the slope conductance of IK_1 is greater in ventricle than in atrium. Between -40 and -20 mV, inward rectification result in a negative slope of the ventricular (but not atrial) current–voltage curve (From refs. [1,2,4,16]).

ated by the electrogenic Na–K pump [5,6]. Thus, the IRK1 current helps to keep the resting membrane potential close to the equilibrium potential for K^+ .

The magnitude of IRK1 current depends on the extracellular K^+ ion concentration. The conductance of IRK1 channels increases with rising extracellular K^+ concentration, resulting in a shortened AP duration. Conversely, low extracellular K^+ ion concentrations decrease the magnitude of IRK1, resulting, in turn, in prolonged repolarization [5].

A cDNA encoding the IRK1 channel has recently been cloned and functionally expressed in *Xenopus* oocytes [6].

2.2. Na–K pump and $IK_{(Na)}$

By extruding three intracellular Na^+ in exchange for two extracellular K^+ , the Na^+ – K^+ pump maintains steep Na^+ and K^+ concentration gradients, inward for Na^+ and outward for K^+ and in the process generates a small outward current. This current is relatively stable during the cardiac cycle and is termed the electrogenic Na^+ – K^+ pump current. Under physiological conditions, the pump works at only a small fraction of a ten-fold-higher Na^+ extrusion capacity, which allows regulation of intracellular Na^+ concentration.

Blockade of the Na^+ – K^+ pump, e.g. by digitalis, increases the level of intracellular sodium. Increased intracellular Na^+ concentrations have been reported to act on a Na^+ -sensitive- K^+ channel resulting in an increased Na^+ dependant K^+ current, known as the $IK_{(Na)}$ current [7]. Activation of this channel, when the Na^+ – K^+ pump is inhibited, contributes to the shortening of the QT interval in patients receiving digitalis [7]. Also, it has recently been stressed that the intracellular Na^+ threshold of $IK_{(Na)}$ may be substantially lower when the Na^+ – K^+ pump is blocked. However, whether this will lead to opportunities for developing new therapeutic approaches in heart failure remains a subject of debate. Nevertheless, most observers feel that $IK_{(Na)}$ is not a significant player except under very unusual circumstances probably incompatible with life [8].

2.3. $IK_{(Ado, Ach)}$ current

Acetylcholine (ACh) and adenosine (Ado) act on

the same potassium-channel through two different receptors, the muscarinic M_2 -receptor and the A_1 adenosine (purinergic) receptor, resulting in an increased conductance for K^+ ions through $IK_{(Ado, Ach)}$ channels of both sinoatrial (SA) node, atrioventricular (AV) node and atrial cells [9].

Thus, stimulation of $IK_{(ACh)}$ channels results in a resting hyperpolarization of SA and AV nodes and atrial cells. Also, $IK_{(ACh)}$ current slows the SA spontaneous depolarization rate, thus decreasing automaticity. Acetylcholine binding elicits a sequence of intracellular events via a GTP regulatory protein (called Gk) signal transduction. Acetylcholine activates the $IK_{(ACh)}$ channels via $G\beta\gamma$ subunits of GK, that interact with the K^+ channel [8]. Application of a G-protein $\beta\gamma$ peptide inhibitor, called peptide G, results in a progressive decline in the $IK_{(ACh)}$ channel opening probability [10].

Acetylcholine causes an increase in the open-time of the muscarinic K^+ channel during the onset of activation, thereby shortening the action potential duration (APD).

Acetylcholine has been reported to desensitize $IK_{(ACh)}$ [11] by intracellular factors such as Mg^{++} -ATP [10].

Recently, it has been shown that adenosine, which is released into the extracellular spaces during ischemia and exerts vasodilatory effects on coronary arteries, can activate $IK_{(Ado, ACh)}$ channels. This action is mediated by A_1 -adenosine receptors and results in a shortening of atrial but not ventricular APD [12]. Also, adenosine can activate the $K_{(ATP)}$ channel in the ventricle [13].

2.4. I_f current or pacemaker current

The I_f current, which is promoted by membrane hyperpolarization, is only partly of potassium origin [14]. Its activation, which occurs at membrane potentials, below -80 mV, generates an inward current through a relatively nonspecific cationic channel in SA and AV node cells and His/Purkinje cells that depolarizes the cell membrane and plays a key-role in cardiac automaticity.

I_f current is modulated by intracellular calcium concentrations and by cAMP and adrenergic stimulation that shift its activation threshold to higher voltages. Conversely, acetylcholine shifts the activa-

tion zone to somewhat more negative voltages and results in an inhibition of the I_f current. Also, pharmacological inhibition of I_f has been achieved by zatebradine, a new specific bradycardic agent that blocks sinus tachycardia [15].

Both I_f and $IK_{(ACh)}$ currents are present in sinoatrial (SA) cells and may be involved in the regulation of the heart rate via acetylcholine stimulation. In contrast to the $IK_{(ACh)}$ current which is quickly desensitized, I_f remains stable over time and is not time-inactivated [11]. Also, it has recently been reported that acetylcholine affects I_f at concentrations lower than those required to affect $IK_{(ACh)}$, resulting in a more prominent role of this former channel in the vagal control of heart rate [11]. Finally, SA nodal automaticity is mediated in part by deactivation of IK (see below).

2.5. $IK_{(ATP)}$ current

In 1983, Noma described a K^+ channel which is activated when cytosolic ATP falls below a critical level [16]. Since then, ATP-sensitive currents, $IK_{(ATP)}$, have been increasingly shown to play physiological and pathological roles. Whereas they are inhibited by physiological concentrations of ATP, they open when cytosolic ATP concentrations decrease, resulting in a major outward potassium current whose magnitude may be larger than that of IK_1 .

Also, the $IK_{(ATP)}$ channels distinguish themselves by several electrophysiological patterns. Short and infrequent opening occurs at normal intracellular ATP concentrations, with complete opening occurring in ATP-depleted cells. Unlike $IRK1$, $IK_{(ATP)}$ exhibits only weak inward rectification for positive membrane potentials (Fig. 1). For these reasons, $IK_{(ATP)}$ persists throughout the action potential and during the whole cardiac cycle [16,17].

2.6. Resting potential electrogenesis : Roles of the potassium currents

Potassium currents and their related regulatory pathways vary widely from one animal species to another and from one cardiac tissue to another, despite striking evidence of phylogenetic structural homology, which is conserved from a billion years ago [18].

In humans, patch-clamp techniques showed that 58% of patches isolated from atrial cells contain $IK_{(ACh)}$ channels, 16% $IK_{(Ado)}$ channels and 18% IK_1 channels. Half the patches share $IK_{(ATP)}$ channels, which are closed in physiological conditions but are activated with the inside-out configuration of patches or after depletion in intracellular ATP.

Apart from the Na^+-K^+ pump, it is the inward rectifier potassium current $IRK1$ that extrudes most potassium flux across the membrane at baseline physiological conditions in humans.

Its conductance is responsible for maintaining the resting potential, especially in the ventricle because the percentage of patches in which IK_1 channels are isolated is 2.5-fold greater in ventricle than in atrium [1]. In contrast, little potassium current passes through the $IK_{(ACh)}$ channels which are almost all closed at rest in physiological conditions [19].

3. Action potential and repolarization

Depolarization of myocyte cell membranes (+10 to +20 mV) during the action potential activates voltage-gated K^+ channels generating outward potassium currents responsible for the subsequent cell repolarization. Thus, both duration and configuration of the cardiac AP are governed by a variety of outward currents during the depolarization phase of the action potential (Fig. 2).

Several outward K^+ currents have been identified in cardiomyocytes. Most are voltage-activated. Others, that are calcium activated, respond to increased cytosolic calcium concentrations, i.e. they open as a result of calcium release from the sarcoplasmic reticulum.

3.1. Delayed rectifier outward K^+ current or IK

The delayed rectifier outward K^+ current, also known as the IK current, is activated upon depolarization. It represents the heart's main repolarizing current. IK activates slowly at potentials near the plateau values (+10 to +20 mV), whereas it provides the major contribution to repolarization as the membrane potential becomes more negative from the plateau voltage through -40 mV [20].

The IK channel, also called K_v (voltage-gated),

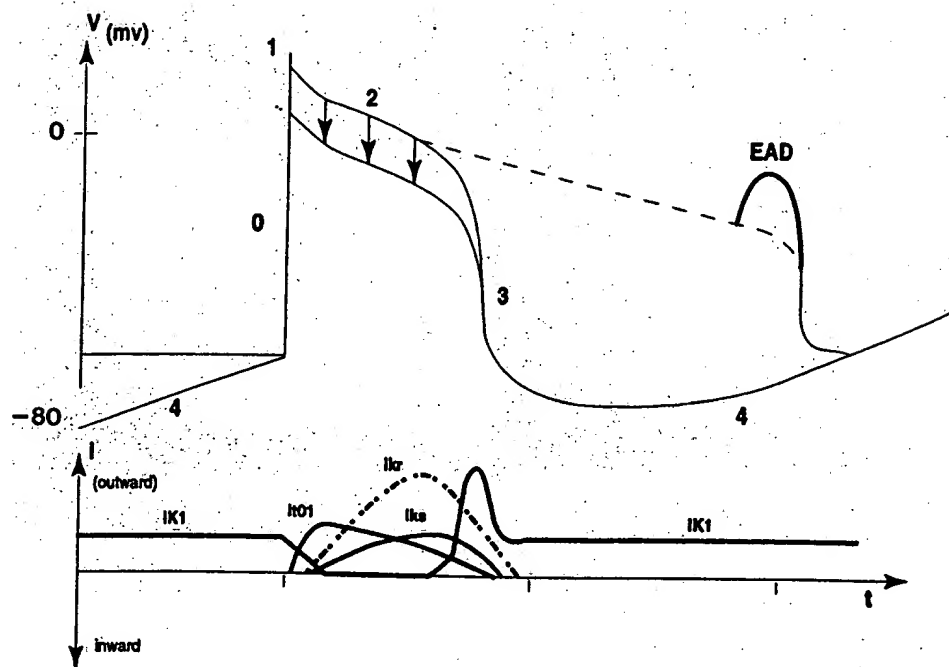


Fig. 2. Repolarizing potassium currents involved in the action potential configuration. The action potential duration (APD) is determined by IK ($IK_r + IK_s$), whereas I_{to} , the K^+ transient outward current, is responsible for the phase two plateau level (arrows). In M cells, dramatic prolongation of APD (dashed lines), promoted by hypokalemia or by a slow stimulation rate, results in an early afterdepolarization (EAD) that may elicit subsequent triggered activity (from refs. [40–42]).

opens with cell depolarization, thus eliciting an outward current, IK, that is enhanced by isoproterenol and the protein-kinase A system through a G protein (G_s) and decreased by β -adrenergic blocking agents. Indeed, the K^+ channels that pass the IK current are modulated by cyclic AMP via the G_s protein, resulting in protein kinase A activation and phosphorylation of the channel, thereby increasing its probability of being open. In addition, IK is modulated by cyclic guanosine monophosphate cGMP and the protein kinase C.

A number of other regulating factors have been documented. IK is controlled by cytosolic calcium concentrations, being increased by calcium release from the sarcoplasmic reticulum, i.e., soon after the onset of the AP [21].

More recently, endothelin, a vasoactive peptide, has been demonstrated to enhance IK in guinea pig ventricular myocytes. This increase in IK is brought about via phospholipase C mediated protein kinase C activation and increased intracellular calcium [22].

The delayed rectifier K^+ outward current IK has been shown to play a major role in repolarizing the

cardiac AP and it therefore governs the APD. Thus, factors that enhance IK shorten the APD and, conversely, inhibition of IK results in a lengthened APD and an increased refractoriness [23].

Pharmacological blockade of IK has been shown to underlie the increase in APD produced by class III antiarrhythmic agents. Indeed, a number of such drugs that block IK either selectively, such as sotalol and dofetilide [20], or less selectively such as amiodarone, flecainide or propafenone [21] are effective in the treatment of clinical arrhythmias. Also, flecainide and E 4031 are potent blockers of IK in cat ventricular myocytes [23].

On the other hand, β -adrenergic receptor stimulation, which shortens the APD by enhancing IK, increases the likelihood of atrial reentry [23–25].

In 1969, Noble and Tsien suggested, with evidence obtained from a mathematical model, that the delayed rectifier outward current, at this time known as the “ I_x ” current, resulted from the addition of two different components called I_{x1} and I_{x2} [20]. This suggestion has since been substantiated by the identification of a fast component (IK_r), which exhibits

inward rectifying properties, and a slow component (IK_s) which does not rectify [21,26].

Moreover, IK has been pharmacologically separated into a rapidly activating component, IK_r , and a slowly activating component IK_s , that is dramatically enhanced in conditions of high sympathetic activity and is similar to the classically described IK [26]. Finally, IK_r activates at more negative potentials than IK_s [26].

Dofetilide is a potent methane sulphonamide anti-arrhythmic agent that attenuates IK_r . Amiodarone and sotalol block IK_r . In contrast, clofilium and quinidine inhibit IK_r and IK_s [24].

Recently, using the patch-clamp technique in an animal model, Furukawa et al. showed that epicardial myocytes manifest slower rates of deactivation of IK_r compared with endocardial myocytes. This phenomenon may provide a substrate for arrhythmogenicity or, at least, heterogeneity of repolarization throughout the myocardium [27].

3.2. Transient outward currents

Whereas IK currents, are responsible for cardiac repolarization during phase three of the AP, the transient outward currents (I_{to}) that occur early during phases one and two of the AP contribute to the generation of the spike and dome configuration of the AP and to the magnitude of the plateau level voltage.

Until recently, transient outward currents have only been documented in humans in atrial cells [28]. Two components have been demonstrated by Coraboeuf and Carmeliet [29]. The first, a brief outward current, known as I_{to} , is in fact a chloride-calcium activated current [28]. The second, however, is a longer lasting, true potassium, transient outward current, designated I_{to} , which is blocked by 4-aminopyridine (4AP) [29,30]. Although I_{to} (also called I_{to1}) has a longer duration than I_{to} (or I_{to2}), both currents inactivate rapidly and both are likely to be fully inactivated before the onset of phase three of the AP [31]. In addition, I_{to1} is the only K^+ current in the heart that shows voltage dependent inactivation [27].

I_{to1} is responsible for the early repolarization (phase one) of the AP, during which the spike potential runs out smoothly in a plateau phase (phase two) in ventricular endocardial cells. In contrast, the I_{to1} -mediated phase one contributes to the generation of the spike and dome configuration to the ventricular

AP that is very prominent in epicardial cells [31]. (Fig. 2).

Recently, this early repolarization of the AP has been shown to disappear in cells surviving chronic infarction. In an animal model of myocardial infarction, Lue et al. demonstrated that this pattern was due to the impairment of I_{to1} [32]. Also, the resulting prolongation of the AP has been reported to contribute to the arrhythmogenic substrate of coronary artery occlusion related ventricular arrhythmias [33].

The channel that passes I_{to1} , known as the $RK5$ channel, has recently been cloned and characterized [34]. Nevertheless, there is still controversy as to what encodes I_{to1} (K_v 4.2 or K_v 1.4).

In a recent study, Wang et al. demonstrated the presence of another potentially important repolarizing current in human atrial myocytes. This "very rapidly activating delayed rectifier K^+ current" shows limited slow deactivation and is therefore referred to as a "sustained" current or I_{sus} [35]. I_{sus} is insensitive to TEA, Ba^{+} and dendrotoxin, but is sensitive to 4AP. Thus, I_{sus} is a K^+ current that can be distinguished from both I_{to1} (from which it differs by voltage dependent inactivation patterns) and IK (sensitivity to 4AP). The kinetic properties of I_{sus} resemble those of the potassium channel encoded by the K_v 1.5 group of human cardiac cDNA libraries [36]. Accordingly, it has been suggested that I_{sus} may be the native counterpart of K_v 1.5 channels cloned from human cardiac tissues [35,36]. Recently I_{sus} , also known as IK_{ur} (ultra-rapid) has been shown to be modulated by adrenergic stimulation. Isoprenaline and other stimulators of protein kinase A enhance, while phenylephrine inhibits, IK_{ur} in human atrial cells. Thus, its autonomic regulation may play a significant role in controlling the occurrence of reentrant atrial arrhythmias [37]. Pharmacologically, block of IK_{ur} may be achieved by zatebradine, a new bradycardic agent that also inhibits the hyperpolarization-activated current I_f [15].

Another recently described plateau K^+ current, IK_p , has been thought to play an important role in late phase two repolarization and in determining the shape of the plateau [38].

3.3. SR-K currents

The release of stored calcium from the sarcoplasmic reticulum as the AP is initiated, generates the

activation-contraction coupling. Calcium release from SR is associated with a K^+ countercurrent entering the SR cisternae, across the SR-K channel to maintain electroneutrality.

This channel is controlled by the amount of calcium stored within the SR. It opens as the stored calcium decreases, i.e. after calcium-induced calcium release across the ryanodine receptor of the SR and, conversely, it closes as the calcium pooled in the SR increases, i.e. when the Ca^{++} -ATPase mediated calcium reuptake initiates the relaxation [39].

Thus, this unique control mechanism is triggered by the cyclic activation of the SR.

3.4. Respective roles of cardiac K^+ currents in repolarization and regional differences in repolarization

Although the kinetic properties of most repolarizing K^+ currents have been extensively reported, their relative importance in determining AP shape and duration remains controversial. Using a theoretical model of ventricular action potential, Zeng et al. showed that IK_s is the major outward current contributing to cardiac repolarization in guinea pig. A >80% block of IK_s results in APD prolongation and early after depolarization whereas IK_r can be completely blocked without similar effects [40]. In the same model, IK_1 becomes more prominent at the end of the action potential, controlling the return to the resting membrane potential [40] (Fig. 2).

On the other hand, a recent study of cardiac K^+ channels by Konarzewska et al. showed that the major repolarizing currents in normal human ventricular myocytes are IK_1 and Ito_1 . Moreover, there is a regional variability in the magnitude of Ito_1 . A large transmural gradient has been documented across the left ventricle, where Ito_1 is two times greater in subepicardial than in subendocardial myocytes [41]. Cells with different morphologies and varying Ito_1 and IK levels were also demonstrated by Antzelevitch [42] and Drouin [43] in the normal ventricular myocardium, including midventricular M cells which are prone to dramatically prolong their AP in response to hypokalemia, slowing heart rate or block of IK_r [42,43].

The kinetic properties of Ito_1 in right ventricular septum subendocardial cells are closely related to those of their subepicardial (rather than subendocar-

dial) left ventricular free wall counterparts, thus suggesting a possible electrophysiological substrate for the functional similarity of these two regions that form the outer wall of the left ventricular chamber [41].

4. Ischemia

Ischemia results in myocardial potassium loss and in increased extracellular K^+ levels. Two mechanisms have been suggested: an increase in K^+ conductance (gK^+) and/or a small inward current causing slight depolarization of the resting potential [44].

4.1. Increased potassium conductance

The $IK_{(ATP)}$ channels may have particular importance in the K^+ efflux of early ischemia. As they are also open during the AP, they participate in the shortening of the AP associated with ischemia [16].

The magnitude of $IK_{(ATP)}$ has been shown to be correlated with tissue levels of ATP. Intracellular ATP depletions as limited as 25% have been reported to enhance $IK_{(ATP)}$ [45]. Nevertheless, the ATP levels observed during acute ischemia are generally above those required to keep the $IK_{(ATP)}$ channel closed [19]. Such discrepancies could be explained by recent findings concerning $IK_{(ATP)}$ current modulation. Lowering intracellular pH and increasing lactate levels have been reported to promote the $IK_{(ATP)}$ current. As the intracellular pH falls quickly in early ischemia, such a stimulating effect of H^+ on $IK_{(ATP)}$ could promote K^+ efflux at higher concentrations of ATP [46].

The $IK_{(ATP)}$ channels are modulated by several pharmacological agents: they are inhibited by sulphonylureas (glibenclamide and tolbutamide) and, conversely, they are activated by aprikalim, cromakalim, pinacidil and nicorandil.

Generation of oxygen free radicals, especially OH^\cdot , also elicits the $IK_{(ATP)}$ channel opening. This activation could not be prevented by glibenclamide, even at high concentrations, thus suggesting a distinct mode of action of the oxygen free radicals on the channel [47].

However, the view that opening of K_{ATP}^+ channels in response to ischemia plays a role in increased K^+ efflux has been criticized. Involvement of other K^+ channels has been advocated. Lysophosphatidylcholine and long chain acylcarnitine resulting from membrane phospholipid metabolism rapidly accumulate in early ischemia and activate the arachidonic acid activated K^+ channel (I_{KAA}) and the phosphatidylcholine activated K^+ channel (I_{KPC}), both also being very sensitive to ischemia-induced low pH [43,48].

4.2. Inward currents associated with potassium loss

The second mechanism involves inward currents associated with K^+ loss. Indeed, the increase in K^+ efflux during ischemia is not only combined with a counter ion movement but may also be induced by such an inward current. Several hypothesis have been proposed. As sodium accumulates shortly after the onset of ischemia, the voltage-sensitive sodium channel, the nonselective cation channel and the Na^+/Ca^{++} exchange (1 Ca^{++} out, 3 Na^+ in) are suggested (review in [43]).

4.3. Coronary blood flow

Finally, recent studies have suggested that changes in myocardial oxygen tension with metabolic mediators such as adenosine may play an important role in local control of coronary blood flow. Katsuda et al. showed that blockade of vascular K_{ATP}^+ channels with intracoronary glibenclamide in anaesthetized dogs inhibited the coronary vasodilatation induced by pacing tachycardia without altering the tachycardia-induced increase in myocardial oxygen consumption. This suggest a key-role of K_{ATP}^+ channels in the mechanisms mediating regulation of coronary blood flow associated with increased myocardial oxygen consumption [49]. Also, the involvement of K_{ATP}^+ channels in the local control of coronary blood flow does not rule out a role for adenosine, since adenosine has also been shown to open these channels [12,13,50,51]. Moreover, vasodilatation elicited by adenosine and other cAMP-dependent mechanisms has been reported to result from opening of endothelial K_{ATP}^+ channels and the subsequent hyperpolarization which, in turn, promotes NO formation [52].

5. Structure of potassium channels

Recent advances in molecular biology have highlighted the structure and function of different types of potassium channels. Several cDNA codings for K^+ channels have been cloned and subsequently expressed in *Xenopus* oocytes and other expression systems allowing further electrophysiological studies using patch-clamp technique. Moreover, the molecular basis of some channel behaviour has also been accurately defined by directed mutagenesis that has clearly identified many regulation sites [18,53,54].

Both structure and function of the channel passing IK_1 have been characterized by this approach [6], leading to revision of the previously held concept of structural uniformity of the K^+ channels. In fact, there are two main types of K^+ channels (Fig. 3).

5.1. Voltage-gated channels (K_v)

The first group includes all voltage-gated K^+ channels (K_v family channels). They are composed of four identical α -subunits, each containing six α -helical hydrophobic segments spanning the cell membrane designated S_1 through to S_6 and four hydrophilic β -subunits associated with the α -subunit on the cytoplasmic side of the membrane [6,52]. A large H5 peptide loop intervenes between the segments S_5 and S_6 of each α -subunit. The loops between transmembrane segments S_5 and S_6 with the homologous H5 counterpart of the remaining three α -subunits are thought to form the outer part of the pore through which ions cross the membrane [6,18,54]. Certainly other regions contribute to the inner mouth. Mutagenesis has confirmed the presence of multiple potassium binding sites arranged in a single line [54].

The S_4 transmembrane segment is the voltage-sensor and is common to all voltage sensitive channels, e.g. the sodium channel [18,53,54].

The transmembrane segments S_1 , S_2 and S_3 vary one from another for each voltage-gated K^+ channel [6].

A large N-terminal peptide sequence prolongs the S_1 transmembrane segment of all voltage-gated K^+ channels. In many of them, it forms the inactivation ball peptide and its chain that produces fast inactivation in many K_v channels. This major structure is

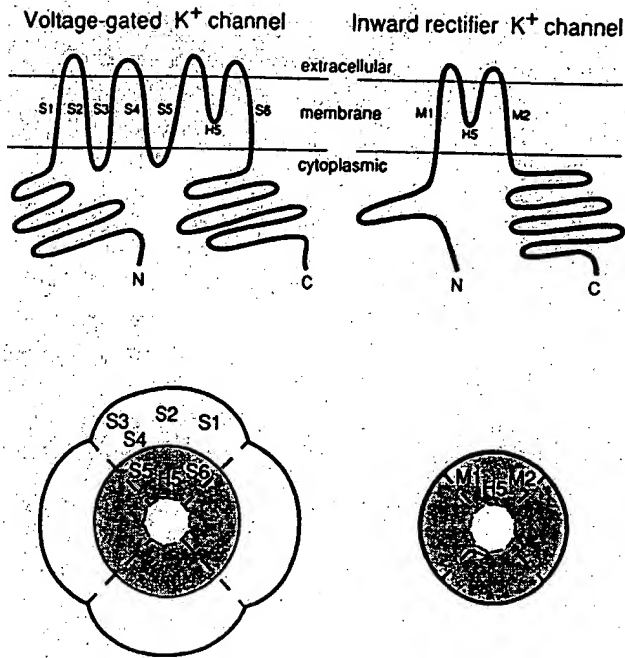


Fig. 3. Membrane arrangement of the two types of potassium channels. Both voltage gated channels (K_v) and IRK_1 are made up of four α -subunits with an inner core sequence (the H5 loop intervening between the segments S_5 - S_6 or M_1 - M_2) that constitute the K^+ channel pore. The voltage gated channel, K_v , distinguishes from IRK_1 by the voltage sensor, S_4 , by the segments S_1 , S_2 and S_3 , and by a longer N-terminal peptide sequence (phosphorylation sites). Reprinted with permission from Nature (ref. [6]). Copyright (1993) Macmillan Magazines Limited.

also likely to contain many other regulatory and/or phosphorylation sites [6].

5.2. Inward rectifier channels (K_{ir})

The second group of K^+ channels (K_{ir} family channels) includes the short N-terminal amino-acid sequence K^+ channels such as those passing IK_1 , $IK_{(ATP)}$ [6,54–56] and $IK_{(Ach)}$ [57].

The structure of IK_1 has been determined. As a result of the deletion of the N-terminal chain, these channels harbour fewer phosphorylation sites than the voltage-gated K^+ channels. However, some homology in the pore region is observed. Like their counterparts, they are made up of four α -subunits but unlike the K_v channels, each subunit contains only two hydrophobic segments, designated M_1 and M_2 . These two segments, between which intervenes the H5 loop, are homologous to the S_5 and S_6 segments and form the K^+ selective pore. The transmembrane

S_4 segment is deleted (there is no voltage sensor) as are the segments S_1 , S_2 and S_3 . Whether inwardly rectifying channels also contain β -subunits is not known [54].

The structures of K_{ATP} and $K_{(Ach)}$ channels are more complex. K_{ATP} channels are formed by co-expression of a K_{ir} channel (K_{ir} 6.1), also designated BIR (β -cell inward rectifier family), with the sulphonylurea receptor protein SUR, a large membrane protein (140 to 170 kD) which is a member of the ATP-binding cassette superfamily and functions as the ATP and ADP sensor that modulates the channel [55,56].

Also, the molecular structure of the G-protein activated channel that underlies IK_{Ach} is now thought to comprise a heterotetramer of two distinct $G\beta\gamma$ -regulated inwardly rectifying K^+ channels, which are the products of the $GIRK_1$ and CIR (cardiac inward rectifier) genes respectively [57].

Finally, the human “ether-a-go-go” related gene (HERG) and min K (or IsK), the genes that encode for the major subunit of the cardiac IK_r channel and the cardiac IK_s channel respectively, have been identified [58–60]. Although IsK, or min K, the cDNA coding for the minimal K^+ channel protein (130 amino acids), a voltage-gated K^+ channel with a single membrane spanning domain, has been isolated from cardiac tissues and expressed in *Xenopus* oocytes, resulting in a K^+ current similar to IK_s , its relationship with IK_s remains controversial [60].

6. Conclusion

New insights brought by the recognition of molecular and electrophysiological properties of K^+ channels provide in depth understanding of the precise electrophysiological targets for pharmacological interventions in man. This will be discussed in the second part of this review.

Acknowledgements

We are indebted to Dr John Evans for careful manuscript revision and to Pascale Granger for secretary assistance.

References

- [1] Koumi SI, Backer CL, Arentzen CE. Characterization of inwardly rectifying K⁺ channel in human cardiac myocytes. *Circulation* 1995;92:164–74.
- [2] Matsuda H, Saigusa A, Irasawa H. Ohmic conductance through the inwardly rectifying K channel and blocking by integral Mg⁺⁺. *Nature* 1987;325:156–9.
- [3] Lopatin AN, Makhina EN, Nichols CG. Potassium channel block by cytoplasmic polyamines as the mechanism of intrinsic rectification. *Nature* 1994;372:366–9.
- [4] Fakler B, Brandle U, Glowatski E, Weidemann S, Zenner HP, Ruppersberg JP. Strong voltage-dependent inward rectification of inward rectifiers K⁺ channels is caused by intracellular spermine. *Cell* 1995;80:149–54.
- [5] Sakmann B, Trube G. Conductance properties of single inwardly rectifying potassium channels in ventricular cells from guinea-pig hearts. *J Physiol* 1984;347:641–57.
- [6] Kubo Y, Baldwin TJ, Jan LY. Primary structure and functional expression of a mouse inward rectifier potassium channel. *Nature* 1993;362:127–33.
- [7] Luk HN, Carmeliet E. Na⁺ activated K⁺ current in cardiac cells: rectification, open probability block and role in digitalis toxicity. *Pflüg Arch Eur J Physiol* 1990;416:766–8.
- [8] Rodrigo GC. The Na⁺ dependence of Na⁺-activated K⁺ channels (IK_(Na)) in guinea-pig ventricular myocytes is different in excised inside/out patches and cell attached patches. *Pflüg Arch Eur J Physiol* 1993;422:530–2.
- [9] Kurachi Y, Nakajima T, Sugimoto T. On the mechanisms of activation of muscarinic K⁺ channels by adenosine in isolated atrial cells. *Pflüg Arch Eur J Physiol* 1986;407:264–74.
- [10] Nair LA, Ingleses J, Stoffel R et al. Cardiac muscarinic potassium channel activity is attenuated by inhibitors of G beta-gamma. *Circ Res* 1995;76:832–8.
- [11] Kim D. Mechanism of rapid desensitization of muscarinic K⁺ current in adult rat and guinea-pig atrial cells. *Circ Res* 1993;73:89–97.
- [12] Xu J, Wang L, Hurt CM, Pelleg A. Endogenous adenosine does not activate ATP-sensitive potassium channels in the hypoxic guinea-pig ventricle in vivo. *Circulation* 1994;89:1209–16.
- [13] Kirsch GE, Codina J, Birnbaumer L, Brown AM. Coupling of ATP-sensitive channels to A1 receptor by G proteins in rat ventricular myocytes. *Am J Physiol* 1990;259:H820–6.
- [14] Di Francesco A. A study the ionic nature of the pace-maker current in calf purkinje fibres. *Physiol (London)* 1981;314:377–93.
- [15] Valenzuela C, Delpon E, Franqueza L, Gay P, Perez O, Tamargo J, Snyders DJ. Class III antiarrhythmic effects of zatebradine. *Circulation* 1996;94:562–70.
- [16] Noma A. ATP regulated K⁺ channels in cardiac muscle. *Nature* 1983;305:147–8.
- [17] Nichols CG, Ripoli C, Lederer WJ. ATP sensitive potassium channel modulation of the guinea pig ventricular action potential and contraction. *Circ Res* 1991;68:280–7.
- [18] Katz AM. Cardiac ion channels. *N Eng J Med* 1993;328:1244–5.
- [19] Heidbuchel H, Vereecke J, Carmeliet E. Three different potassium channels in human atrium. Contribution to the basal potassium conductance. *Circ Res* 1990;66:1277–86.
- [20] Noble D, Tsien RW. Outward membrane current activated in the plateau range of potentials in cardiac Purkinje fibres. *J Physiol (London)* 1969;200:205–31.
- [21] Sanguinetti MC, Jurkiewicz NK. Delayed rectifier outward K⁺ current is composed of two currents in guinea-pig atrial cells. *Am J Physiol* 1991;260:H393–9.
- [22] Habuchi Y, Tanaka H, Furukawa T, Tsujimura Y, Takahashi H, Yoshimura M. Endothelin enhances delayed rectifier potassium current via phospholipase C in guinea-pig ventricular myocytes. *Am J Physiol* 1992;262:H435–54.
- [23] Follmer CH, Colatsky TJ. Block of delayed rectifier potassium current I_k by flecainide an E-4031 in cat ventricular myocytes. *Circulation* 1990;82:289–93.
- [24] Chadwick CC, Ezrin AM, O'Connor B et al. Identification of a specific radioligand for the cardiac rapidly activating delayed rectifier K⁺ channel. *Circ Res* 1993;72:707–14.
- [25] Duan D, Fermini B, Nattel S. Potassium channel blocking properties of propafenone in rabbit atrial myocytes. *J Pharmacol Exp Ther* 1993;264:1113–.
- [26] Sanguinetti MC, Jurkiewicz NK. Two components of cardiac delayed rectifier K⁺ current. differential sensitivity to block by class III antiarrhythmic agents. *J Gen Physiol* 1990;96:195–215.
- [27] Furukawa T, Kimura S, Furukawa N, Bassett AL, Myerburg RJ. Potassium rectifier current differences in myocytes of endocardial and epicardial origin. *Circ Res* 1992;70:91–103.
- [28] Escande D, Coulombe A, Faivre JF. Two types of transient outward current in adult human atrial cells. *Am J Physiol* 1987;282:H142–8.
- [29] Coraboeuf E, Carmeliet E. Existence of two transient outward currents in sheep cardiac Purkinje fibers. *Pflüg Arch Eur J Physiol* 1982;392:352–935.
- [30] Carmeliet E. Mechanisms and control of repolarization. *Eur Heart J* 1993;14(suppl H):3–13.
- [31] Wang Z, Fermini B, Nattel S. Delayed rectifier outward current and repolarization in human atrial myocytes. *Circ Res* 1993;73:276–85.
- [32] Lue WM, Boyden PA. Abnormal electrical properties of myocytes from chronically infarcted canine heart. Alterations in V_{max} and the transient outward current. *Circulation* 1992;85:1175–88.
- [33] Jeck C, Pinto J, Boyden P. Transient outward currents in subendocardial Purkinje myocytes surviving in the infarcted heart. *Circulation* 1995;92:465–73.
- [34] Blair TA, Roberts SL, Tamkun MM, Hartshorne RP. Functional characterization of RK5 a voltage gated K⁺ channel cloned from the rat cardiovascular system. *FEBS Lett* 1991;295:211–3.
- [35] Wang Z, Fermini B, Nattel S. Sustained depolarization induced outward current in human atrial myocytes. evidence for a novel delayed rectifier K⁺ current similar to Kv 1.5 cloned channel currents. *Circ Res* 1993;73:1061–76.
- [36] Chandy KG. Simplified gene nomenclature. *Nature* 1991;352:26.
- [37] Li GR, Feng J, Nattel S. Adrenergic modulation of the ultra-rapid delayed rectifier—a novel control mechanism for human atrial repolarization. *Circulation* 1994;90:1–526.
- [38] Backx PH, Marban E. Background potassium current active during the plateau of the action potential in guinea pig ventricular myocytes. *Circ Res* 1993;72:890–900.
- [39] Liu QY, Strauss HC. Blockade of cardiac sarcoplasmic reticulum K⁺ channel by Ca²⁺. *Biophys J* 1991;60:198–203.
- [40] Zeng J, Laurita KR, Rosenbaum DS, Rudy Y. Two components of the delayed rectifier K⁺ current in ventricular myocytes of the guinea pig type. Theoretical formulation and their role in repolarization. *Circ Res* 1995;77:140–52.
- [41] Konarzewska H, Peeters GA, Sanguinetti MC. Repolarizing K⁺ currents in nonfailing human hearts. Similarities between right septal subendocardial and left subepicardial ventricular myocytes. *Circulation* 1995;92:1179–87.

- [42] Antzelevitch C, Sicouri S. Clinical relevance in the generation of V waves, triggered activity and torsades de pointes. *J Am Coll Cardiol* 1994;23:259–77.
- [43] Drouin E, Charpentier F, Gauthier C, Laurent K, Le Marec H. Electrophysiology characteristics of cells spanning the left ventricular wall of human heart. evidence for presence of M cells. *J Am Coll Cardiol* 1995;26:185–92.
- [44] Wilde AM, Aksnes G. Myocardial potassium loss and cell depolarization in ischemia and hypoxia. *Cardiovasc Res* 1995;29:1–15.
- [45] Deutsch N, Klitzner TS, Lamp SC, Weiss JN. Activation of cardiac ATP sensitive K^+ current during hypoxia. correlation with tissue ATP levels. *Am J Physiol* 1991;261:H671–6.
- [46] Fan Z, Makielski JC. Intracellular H^+ and Ca^{++} modulation of trypsin modified ATP sensitive K^+ channels in rabbit ventricular myocytes. *Circ Res* 1993;72:715–22.
- [47] Tokube K, Kiyosue T, Arita M. Opening of ATP-sensitive potassium channel by different species of oxygen free radicals. *Circulation* 1994;90:1–525.
- [48] Van Der Vusse GJ, Glatz JFC, Stam HCG, Reneman RS. Fatty acid homeostasis in the normoxic and ischemic heart. *Physiol Rev* 1992;72:881–940.
- [49] Katsuda Y, Egashira K, Ueno H et al. Glibenclamide, a selective inhibitor of ATP-sensitive K^+ channels, attenuates metabolic coronary vasodilatation induced by pacing tachycardia in dogs. *Circulation* 1995;92:511–7.
- [50] Nakhostine N, Lamontagne D. Adenosine contributes to hypoxia-induced vasodilatation through ATP-sensitive K^+ channel activation. *Am J Physiol* 1993;34:H1289–34.
- [51] Dart C, Standen NB. Adenosine-activated potassium current in smooth muscle cells isolated from the pig coronary artery. *J Physiol* 1993;471:767–86.
- [52] Ming Z, Parent R, Lavallee M. Beta-2 adrenergic dilatation of resistance coronary vessels involves K_{ATP}^+ channels and nitric oxide in conscious dog. *Circulation* 1997;95:1568–76.
- [53] Folander K, Smith JS, Antanavage J, Bennett C, Stein S, Swanson R. Cloning and expression of the delayed-rectifier channel from neonatal rat heart and diethylstilbestrol uterus. *Proc Natl Acad Sci USA* 1990;87:2975–9.
- [54] Yeh Jan L, Nung Jan Y. Potassium channels and their evolving gates. *Nature* 1994;371:119–22.
- [55] Inagaki N, Gonoi T, Clement JP et al. Reconstitution of I_{KATP} : an inward rectifier subunit plus the sulfonylurea receptor. *Science* 1995;270:1166–9.
- [56] Aguilar-Bryan L, Nichols CG, Wechsler SW et al. Cloning of the beta-cell high affinity sulfonylurea receptor: a regulator of insulin secretion. *Science* 1995;268:423–5.
- [57] Krapivinsky G, Gordon EA, Wickman K, Velimirovic B, Krapivinsky L, Clapham DE. The G-protein-gated atrial K^+ channel IK_{Ach} is a heteromultimer of two inwardly rectifying K^+ channel proteins. *Nature* 1995;374:135–41.
- [58] Curran ME, Splawski I, Timothy KW, Vincent GM, Green ED, Keating MT. A molecular basis for cardiac arrhythmia. HERG mutations cause long QT syndrome. *Cell* 1995;80:795–803.
- [59] Sanguinetti MC, Jiang C, Curran ME, Keating MT. A mechanistic link between an inherited and an acquired cardiac arrhythmia. HERG encodes the IKr potassium channel. *Cell* 1995;81:299–307.
- [60] Yang T, Kupersmidt S, Roden DM. Anti-min K antisense decrease the amplitude of the rapidly activating cardiac delayed rectifier K^+ current. *Circ Res* 1995;77:1246–53.



Protective Effect of the K⁺ Channel Opener KRN4884 on Peripheral Occlusive Arterial Disease in Rats

Tetsuya Yoshino,
Hideo Ohta, Yasuhiro Jinno, Yoshifumi Torii,
Nobuyuki Ogawa, Toshio Izawa and Yuji Okada*

PHARMACEUTICAL RESEARCH LABORATORY, KIRIN BREWERY COMPANY, LTD.,
MIYAHARA-CHO 3, TAKASAKI, GUNMA 370-1295, JAPAN [TEL: 81-273-46-9745; FAX: 81-273-47-5280]

ABSTRACT. 1. The effect of the potassium channel opener KRN4884 on the peripheral arterial occlusion model induced by laurate was examined and compared with that of beraprost sodium and nilvadipine.

2. KRN4884 or beraprost sodium prevented macroscopic changes in the paw after the injection of laurate. In contrast, nilvadipine did not improve the lesions.

3. KRN4884 produced a dose-dependent increase in gastrocnemius blood flow in the chronic femoral artery-ligated rats. The effect of KRN4884 on the blood flow was stronger in the hypoxic muscle than in the normal muscle.

4. KRN4884 did not have a direct antiplatelet aggregation activity.

5. These findings suggest that KRN4884 is useful for the therapy of peripheral arterial occlusive disease and that the effect of KRN4884 is associated with an increase in blood flow in ischemic skeletal muscle. GEN PHARMAC 3131;11:59–62, 1998. © 1998 Elsevier Science Inc.

KEY WORDS. KRN4884, arterial occlusion, K⁺ channel opener

INTRODUCTION

Peripheral vascular disease is an increasing problem in an aging population. The K⁺ channel openers cromakalim, pinacidil and nicorandil caused a significant increase in hypoxic muscle blood flow and pO₂ in an occlusive arterial disease model (Angersbach and Nicholson, 1988). Cook *et al.* (1993) showed that K⁺ channel openers SDZ-PCO 400 and cromakalim have a beneficial effect on muscle high-energy phosphate levels in the hind limb of the occlusive arterial disease model rat. On the other hand, Weselcouch and Baird (1994) reported that cromakalim does not affect skeletal muscle blood flow or function during acute ischemia in a hindlimb in ferrets. Moreover, Weselcouch *et al.* (1993) showed the nonbeneficial effect of cromakalim on the treatment of skeletal muscle ischemia in rats. Thus, it is not clear that K⁺ channel openers have beneficial therapeutic effects on occlusive arterial disease.

KRN4884, 5-amino-N-[2-(2-chlorophenyl)ethyl]-N'-cyano-3 pyridinecarboxamidine (Fig. 1), is a novel and potent vasodilator, and its mechanism of action is K⁺ channel opening in the vascular smooth muscle (Izumi *et al.*, 1995, 1996; Kawahara *et al.*, 1996). In the present study, we examined the effects of KRN4884 on laurate-induced peripheral circulation insufficiency rats as a thromboangiitis obliterans (TAO) model and on muscle circulation in chronic occlusion of the femoral artery as an arteriosclerosis obliterans (ASO) model.

MATERIALS AND METHODS

Laurate-induced occlusion model

A rat model of peripheral circulation insufficiency was made according to the method of Ashida *et al.* (1980). Briefly, male Wistar rats (Charles River Japan Inc., Japan), weighing 350–480 g, were

anesthetized with sodium pentobarbital intraperitoneally at 50 mg/kg. The right femoral artery was exposed by surgical incision. One-tenth milliliter of lauric acid solution (10 mg/ml saline) was injected into the right femoral artery. KRN4884 (1 and 3 mg/kg), beraprost sodium (0.3 mg/kg) or vehicle (0.5% CMC-Na water) was administered orally 30 min before surgery and twice a day for the next 3 days and once a day on the 4th–10th days after surgery (Experiment 1). KRN4884 (0.3, 1 and 3 mg/kg), beraprost sodium (0.3 mg/kg), nilvadipine (30 mg/kg) or vehicle (0.5% CMC-Na water) was administered orally 1 hr before and twice a day for 10 days after injection of laurate (Experiment 2). We decided on the dose of beraprost sodium (0.3 mg/kg) according to a report (Murai *et al.*, 1989) that showed the effectiveness of beraprost sodium at the dose of 0.3 mg/kg. The dose of nilvadipine (30 mg/kg) was determined by a previous study; that is, nilvadipine at 30 mg/kg may induce hypotension equal to that induced by 3 mg/kg KRN4884 in normal rats. The macroscopic observation of the treated hind limbs was carried out on the 3rd and 10th day after the laurate injection. The degree of lesions was classified into the following six grades: Grade 0, normal appearance; Grade 1, edema or erythema; Grade 2, the region was limited to the nail; Grade 3, the region was limited to the fingers; Grade 4, the region was limited to half the paw; and Grade 5, the region was limited to the whole paw.

Blood pressure measurements

Systolic blood pressure was measured by the tail-cuff method (PS-200; Riken Kaihatsu, Japan) 1 hr after the administration of drugs on the 7th or 8th day of Experiment 2.

Muscle blood flow measurements

Rat resting gastrocnemius muscle blood flow was measured by using a laser Doppler flowmeter (Laserflo BPM403A, TSI, USA) ac-

*To whom correspondence should be addressed.

Received 5 June 1997; accepted 3 October 1997.

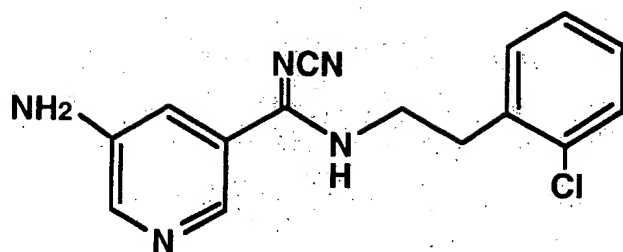


FIGURE 1. Chemical structure of KRN4884.

cording to the method of Angersbach and Nicholson (1988). The relative blood flow was indicated as the flux (number \times velocity) of blood cells in the illuminated volume of muscle (Nicholson *et al.*, 1985). Effect of KRN4884 on muscle blood flow was measured in rats with and without a femoral artery ligation. Male Wistar rats (age 7–9 weeks) were purchased from Charles River Japan Inc. (Japan) and housed until 8–11 weeks of age, and then chronic (6–9 weeks) ligation of the left femoral artery was performed. Chronically ligated rats or nonligated rats were anesthetized with sodium pentobarbital intraperitoneally at 50 mg/kg. The left gastrocnemius muscle was exposed by surgical incision, and the muscle blood flow was measured. The right femoral artery and vein were cannulated for the recording of blood pressure and for KRN4884 administration (1, 3 and 10 μ g/kg).

Antiplatelet activity

Blood was collected from male Wistar rats (12–13 weeks old, Charles River Japan Inc., Japan) with a plastic syringe containing 1/10 volume of 3.1% trisodium citrate solution. Platelet-rich plasma (PRP) was prepared by centrifugation at 80 \times g for 15 min. Platelet-poor plasma (PPP) was obtained from the precipitated fraction of PRP by centrifugation at 1,200 \times g for 15 min. The platelets in PRP were suspended in PPP to adjust the platelet count to $5 \times 10^5/\mu$ l. Platelet aggregation was determined by using an aggregometer (Hema Tracer, Niko Bioscience Inc., Japan). A 100- μ l sample of PRP was placed in the cuvette to which 5 μ l of KRN4884 was added for a 3-min preincubation at 37°C. Then, 10 μ l of each aggregator (ADP and collagen) solution was added to the reaction medium.

Chemicals

KRN4884 (lot. no. YH-005) was synthesized at Kirin Brewery Co. Beraprost sodium (Kaken Pharmaceutical Co., Japan), nilvadipine (Fujisawa Pharmaceutical Co., Japan), lauric acid (Tokyou Kasei

Co., Japan), ADP (NBS Co., Japan) and collagen (MC Medical Co., Japan) were purchased. KRN4884, beraprost sodium and nilvadipine were suspended in 0.5% carboxymethyl cellulose (Sigma Chemical Co., USA) in the study using the laurate-induced model. KRN4884 was dissolved in 30% polyethylene glycol 200 (Wako Pure Chemical Co., Japan)-saline solution or dimethyl sulfoxide (Wako Pure Chemical Co., Japan) in the blood flow measurement study or antiplatelet aggregation study, respectively.

Statistical analysis

Results were expressed as the mean \pm SE. The significance of the data was evaluated by using Mann-Whitney's U-test or paired *t*-test or Dunnett's multiple comparisons test. A significance level of more than 95% was taken to indicate statistical significance ($P < 0.05$).

RESULTS

Effects of KRN4884 and beraprost sodium on laurate-injected rats (Experiment 1)

Injection of laurate into the femoral artery mummified the fingers or part of the paw 3 days after the injection, and then the gangrene area extended to the part or whole of the paw 10 days after the injection in the vehicle group (Table 1). KRN4884 (1 and 3 mg/kg, PO) and beraprost sodium (0.3 mg/kg), which is used as a positive control, markedly ($P < 0.05$) inhibited the progression of the lesions at 3 and 10 days after the injection of laurate (Table 1).

Effects of KRN4884 and other drugs on laurate-injected rats (Experiment 2)

KRN4884 (1 and 3 mg/kg, PO) significantly ($P < 0.05$) inhibited the progression of the lesions at 10 days after the injection of laurate (Fig. 2). KRN4884 (0.3 mg/kg) and beraprost sodium (0.3 mg/kg) tended to suppress the lesions, but nilvadipine (30 mg/kg) was ineffective for the treatment of this model. Systolic blood pressures in vehicle-treated laurate-injected rats were about 130 mmHg (Fig. 3). Treatment with KRN4884 dose dependently reduced blood pressure in the rats. KRN4884 (0.3 mg/kg) and beraprost sodium (0.3 mg/kg) did not reduce blood pressure in the rats. Nilvadipine (30 mg/kg) and KRN4884 (3 mg/kg) reduced blood pressure to the same extent, by about 30 mmHg, compared with the vehicle-treated rats.

Effects of KRN4884 on the skeletal muscle blood flow in femoral artery-ligated rats

The blood flow of the resting (just before injection of 1 μ g/kg KRN4884) gastrocnemius muscle of femoral artery-ligated rats

TABLE 1. Effect of KRN4884 on laurate-induced hind limb lesions (Experiment 1)

Drug	n	Grade						Mean \pm SE
		0	1	2	3	4	5	
Day 3								
Vehicle	7	0	0	1	4	1	1	3.29 \pm 0.36
KRN4884 (1 mg/kg)	8	4	1	1	2	0	0	1.13 \pm 0.48, $P < 0.01$
KRN4884 (3 mg/kg)	11	7	0	3	1	0	0	0.82 \pm 0.35, $P < 0.01$
Beraprost (0.3 mg/kg)	10	2	3	5	0	0	0	1.30 \pm 0.26, $P < 0.01$
Day 10								
Vehicle	7	0	0	1	0	4	2	4.00 \pm 0.38
KRN4884 (1 mg/kg)	8	5	0	2	0	1	0	1.00 \pm 0.54, $P < 0.05$
KRN4884 (3 mg/kg)	11	6	1	3	1	0	0	0.91 \pm 0.34, $P < 0.01$
Beraprost (0.3 mg/kg)	10	3	2	0	5	0	0	1.70 \pm 0.45, $P < 0.01$

Each value represents the number of rats. *P* values: drug-treated group versus vehicle group (U-test).

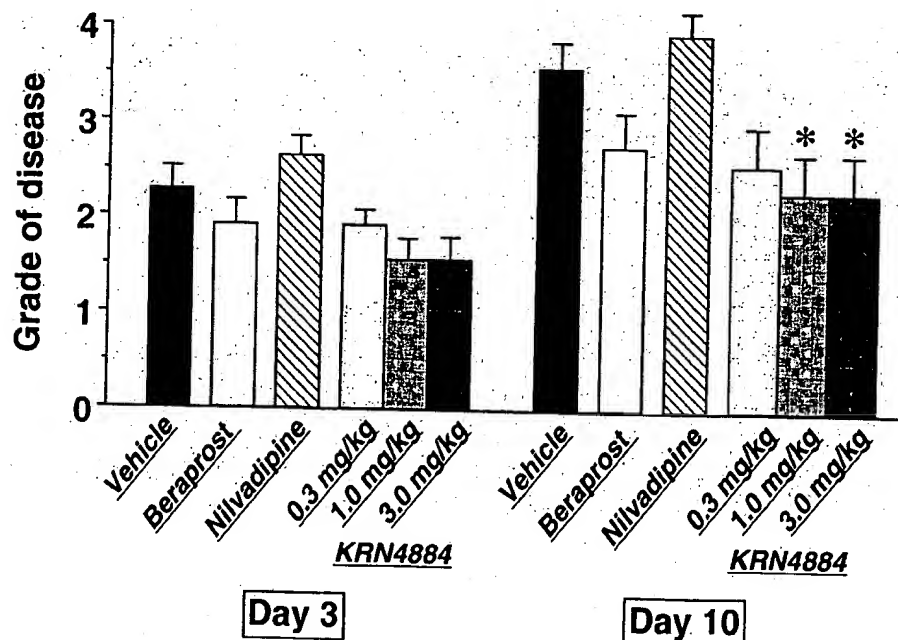


FIGURE 2. The effect of KRN-4884 (0.3–3.0 mg/kg), beraprost sodium (0.3 mg/kg) and nilvadipine (30 mg/kg) on laurate-induced arterial occlusive rats (Experiment 2). The macroscopic observation of the hind limbs was carried out on the 3rd and 10th day after the laurate injection. The degree of lesions was classified into six grades. Data represent mean ± SEM (n=11); *P<0.05: significantly different from vehicle group (U-test).

(5.5 ± 0.5 V, n=6) was significantly ($P<0.001$) reduced compared with that of nonligated (14.6 ± 1.2 V, n=5). There was no significant difference in the mean arterial blood pressure between the two groups (not shown). KRN4884 produced a dose-dependent reduction in the arterial blood pressure in the ligated and nonligated rats (Fig. 4).

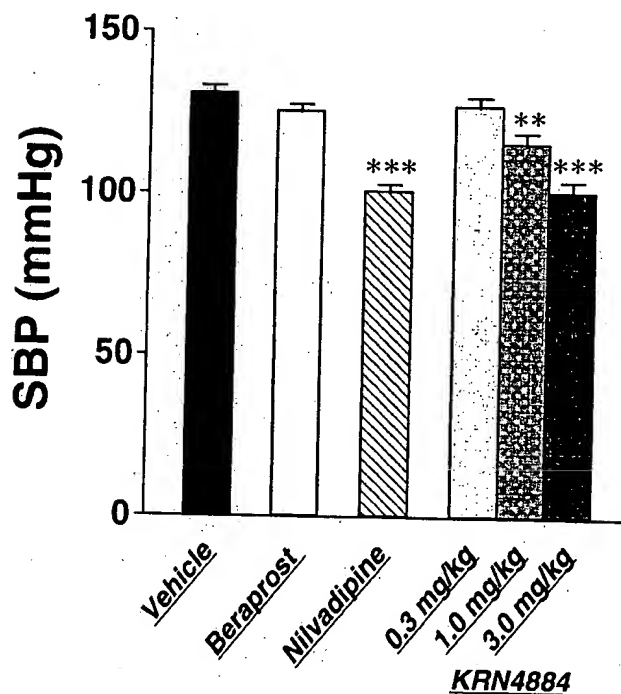


FIGURE 3. Hypotensive effect of KRN4884 (0.3–3.0 mg/kg), beraprost sodium (0.3 mg/kg) and nilvadipine (30 mg/kg) on laurate-induced arterial occlusive rats in Experiment 2. Systolic blood pressure (SBP) was measured 1 hr after administration of the drugs on the 7th or 8th day after the laurate injection. Data represent mean ± SEM (n=8–9); **P<0.01, ***P<0.001: significantly different from vehicle group (Dunnett's multiple comparisons test).

KRN4884 (3 and 10 μ g/kg, IV) significantly increased the muscle blood flow in the femoral artery-ligated rats but not in nonligated rats.

Effects of KRN4884 on platelet aggregation

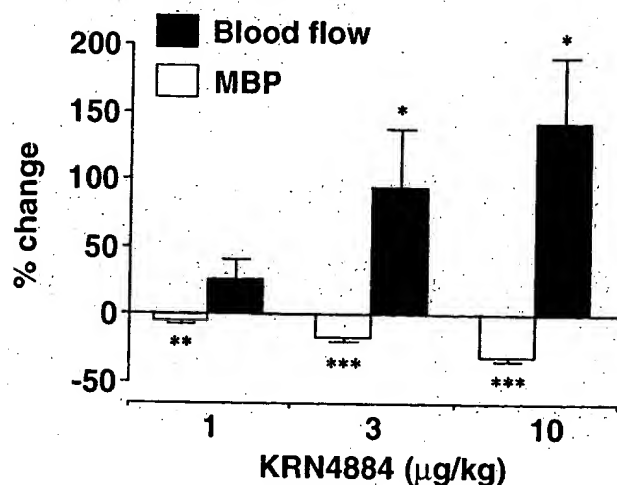
KRN4884 (10^{-8} – 2.5×10^{-5} M) did not affect rat platelet aggregation induced by ADP (1 μ M) and collagen (3 μ M) *in vitro* (not shown).

DISCUSSION

In the present study, we demonstrated that KRN4884 had a protective effect in the laurate-induced model of peripheral circulation insufficiency. Ashida *et al.* (1980) reported that injection of laurate into the artery causes degeneration and denudation of the endothelium, and its damage triggers platelet adherence and aggregation to form occlusive thrombosis. The antiplatelet agent ticlopidine was effective in the laurate-induced model (Ashida *et al.*, 1980). They showed a major participation of platelets in the progression of the model.

KRN4884 did not have antiplatelet action but was effective in this model. K^+ channel openers cromakalim, pinacidil and nicorandil significantly increased muscle blood flow and pO_2 in an occlusive arterial disease model (Angersbach and Nicholson, 1988). Furthermore, K^+ channel openers SDZ-PCO 400 and cromakalim had a beneficial effect on muscle high-energy phosphate levels in the hind limb of the occlusive arterial disease model rat (Cook *et al.*, 1993), suggesting that K^+ channel openers vasodilate collateral blood vessels in the ischemic limb. KRN4884 also increased muscle blood flow in the femoral artery-ligated gastrocnemius muscle in this study. Thus, the protective effect of KRN4884 in the laurate-induced model may be related to an improvement of peripheral circulation through an increase in blood flow of the collateral artery. In contrast, the Ca^{2+} channel blocker nilvadipine had no effect on the laurate-induced rat model. The result in our study is consistent with the results from studies by Angersbach and Nicholson (1988) and Cook *et al.* (1993). Angersbach and Nicholson (1988) observed that the Ca^{2+} channel blockers nifedipine, verapamil and diltiazem do not increase blood flow in the hypoxic skeletal muscle, and Cook *et al.* (1993) demonstrated that nitrendipine has no effect on ischemic muscle high-energy phosphate levels in the animal model.

A. ligated femoral artery



B. non-ligated femoral artery

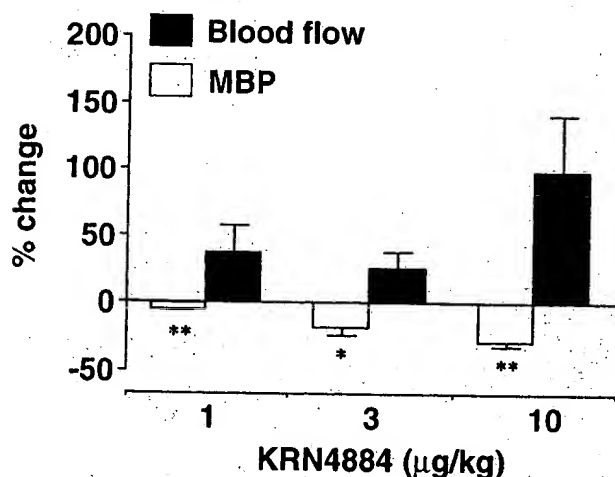


FIGURE 4. The effect of KRN4884 on mean arterial blood pressure and rat gastrocnemius muscle blood flow (A) with or (B) without ligated femoral artery. Peak changes in mean blood pressure (MBP, open column) and blood flow (solid column) produced by intravenous administration of KRN4884. Data represent mean \pm SEM ($n=4-7$); * $P<0.05$, ** $P<0.01$, *** $P<0.001$: significantly different from the value before administration of KRN4884 (paired t -test).

They suggested that the collateral vessels are more sensitive to the K^+ channel openers than to the Ca^{2+} channel blockers.

Thromboangiitis obliterans (TAO) and arteriosclerosis obliterans (ASO) are produced by the occlusion of the distal and proximal artery in the legs, respectively. Drug therapy for TAO and ASO has been mainly used with antiplatelet drugs; but, on the other hand, vasodilators that have no antiplatelet effect (i.e., dihydropyridine Ca^{2+} channel blockers, α -adrenergic blockers and β -adrenergic agonists) have been confirmed to be ineffective in intermittent claudication (Boobis and Bell, 1982; Creager and Roddy, 1990; Lorentsen and Landmark, 1983).

In this study, the K^+ channel opener KRN4884 was effective in both the TAO and the ASO models. These findings suggest a new drug therapy, which improves peripheral circulation in the ischemic region without antiplatelet action. Clinical studies are needed to establish the therapy using KRN4884 for TAO and ASO.

SUMMARY

The effect of the potassium channel opener KRN4884 on the peripheral arterial occlusion model induced by laurate (1.0 mg/leg, IA) was examined and compared with that of beraprost sodium, prostaglandin I_2 analog, and the Ca^{2+} channel blocker nilvadipine. Treatment of the rats with KRN4884 (1 and 3 mg/kg, PO) or beraprost sodium (0.3 mg/kg, PO) prevented macroscopic changes in the paw after injection of laurate. In contrast, nilvadipine did not improve the lesions induced by laurate. KRN4884 produced a dose-dependent increase in gastrocnemius blood flow in the chronic femoral artery-ligated rats. The effect of KRN4884 on blood flow was stronger in the hypoxic muscle than in the normal muscle. KRN4884 did not have a direct antiplatelet aggregation activity. These findings suggest that KRN4884 is useful for the therapy of peripheral arterial occlusive disease and that the effect of KRN4884 is associated with an increase in blood flow in ischemic skeletal muscle.

References

- Ashida S., Ishihara M., Ogawa H. and Abiko Y. (1980) Protective effect of ticlopidine on experimentally induced peripheral arterial occlusive disease in rats. *Thromb. Res.* 18, 55-67.
- Angersbach D. and Nicholson C. D. (1988) Enhancement of muscle blood cell flux and pO_2 by cromakalim (BRL34915) and other compounds enhancing membrane K^+ conductance, but not Ca^{2+} antagonists or hydralazine, in an animal model of occlusive arterial disease. *Naunyn-Schmiedeberg's Arch. Pharmac.* 337, 341-346.
- Boobis L. H. and Bell P. R. F. (1982) Can drugs help patients with lower limb ischaemia? *Br. J. Surg.* 69(Suppl.), S17-S23.
- Cook N. S., Rudin M., Pally C., Blarer S., and Quast U. (1993) Effects of the potassium channel openers SDZ-PCO 400 and cromakalim in an *in vivo* rat model of occlusive arterial disease assessed by ^{31}P -NMR spectroscopy. *J. Vasc. Med. Biol.* 4, 14-22.
- Creager M. A. and Roddy M. A. (1990) The effect of nifedipine on calf blood flow and exercise capacity in patients with intermittent claudication. *J. Vasc. Med. Biol.* 2, 94-99.
- Izumi H., Jinno Y., Kaneta S., Tanaka Y., Okada Y., Izawa T. and Ogawa M. (1995) Effect of KRN488, a novel K channel opener, on the cardiovascular system in anesthetized dogs: a comparison with levromakalim, nilvadipine, and nifedipine. *J. Cardiovasc. Pharmac.* 26, 189-197.
- Izumi H., Tanaka Y., Okada Y., Ogawa M. and Izawa T. (1996) Structure-activity relationship of a novel K^+ channel opener, KRN4884, and related compounds in porcine coronary artery. *Gen. Pharmac.* 27, 985-989.
- Kawahara J., Izumi H., Okada Y. and Izawa T. (1996) Effects of the potassium channel openers KRN4884 and levromakalim on the contraction of rat aorta induced by A23187, compared with nifedipine. *Naunyn-Schmiedeberg's Arch. Pharmac.* 354, 460-465.
- Lorentsen E. and Landmark K. (1983) The acute effects of nifedipine on calf and forefoot blood flow in patients with peripheral arterial insufficiency. *Angiology* 34, 46-52.
- Murai T., Muraoka K., Saga K., Sakai A., Sato N., Amemiya K., Yajima M., Murata T., Umetsu T. and Nishio S. (1989) Effect of beraprost sodium on peripheral circulation insufficiency in rats and rabbits. *Arzneim.-Forsch. Drug Res.* 39, 856-859.
- Nicholson C. D., Schmitt R. M. and Wilke R. (1985) The effect of acute and chronic femoral artery ligation on the blood flow through the gastrocnemius muscle of the rat examined using laser Doppler flowmetry and xenon-113 clearance. *Int. J. Microcirc. Clin. Exp.* 4, 157-171.
- Weselcouch E. O. and Baird A. J. (1994) Effect of cromakalim on skeletal muscle function and blood flow in the ferret ischemic hindlimb. *Pharmacology* 49, 75-85.
- Weselcouch E. O., Sargent C., Wilde M. W. and Smith M. A. (1993) ATP-sensitive potassium channels and skeletal muscle function *in vitro*. *J. Pharmac. Exp. Ther.* 267, 410-416.

Contribution of ATP-Sensitive Potassium Channels to Hypoxic Hyperpolarization in Rat Hippocampal CA1 Neurons In Vitro

N. FUJIMURA,^{1,2} E. TANAKA,¹ S. YAMAMOTO,¹ M. SHIGEMORI,² AND H. HIGASHI¹

Departments of ¹Physiology and ²Neurosurgery, Kurume University School of Medicine, Kurume 830, Japan

Fujimura, N., E. Tanaka, S. Yamamoto, M. Shigemori, and H. Higashi. Contribution of ATP-sensitive potassium channels to hypoxic hyperpolarization in rat hippocampal CA1 neurons in vitro. *J. Neurophysiol.* 77: 378–385, 1997. To investigate the mechanism of generation of the hypoxia-induced hyperpolarization (hypoxic hyperpolarization) in hippocampal CA1 neurons in rat tissue slices, recordings were made in current-clamp mode and single-electrode voltage-clamp mode. Superfusion with hypoxic medium produced a hyperpolarization and corresponding outward current, which were associated with an increase in membrane conductance. Reoxygenation produced a further hyperpolarization, with corresponding outward current, followed by a recovery to the preexposure level. The amplitude of the posthypoxic hyperpolarization was always greater than that of the hypoxic hyperpolarization. In single-electrode voltage-clamp mode, it was difficult to record reproducible outward currents in response to repeated hypoxic exposure with the use of electrodes with a high tip resistance. The current-clamp technique was therefore chosen to study the pharmacological characteristics of the hypoxic hyperpolarization. In 60–80% of hippocampal CA1 neurons, glibenclamide or tolbutamide (3–100 μ M) reduced the amplitude of the hypoxic hyperpolarization in a concentration-dependent manner by up to ~70%. The glibenclamide or tolbutamide concentrations producing half-maximal inhibition of the hypoxic hyperpolarization were 6 and 12 μ M, respectively. The chord conductance of the membrane potential between –80 and –90 mV in the absence of glibenclamide (30 μ M) or tolbutamide (100 μ M) was 2–3 times greater than that in the presence of glibenclamide or tolbutamide. In contrast, the reversal potential of the hypoxic hyperpolarization was approximately –83 mV in both the absence and presence of tolbutamide or glibenclamide. In ~40% of CA1 neurons, diazoxide (100 μ M) or nicorandil (1 mM) mimicked the hypoxic hyperpolarization and pretreatment of these drugs occluded the hypoxic hyperpolarization. When ATP was injected into the impaled neuron, hypoxic exposure could not produce a hyperpolarization. The intracellular injection of the nonhydrolyzable ATP analogue 5'-adenylylimidodiphosphate lithium salt reduced the amplitude of the hypoxic hyperpolarization. Furthermore, application of dinitrophenol (10 μ M) mimicked the hypoxic hyperpolarization, and the dinitrophenol-induced hyperpolarization was inhibited by either pretreatment of tolbutamide or intracellular injection of ATP, indicating that the hypoxic hyperpolarization is highly dependent on intracellular ATP. It is therefore concluded that in the majority of hippocampal CA1 neurons, exposure to hypoxic conditions resulting in a reduction in the intracellular level of ATP leads to activation of ATP-sensitive potassium channels with concomitant hyperpolarization.

INTRODUCTION

In the CNS, hippocampal CA1 neurons are known to be extremely vulnerable to anoxia and ischemia (Siesjö 1988). In tissue slices, exposure of hippocampal CA1 neurons to

hypoxia for a short period (2–4 min) induces a hyperpolarization with decreases in input resistance and in synaptic noise (Fujiwara et al. 1987; Krnjević and Leblond 1989; Leblond and Krnjević 1989). The hypoxia-induced hyperpolarization (hypoxic hyperpolarization) is most likely to be mediated by an increase in K^+ conductance (Fujiwara et al. 1987; Hansen et al. 1982; Leblond and Krnjević 1989), but the subtype(s) of K^+ channels involved in the hyperpolarization is still unclear. It has been suggested that the hypoxic hyperpolarization is due to activation of a Ca^{2+} -dependent K^+ conductance, because hypoxia induces an early increase in the intracellular Ca^{2+} concentration as a result of Ca^{2+} mobilization from intracellular stores (Belousov et al. 1995; Katchman and Hershkowitz 1993; Krnjević and Xu 1989). Direct evidence supporting this is, however, either lacking (Fujiwara et al. 1987) or inconclusive (Leblond and Krnjević 1989). The involvement of ATP-sensitive potassium (K_{ATP}) channels in the hyperpolarization has been suggested by an inverse correlation between the ATP content of patch electrodes and conductance changes induced by hypoxia (Zhang and Krnjević 1993). The highest binding densities of glibenclamide, a K_{ATP} channel blocker, have been reported in the cortex, hippocampus, cerebellum, and substantia nigra in the CNS (Jiang et al. 1992; Mourre et al. 1989; Xia and Haddad 1991). Moreover, it has been reported that in substantia nigra neurons and dorsal vagal neurons, anoxia induces a hyperpolarization that is mediated by an activation of K_{ATP} channels (Jiang et al. 1994; Murphy and Greenfield 1992; Trapp and Ballanyi 1995). Nevertheless, the contribution of the K_{ATP} channel to the hypoxic hyperpolarization is still controversial in hippocampal CA1 neurons. K_{ATP} channel blockers, such as tolbutamide and glibenclamide, have yielded equivocal results: tolbutamide depressed the hypoxic hyperpolarization (Godfraind and Krnjević 1993; Grigg and Anderson 1989), but neither tolbutamide nor glibenclamide had comparable effects (Godfraind and Krnjević 1993; Leblond and Krnjević 1989).

The aim of this study is, therefore, to investigate the involvement of activation of K_{ATP} channels in the hypoxic hyperpolarization. By observing the effects of selective K_{ATP} channel antagonists, agonists and intracellular injection of ATP, attempts were made to examine whether the hypoxic hyperpolarization is specifically mediated by K_{ATP} channels. In addition, attempts were made to mimic the hyperpolarization with the use of a metabolic inhibitor. The accompanying paper (Yamamoto et al. 1997) describes the contribution of the Ca^{2+} -dependent K^+ conductance to the hypoxic hyperpolarization.

METHODS

The forebrains of adult Wistar rats (male, weight 200–250 g) were quickly removed under ether anesthesia and placed in chilled (4–6°C) Krebs solution that was aerated with 95% O₂–5% CO₂. The composition of the solution was (in mM) 117 NaCl, 3.6 KCl, 2.5 CaCl₂, 1.2 MgCl₂, 1.2 NaH₂PO₄, 25 NaHCO₃, and 11 glucose. The hippocampus was dissected and then sliced with a Vibratome (Oxford) to a thickness of ~400 μ m. A slice was placed on a nylon net in a recording chamber (volume 500 μ l) and immobilized with a titanium grid placed on the upper surface of the section. The preparation was completely submerged in the superfusing solution. The temperature in the recording chamber was continuously monitored and maintained at 36–37°C, and the solution was perfused at a constant rate of 6–8 ml/min. Intracellular recordings from CA1 pyramidal cells were made with glass micropipettes filled with potassium acetate (2 M) or KCl (2 M). The electrode resistance was 20–90 M Ω . The membrane potential was determined by the baseline level recorded from an X-Y recorder with a low-pass filter. In another series of experiments, voltage clamping was performed with a single-electrode voltage-clamp amplifier (Axon Instruments, Axoclamp-2A), employing a switching frequency of 4–5 kHz and a 30% duty cycle. The headstage voltage was continuously monitored to ensure complete settling of the voltage at the end of each switching cycle. Particular efforts were made to select electrodes with optimal current-passing characteristics: tip resistance of 20–90 M Ω and minimal rectification. In some neurons, recording electrodes containing adenosine 5'-triphosphate dipotassium salt (K₂-ATP, 20 mM), adenosine 5'-triphosphate magnesium salt (Mg-ATP, 10 mM), or 5'-adenylylimido-diphosphate lithium salt (AMP-PNP, 20 mM)/potassium acetate (2 M) were used for intracellular ATP or AMP-PNP injection. ATP or AMP-PNP was injected by passing hyperpolarizing current pulses (0.4–0.9 nA in intensity, 200 ms in duration, and 3.3 Hz in frequency) for 10–15 min.

Slice preparations were made "hypoxic" by superfusing medium equilibrated with 95% N₂–5% CO₂ (hypoxic medium). The dead space of the superfusing system resulted in a delay of 15–20 s before the new medium reached the chamber.

Drugs used were tolbutamide and glibenclamide (Research Biochemicals International); diazoxide (Sigma); nicorandil (gift from Chugai Pharmaceutical); 2,4-dinitrophenol (Tokyo Kasei Organic Chemical); and Mg-ATP, K₂-ATP, and AMP-PNP (Sigma). All quantitative results are expressed as means \pm SD. The number of neurons examined is given in parentheses. The unpaired and paired Student's *t*-test was used to compare data, with *P* < 0.05 considered significant.

RESULTS

This study was based on recordings from ~100 CA1 pyramidal neurons of adult rats with stable membrane potentials more negative than –60 mV. The resting membrane potential and the apparent input resistance were -71.4 ± 4.9 mV and 33.3 ± 8.8 M Ω (*n* = 67), respectively, recorded with 2 M potassium acetate electrodes and -70.1 ± 2.7 mV and 40.4 ± 4.2 M Ω (*n* = 38), respectively, recorded with 2 M KCl electrodes. In either current-clamp or voltage-clamp recording, unless specified otherwise, the membrane potential was held at –60 mV by current injection from the recording electrode before hypoxic exposure.

Hypoxia-induced hyperpolarization

Figure 1 illustrates typical changes in membrane potential or membrane current in response to oxygen deprivation, with

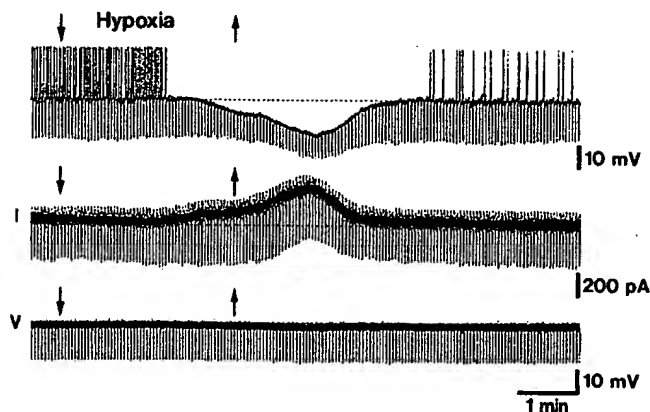


FIG. 1. Hypoxic hyperpolarizations and the corresponding outward currents in hippocampal CA1 neurons. In this and subsequent figures, the hypoxic medium was applied between the downward and upward arrows and, in each trace, the dotted line indicates the preexposure level of the membrane potential or membrane current, unless specified otherwise. *Top trace*: membrane potential recorded with a high (80 M Ω) electrode resistance under current-clamp conditions. *Middle and bottom traces*: membrane potential and voltage, respectively, recorded from the same neuron under voltage-clamp condition. Downward deflections in voltage recordings are hyperpolarizing electrotonic potentials elicited by anodal current pulses (0.3 nA, applied for 200 ms every 3 s), and downward deflections in voltage and current recordings under the voltage clamp are voltage steps (14 mV for 200 ms every 3 s) and the resultant currents.

the use of 2 M KCl-filled electrodes with a high tip resistance (80 M Ω). Superfusion with hypoxic medium produced a hyperpolarization that was associated with a reduction in apparent input resistance. When oxygen was readmitted, the membrane potential was transiently shifted to a more negative level (posthypoxic hyperpolarization) before it recovered to the preexposure level. In the same neuron under the voltage-clamp mode, hypoxia now evoked a corresponding outward current that was accompanied by a large increase in conductance. Reoxygenation prolonged the decay of the outward current by a transient outward shift, which corresponded to the posthypoxic hyperpolarization. Our previous study indicates that the hypoxic hyperpolarization is mainly due to an increase in K⁺ conductance and the posthypoxic hyperpolarization is caused by reactivation of the Na⁺–K⁺ pump (Fujiwara et al. 1987).

The peak amplitudes of the hypoxic responses, the posthypoxic hyperpolarization, and the corresponding currents, with the use of KCl or potassium acetate electrodes with high and low tip resistances, are summarized in Table 1. As the tip resistance of KCl or potassium acetate electrodes decreased, the peak amplitudes of the hypoxic hyperpolarization and its corresponding outward current were reduced, whereas the posthypoxic hyperpolarization and its corresponding outward current were not altered. When the neurons were impaled by KCl or potassium acetate electrodes with extremely low tip resistances (20- to 30-M Ω KCl electrodes and 35- to 45-M Ω potassium acetate electrodes), hypoxia produced a depolarization and its corresponding current. Both responses were associated with an increase in conductance. The peak amplitudes of the hypoxic depolarization, the hypoxic hyperpolarization, and their corresponding currents were not significantly different between potassium acetate and KCl electrodes.

TABLE 1. Peak amplitudes of hypoxic depolarization or hyperpolarization, posthypoxic hyperpolarization, and corresponding currents using KCl and potassium acetate electrodes

	Hypoxic Depolarization, mV	Hypoxic Inward Current, pA	Hypoxic Hyperpolarization, mV	Hypoxic Outward Current, pA	Posthypoxic Hyperpolarization, mV	Posthypoxic Outward Current, pA
KCl electrode						
20–30 M Ω	7.0 \pm 1.0 (5)	228 \pm 74 (5)	None	None	11.9 \pm 1.7 (5)	282 \pm 111 (5)
30–50 M Ω	None	None	5.7 \pm 2.5 (8)	161 \pm 64 (5)	11.2 \pm 5.2 (8)	259 \pm 73 (5)
>50 M Ω	None	None	9.8 \pm 2.6 (30)*	242 \pm 78 (5)	13.4 \pm 4.8 (30)	278 \pm 78 (5)
Potassium acetate electrode						
35–45 M Ω	6.1 \pm 1.6 (5)	192 \pm 70 (5)	None	None	11.4 \pm 2.0 (5)	276 \pm 102 (5)
45–70 M Ω	None	None	6.3 \pm 2.3 (10)	168 \pm 61 (5)	10.8 \pm 5.5 (10)	253 \pm 70 (5)
>70 M Ω	None	None	9.2 \pm 4.0 (57)*	234 \pm 84 (5)	13.6 \pm 4.4 (57)	283 \pm 68 (5)

Values are means \pm SD, with number of neurons in parentheses. $P < 0.01$, unpaired t -test.

Moreover, when the neuron was impaled by electrodes with relatively high tip resistances (60–80 M Ω), repeated exposure to hypoxia at the interval of every 10 min gradually attenuated both the hypoxic and posthypoxic outward currents, but not both the hypoxic and posthypoxic hyperpolarizations. This result suggests that the neuron in the voltage-clamp mode would be deteriorated more easily than that in the current-clamp mode. In other words, the hypoxic hyperpolarization would prevent the accumulation of intracellular Ca^{2+} concentration that triggers the cell deterioration (cf. Siesjö 1988). Thus we used the current-clamp technique to study the pharmacological characteristics of the hypoxic hyperpolarization in the following section.

Effects of K_{ATP} channel blockers

The hippocampal slice preparation was pretreated with the K_{ATP} channel blockers tolbutamide (3–100 μM) or glibenclamide (3–100 μM) for 10 min before hypoxic exposure. Each drug caused a small, sustained depolarization that was accompanied by an increase in apparent input resistance. The amplitude of the depolarization was 3.6 ± 1.5 mV ($n = 9$) in the presence of 100 μM tolbutamide and 3.4 ± 1.5 mV ($n = 7$) in the presence of 100 μM glibenclamide. In the majority of neurons tested, both tolbutamide and glibenclamide reduced the amplitude of the hypoxic hyperpolarization and/or prolonged the onset time of the hyperpolarization in a concentration-dependent manner (Fig. 2, *A* and *B*). In 8 of 10 hippocampal CA1 neurons tested, the minimal effective concentration and the maximal inhibitory concentration of tolbutamide were 3 and 100 μM , respectively. Tolbutamide (100 μM) significantly reduced the amplitude of the hypoxic hyperpolarization by $71 \pm 16\%$ ($n = 8$, $P < 0.01$) of the control. The half-maximum inhibition was achieved at a concentration of 12 μM (Fig. 2*B*). In the remaining two neurons, tolbutamide had no effect. Glibenclamide had similar effects; in 13 of 22 CA1 neurons, the minimal effective concentration, half-maximum inhibition and maximal inhibitory concentration were 3, 6, and 100 μM , respectively (Fig. 2*C*). Glibenclamide (100 μM) significantly reduced the amplitude of the hypoxic hyperpolarization by $67 \pm 15\%$ ($n = 13$, $P < 0.01$) of the control. In two other neurons, glibenclamide prolonged the onset time without affecting the amplitude. In the remaining five neu-

rons, glibenclamide had no effect. Moreover, tolbutamide or glibenclamide at the high concentration (100 μM) did not significantly affect the amplitude of the posthypoxic hyperpolarization (Fig. 2*A* for tolbutamide). Thus, in 60–80% of the neurons, tolbutamide and glibenclamide depressed the hypoxic hyperpolarization in a concentration-dependent manner, but were unable to block the posthypoxic hyperpolarization.

To further study the inhibitory action of glibenclamide or tolbutamide, steady-state current-voltage plots before and during the hypoxic hyperpolarization were obtained by passing hyperpolarizing and subsequent depolarizing ramp currents through the recording electrode. The conductance change during hypoxia was much greater than that in normoxic media (Fig. 3, *A* and *C*), indicating that it is not likely to result from the reduction of a tonic inward current. The net outward current induced by hypoxia was markedly depressed by tolbutamide (100 μM) or glibenclamide (30 μM) (compare Fig. 3, *A* and *C*, *insets*, with Fig. 3, *B* and *D*, *insets*, respectively). The chord conductance of the membrane potential between -80 and -90 mV in the absence of tolbutamide was significantly greater than that in the presence of tolbutamide (100 μM), being 12.3 ± 6.1 nS ($n = 8$) in the absence and 3.7 ± 1.5 nS ($n = 6$) in the presence of tolbutamide. Similar results were obtained in the absence and presence of glibenclamide (30 μM), being 14.3 ± 7.5 nS ($n = 4$) in the absence and 6.3 ± 3.3 nS ($n = 4$) in the presence of glibenclamide. In contrast, the reversal potential of the hypoxic hyperpolarization was not different at -83.7 ± 3.5 mV ($n = 8$) and -83.3 ± 2.6 mV ($n = 6$) in the absence and presence of tolbutamide (100 μM), respectively. The reversal potential of the hypoxic hyperpolarization was -82.6 ± 1.9 mV ($n = 4$) and -83.4 ± 1.7 mV ($n = 4$) in the absence and presence of glibenclamide (30 μM), respectively.

Effects of activators of K_{ATP} channels

Diazoxide and nicorandil are well known to be activators of K_{ATP} channels in pancreatic β -cells (Ashcroft and Ashcroft 1990; Dunne 1990; Trube et al. 1986). To confirm the contribution of K_{ATP} channels to the hypoxic hyperpolarization, these activators were applied to hippocampal CA1 neurons. In 10 of 36 neurons, application of diazoxide (100

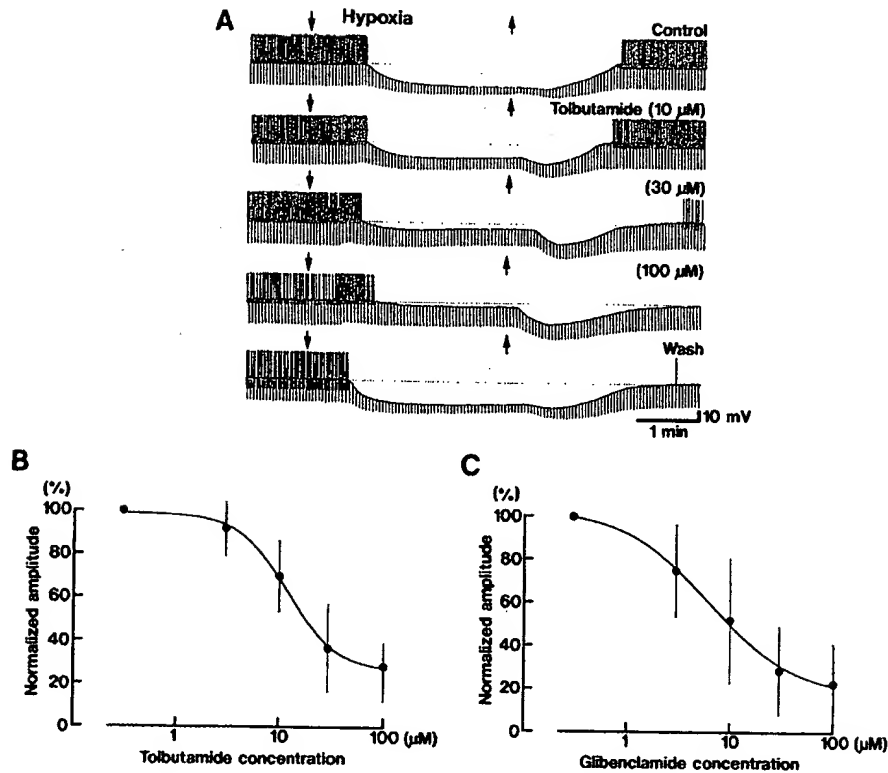


FIG. 2. Effects of the ATP-sensitive potassium (K_{ATP}) channel blockers on the hypoxic hyperpolarization. *A*: hypoxic hyperpolarization before blockers (top trace), after pretreatment with tolbutamide at a concentration of 10 μM (2nd trace), 30 μM (3rd trace), and 100 μM (4th trace) for 10 min, and after washing out of the drug for 30 min (bottom trace). *B* and *C*: concentration dependence of inhibition by tolbutamide (*B*) and glibenclamide (*C*). The peak amplitudes of the hypoxic hyperpolarizations at various concentrations of tolbutamide or glibenclamide were normalized with those of the respective controls. Error bars: SD. The curves fitting the points were drawn by the Hill's equation. The Hill coefficient was 1.8 for tolbutamide and 1.0 for glibenclamide. Downward deflections in voltage recordings are hyperpolarizing electrotonic potentials elicited by anodal current pulses (0.4 nA, applied for 200 ms every 3 s).

μM) or nicorandil (1 mM) produced a hyperpolarization that was accompanied by a fall in apparent input resistance. The hyperpolarization reversed rapidly when the application

was discontinued. The peak amplitudes of the hyperpolarization induced by diazoxide (100 μM) and nicorandil (1 mM) were 6.0 ± 2.6 mV ($n = 4$) and 2.8 ± 1.2 mV ($n = 6$),

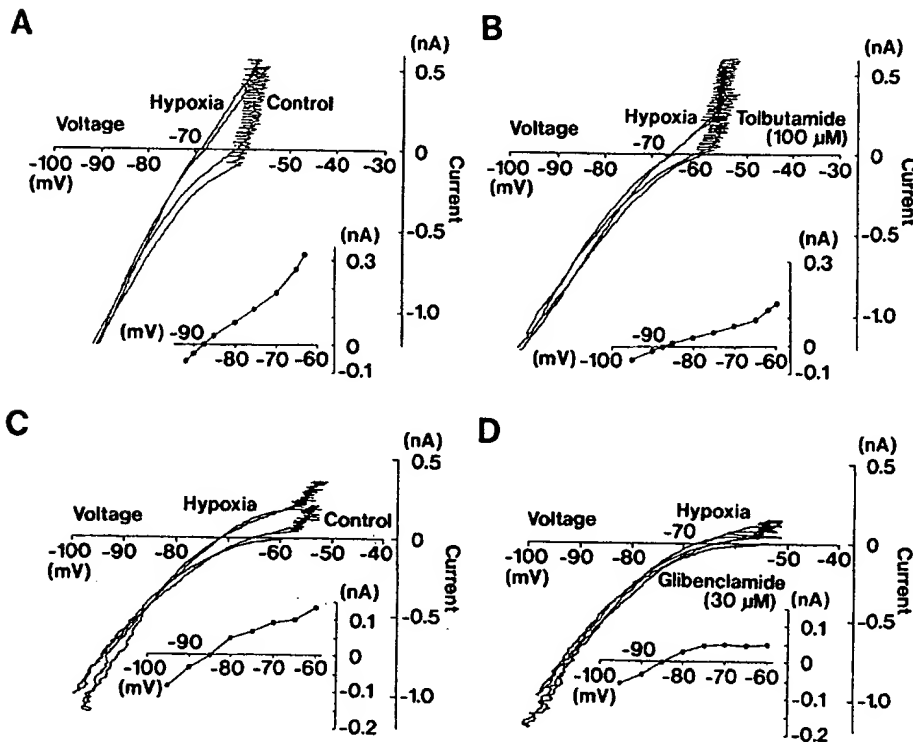


FIG. 3. Effects of the K_{ATP} channel blockers on the membrane conductance during the hypoxic hyperpolarization. Slow hyperpolarizing and depolarizing DC ramp currents (1–2 mV/s) were passed through the recording electrode to obtain steady-state current-voltage relationships before and during hypoxic exposure (not shown). *A* and *B*: steady-state current-voltage curves before (Control) and during hypoxic exposure (Hypoxia) in the absence (*A*) and presence (*B*) of tolbutamide (100 μM). *Insets*: net outward currents produced by hypoxia, which were obtained by subtraction of the steady-state current-voltage relation at preexposure level from that during hypoxic exposure. For subtraction, steady-state current-voltage relations, which were continuously recorded from the most hyperpolarizing level (–95 mV) to –60 mV, were used. Note that the net outward current was markedly depressed by tolbutamide. *C* and *D*: steady-state current-voltage curves before (Control) and during hypoxic exposure (Hypoxia) in the control condition and in the presence of glibenclamide (30 μM), respectively. The outward current in the control condition was markedly depressed by glibenclamide. Note that the reversal potential of the net outward current was not affected by either tolbutamide or glibenclamide.

respectively. The neuronal input resistance measured at the peak of the hyperpolarization was reduced to $79 \pm 11\%$ ($n = 4$) of the control before application of diazoxide and to $85 \pm 11\%$ ($n = 6$) of the control before application of nicorandil. Next, the hypoxic hyperpolarization was compared in the absence and presence of the K_{ATP} channel activator. The peak amplitude of the hypoxic hyperpolarization was significantly reduced to $82 \pm 4\%$ ($n = 4$) of the control in the presence of $100 \mu\text{M}$ diazoxide and to $63 \pm 12\%$ ($n = 6$) of the control in the presence of 1 mM nicorandil. In the remaining 26 neurons, application of diazoxide or nicorandil did not significantly affect the membrane potential and apparent input resistance.

Effects of a metabolic inhibitor

Metabolic inhibitors, such as 2,4-dinitrophenol and cyanide, have been used to produce the anoxic/ischemic insult by blocking oxidative respiration and thereby lowering intracellular ATP levels ($[\text{ATP}]_i$) (Murphy and Greenfield 1991; Reiner et al. 1990). A short period (15–60 s) of superfusion with dinitrophenol ($10 \mu\text{M}$) caused a hyperpolarization that was associated with a reduction of the neuronal input resistance. As the application period increased, the duration of the hyperpolarization was prolonged (Fig. 4A). The amplitude of the dinitrophenol-induced hyperpolarization was $4 \pm 2 \text{ mV}$ ($n = 4$), $7 \pm 3 \text{ mV}$ ($n = 4$), and $9 \pm 4 \text{ mV}$ ($n = 9$) with 15, 30, and 60 s of superfusion with medium containing dinitrophenol ($10 \mu\text{M}$). The duration of the dinitrophenol-induced hyperpolarization was $1.4 \pm 0.3 \text{ min}$ ($n = 4$), $4 \pm 0.5 \text{ min}$ ($n = 4$), and $5.2 \pm 0.7 \text{ min}$ ($n = 9$) with 15, 30, and 60 s of superfusion with medium containing dinitrophenol ($10 \mu\text{M}$). On superfusion with dinitrophenol ($10 \mu\text{M}$) for 60 s, the neuronal input resistance measured at the peak of the dinitrophenol-induced hyperpolarization was decreased to $60 \pm 13\%$ ($n = 9$) of the control.

Because the posthypoxic hyperpolarization is generated by reactivation of the $\text{Na}^+ - \text{K}^+$ pump (Fujiwara et al. 1987), it is possible that a hyperpolarization generated by reactivation of the $\text{Na}^+ - \text{K}^+$ pump may follow some periods after superfusion with metabolic inhibitors. It was, however, difficult to detect two components in dinitrophenol-induced hyperpolarization. It may be possible to detect reactivation of the $\text{Na}^+ - \text{K}^+$ pump in the presence of a high concentration of tolbutamide ($100 \mu\text{M}$), because the hypoxic hyperpolarization was inhibited by $\sim 70\%$ whereas the posthypoxic hyperpolarization was not affected (see Fig. 2A). We therefore compared the peak amplitude and neuronal input resistance of the dinitrophenol-induced hyperpolarization in the absence and presence of tolbutamide ($100 \mu\text{M}$) by comparison of two arbitrary points of the time when the dinitrophenol-induced hyperpolarization reached a peak in the absence (t_1) and presence (t_2) of tolbutamide, as shown in Fig. 4B. The amplitudes of the dinitrophenol-induced hyperpolarization at t_1 and t_2 in the absence of tolbutamide were $12.7 \pm 1.1 \text{ mV}$ ($n = 4$) and $11.9 \pm 3.9 \text{ mV}$ ($n = 4$), respectively. In the absence of tolbutamide, the neuronal input resistances measured at t_1 and t_2 were reduced to $51 \pm 8\%$ ($n = 4$) and $58 \pm 8\%$ ($n = 4$) of the controls, respectively. The amplitudes of the dinitrophenol-induced hyperpolarization at t_1 and t_2 in the presence of tolbutamide were $1.0 \pm 1.7 \text{ mV}$

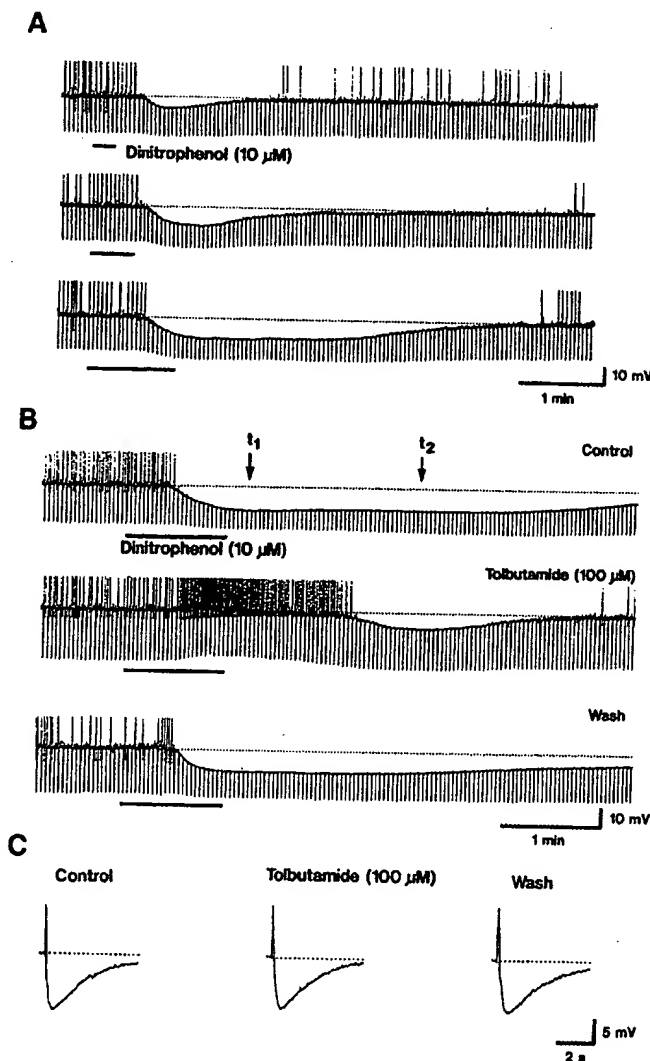


FIG. 4. Effects of dinitrophenol on the hippocampal CA1 neurons. In this and subsequent figures, downward deflections in voltage recordings are hyperpolarizing electrotonic potentials elicited by anodal current pulses (in the range of 0.2–0.5 nA, applied for 200 ms every 3 s). A: dinitrophenol ($10 \mu\text{M}$) produced a hyperpolarization associated with a fall in apparent input resistance. Prolonged applications (indicated by black bars) increased the duration of the hyperpolarization. B: dinitrophenol-induced hyperpolarization in the control condition (top trace), after pretreatment with tolbutamide ($100 \mu\text{M}$) for 10 min (middle trace), and after washing out of the drug for 30 min (bottom trace). Arrows: point of time of the peak of the dinitrophenol-induced hyperpolarization produced in the control condition (t_1) and in the presence of tolbutamide (t_2). Note that the dinitrophenol-induced hyperpolarization was markedly depressed by tolbutamide. C: after hyperpolarization following the spikes in the control condition (left), after pretreatment with tolbutamide ($100 \mu\text{M}$) for 10 min (middle), and after washing out of the drug for 30 min (right).

($n = 4$) and $6.3 \pm 2.8 \text{ mV}$ ($n = 4$), respectively. In the presence of tolbutamide, the neuronal input resistances measured at t_1 and t_2 were reduced to $88 \pm 6\%$ ($n = 4$) and $84 \pm 18\%$ ($n = 4$) of the controls, respectively (Fig. 4B). Thus tolbutamide significantly depressed the peak amplitude of the dinitrophenol-induced hyperpolarization at t_1 ($P < 0.01$), but not the peak amplitude at t_2 . Tolbutamide reversed the reduction in both the neuronal input resistances during the dinitrophenol-induced hyperpolarizations at t_1 ($P <$

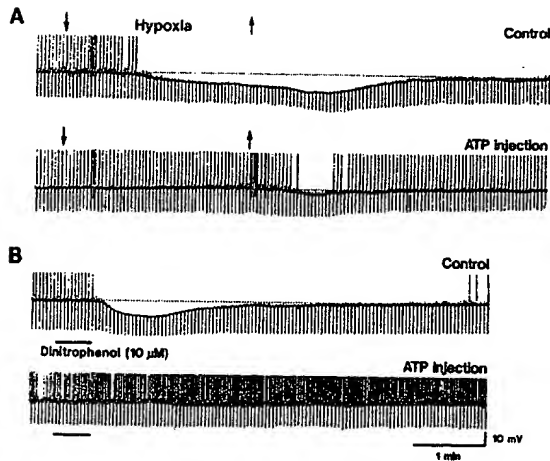


FIG. 5. Effects of intracellular injection of ATP on the hyperpolarization induced by hypoxia (\downarrow) or dinitrophenol (bars). ATP was injected after recording of the 1st response to hypoxic medium or dinitrophenol-containing medium by passing hyperpolarizing current pulses (0.3–0.9 nA for 200 ms every 3 s) through the recording electrode for 10 min. *A*: hypoxic hyperpolarization recorded 5 min after impalement with an electrode containing 20 mM adenosine 5'-triphosphate dipotassium salt (K_2 -ATP)/2 M KCl (*top trace*) was virtually abolished after intracellular ATP injection (*bottom trace*). *B*: dinitrophenol-induced hyperpolarization 5 min after impalement with an electrode containing 20 mM adenosine 5'-triphosphate magnesium salt (Mg-ATP)/2 M KCl (*top trace*) was abolished after intracellular ATP injection (*bottom trace*).

0.01) and t_2 ($P < 0.05$). These results suggest that the dinitrophenol-induced hyperpolarization at t_2 is partially due to the reactivation of Na^+ - K^+ pump. Moreover, neither tolbutamide (100 μ M) nor glibenclamide (30 μ M) affected the afterhyperpolarization that followed action potentials (spike afterhyperpolarization) ($n = 8$, Fig. 4C).

Effects of intracellular injection of ATP and AMP-PNP

K_{ATP} channels in pancreatic β -cells can be closed by high concentrations (>1 mM) of [ATP]_i (Kakei et al. 1985; Rorsman and Trube 1985). Thus ATP was injected intracellularly by the use of recording electrodes containing 20 mM K_2 -ATP or Mg-ATP. Figure 5A shows changes in the membrane potential in response to hypoxia recorded by the use of recording electrodes containing 20 mM K_2 -ATP/2 M KCl. Hypoxia produced a hyperpolarization of 7.7 ± 1.5 mV ($n = 6$) in amplitude 5 min after the neuron was impaled (*top trace*), but it could not induce any hyperpolarization after intracellular injection of ATP by passing hyperpolarizing current pulses for 10 min (*bottom trace*). The amplitude of the posthypoxic hyperpolarization was also significantly reduced from 10.7 ± 1.5 mV before ATP injection to 3.3 ± 1.0 mV ($n = 6$, $P < 0.01$) after the injection. When electrodes containing 20 mM Mg-ATP/2 M KCl were used, similar results were obtained: the hypoxic hyperpolarization could not be obtained 10 min after ATP injection was started ($n = 5$). The intracellular injection of the nonhydrolyzable ATP analogue AMP-PNP (20 mM) markedly depressed the hypoxic hyperpolarization without affecting the posthypoxic hyperpolarization. In five neurons tested, the amplitude of the hypoxic hyperpolarization was significantly reduced to 3.5 ± 1.0 mV ($P < 0.01$) compared with 8.5 ± 2.6 mV

before the injection, whereas the amplitude of the posthypoxic hyperpolarization was 11.2 ± 1.3 mV before the injection and 11 ± 2.4 mV after the injection. Similarly, hyperpolarizations of 7.3 ± 3.2 mV induced by 10 mM dinitrophenol were abolished by intracellular ATP injection in all five neurons tested (Fig. 5B).

DISCUSSION

Our previous study demonstrates that the hypoxic hyperpolarization in hippocampal CA1 neurons is unaffected by Co^{2+} (2 mM) or tetrodotoxin (0.3 μ M) medium, which completely blocks spontaneous and evoked synaptic potentials (Fujiwara et al. 1987). This finding indicates that the response is brought about by a direct action of hypoxia on the impaled neuron. The hyperpolarization is markedly enhanced in K^+ -free media and is depressed in high- K^+ (10 mM) solutions, whereas the hyperpolarization is not significantly affected by low- Cl^- or low- Na^+ medium. The hyperpolarization reverses in polarity at -83 mV (Fujiwara et al. 1987), which is comparable with the value in the present study. These results suggest that the hypoxic hyperpolarization is mainly due to activation of K^+ channels. The contribution of the activation of K_{ATP} channels in the hypoxic hyperpolarization will be discussed in the following section.

Antagonists and agonists of K_{ATP} channels

The highest binding densities of radioactively labeled glibenclamide, a sulfonylurea, which is a specific K_{ATP} channel blocker (Bernardi et al. 1988; Geisen et al. 1985), have been reported in the cortex, hippocampus, cerebellum, and substantia nigra in the CNS (Jiang et al. 1992; Mourre et al. 1989; Xia and Haddad 1991). The binding densities of glibenclamide in rat brain appear to be dense after birth; most of the binding sites are well developed within 3 wk after birth (Xia et al. 1993). The present study shows that in $\sim 80\%$ of hippocampal CA1 neurons tested, the sulfonylureas tolbutamide and glibenclamide depressed both the hypoxic hyperpolarization and the corresponding net outward current. The half-maximum inhibition of tolbutamide for the K_{ATP} channel activity is 3–17 μ M in pancreatic β -cells (Belles et al. 1987; Gillis et al. 1989; Trube et al. 1986; Zünkler et al. 1988), 60 μ M in skeletal muscle (Woll et al. 1989), and 380 μ M in cardiac muscle (Strugess et al. 1988). On the other hand, the half-maximum inhibition of glibenclamide is 4–27 nM in pancreatic β -cells (Belles et al. 1987; Zünkler et al. 1988) and 20 μ M in smooth muscle cells (Standen et al. 1989; also cf. Ashcroft and Ashcroft 1990). In the present study, the values for the half-maximum inhibition of tolbutamide and glibenclamide of the hypoxic hyperpolarization were 12 and 6 μ M, respectively. Thus these values are comparable with those in β -cells and smooth muscle, respectively.

Neither tolbutamide nor glibenclamide at high concentrations (100 μ M) affected a slow spike afterhyperpolarization, which is induced by increased Ca^{2+} -dependent K^+ conductance (Lancaster and Nicoll 1987), and a posthypoxic hyperpolarization, which is produced by reactivation of the electrogenic Na^+ - K^+ pump (Fujiwara et al. 1987). Moreover, the reversal potential of the hypoxic hyperpolarization was

not affected by these sulfonylurea compounds. The results suggest that tolbutamide and glibenclamide (3–100 μ M) act on sulfonylurea receptors in CA1 neurons, with concomitant inactivation of the coupled K_{ATP} channels. The K_{ATP} channels characterized in heart, skeletal and smooth muscles, and pancreatic β -cells are only activated when the $[ATP]_i$ declines by 30–50% of normal levels (Noma and Shibasaki 1985). In guinea pig hippocampal slice preparations, $[ATP]_i$ is decreased by $\sim 15\%$ within 2 min of exposure to hypoxia (Lipton and Whittingham 1982). Thus a brief application of hypoxia for 2–4 min would be expected to activate K_{ATP} channels in $\sim 80\%$ of hippocampal CA1 neurons. Even in the presence of 100 μ M tolbutamide or glibenclamide, however, the hypoxic hyperpolarization was not completely blocked; 30–36% of the amplitude of the hypoxic hyperpolarization was resistant to K_{ATP} channel blockers. Furthermore, in the remaining 20% of CA1 neurons, up to 100 μ M concentrations of tolbutamide or glibenclamide did not affect the hypoxic hyperpolarization. The sensitivity of K_{ATP} channels for tolbutamide or glibenclamide is different in various tissues, described above. In epithelial cells, K_{ATP} channels are not affected by either tolbutamide or glibenclamide (cf. Ashcroft and Ashcroft 1990). It is therefore possible that the K_{ATP} channels in hippocampus are heterogeneous and some of them are insensitive to tolbutamide and glibenclamide. On the other hand, there is another possibility that the sulfonylurea-insensitive hypoxic hyperpolarization could be mediated by activation of another species of K^+ channels, such as Ca^{2+} -dependent K^+ channels (Yamamoto et al. 1997).

In $\sim 40\%$ of CA1 neurons tested in the present study, activators of K_{ATP} channels, such as diazoxide and nicorandil (Trube et al. 1986; also cf. Ashcroft and Ashcroft 1990), mimicked the hypoxic hyperpolarization, and pretreatment with these drugs occluded the hypoxic hyperpolarization. These results indicate that in these neurons the activation of K_{ATP} channels may contribute to the hypoxic hyperpolarization. Nevertheless, diazoxide or nicorandil did not produce any hyperpolarization in the remaining 60% of neurons, whereas tolbutamide or glibenclamide produced a depolarization and depressed the hypoxic hyperpolarization in $\sim 80\%$ of the neurons tested. This discrepancy may be due to the fact that in the experiments in which diazoxide and nicorandil were used the slices were prepared from relatively young (just after 3 wk postnatal) rats, which may only have a small number of K_{ATP} channels. The activation of K_{ATP} channels by diazoxide depends on the $[ATP]_i$; diazoxide induces openings of the channel at < 1 mM $[ATP]_i$, but has little effect at > 1 mM (Trube et al. 1986). The cortical concentration of $[ATP]_i$ is ~ 3 μ M per g wet wt (Hansen 1985). Thus an alternative explanation is that the infrequent, small responses to activators of K_{ATP} channels are due to high concentrations (> 1 mM) of $[ATP]_i$ in hippocampal CA1 neurons (Lipton and Whittingham 1982).

ATP dependency of the hypoxic hyperpolarization

When ATP was injected into the recording neuron, hypoxia failed to induce a hyperpolarization, suggesting that the hypoxic hyperpolarization is highly dependent on $[ATP]_i$. Furthermore, application of the metabolic inhibitor dinitro-

phenol mimicked the hypoxic hyperpolarization, and the dinitrophenol-induced hyperpolarization was reduced by pretreatment with tolbutamide and inhibited by intracellular injection of ATP. Dinitrophenol reduces the transmembrane proton concentration gradient across an inner mitochondrial membrane, which results in a decline of ATP synthesis from mitochondria (Darnell et al. 1990). Taken together, these results support the hypothesis that deprivation of ATP induces the hypoxic hyperpolarization.

Intracellular ATP injection by the use of electrodes containing Mg-ATP or K_2 -ATP similarly inhibited the generation of the hypoxic hyperpolarization. It is therefore unlikely that some leakage of Mg^{2+} or K^+ through the electrode is involved in the depression of hypoxic hyperpolarization after ATP injection. Like ATP, the nonhydrolyzable ATP analogues AMP-PNP and adenylyl (β, γ -methylene)-diphosphate have been reported to block K_{ATP} channels in heart, pancreatic β -cells, and skeletal muscle (Ashcroft and Kakei 1989; Cook and Hales 1984; Kakei et al. 1985; Spruce et al. 1987; Trube and Hescheler 1984). Similar results were observed in the present study; intracellular injection of AMP-PNP markedly reduced the hypoxic hyperpolarization. This result suggests that the blocking action of ATP on the generation of the hypoxic hyperpolarization is not due to energy supply by hydrolyzation of ATP.

In conclusion, the present study suggests that the hypoxic hyperpolarization is mainly due to the activation of K_{ATP} channels caused by the reduction of $[ATP]_i$ following hypoxic exposure.

We thank Drs. G. M. Lees and S. M. C. Cunningham for valuable comments and suggestions on the manuscript.

This work was supported in part by a Grant-in-Aid for Scientific Research of Japan and an Ishibashi Foundation Grant.

Address for reprint requests: E. Tanaka, Dept. of Physiology, Kurume University School of Medicine, 67 Asahi-machi, Kurume 830, Japan.

Received 19 June 1996; accepted in final form 12 September 1996.

REFERENCES

- ASHCROFT, S. J. H. AND ASHCROFT, F. M. Properties and functions of ATP-sensitive K-channels. *Cell. Signalling* 2: 197–214, 1990.
- ASHCROFT, F. M. AND KAKEI, M. ATP-sensitive K^+ channels in rat pancreatic β -cells: modulation by ATP and Mg^{2+} ions. *J. Physiol. Lond.* 416: 349–367, 1989.
- BELLES, B., HESCHELER, J., AND TRUBE, G. Changes of membrane currents in cardiac cells induced by long whole-cell recordings and tolbutamide. *Pfluegers Arch.* 409: 582–588, 1987.
- BELOUSOV, A. B., GODFRAIND, J.-M., AND KRNEVIC, K. Internal Ca^{2+} stores involved in anoxic responses of rat hippocampal neurons. *J. Physiol. Lond.* 486: 547–556, 1995.
- BERNARDI, H., FOSSET, M., AND LAZDUNSKI, M. Characterization, purification, and affinity labeling of the brain [3H]glibenclamide-binding protein, a putative neuronal ATP-regulated K^+ channel. *Proc. Natl. Acad. Sci. USA* 85: 9816–9820, 1988.
- COOK, D. L. AND HALES, C. N. Intracellular ATP directly blocks K^+ channels in pancreatic β -cells. *Nature Lond.* 311: 271–273, 1984.
- DARNELL, J. E., LODISH, H. F., AND BALTIMORE, D. *Molecular Cell Biology*. New York: Scientific American, 1990, p. 583–616.
- DUNNE, M. J. Effects of pinacidil, RP 49356 and nicorandil on ATP-sensitive potassium channels in insulin-secreting cells. *Br. J. Pharmacol.* 99: 487–492, 1990.
- FUJIWARA, N., HIGASHI, H., SHIMOJI, K., AND YOSHIMURA, M. Effects of hypoxia on rat hippocampal neurons in vitro. *J. Physiol. Lond.* 384: 131–151, 1987.
- GEISEN, K., HITZEL, V., OKOMONPOULOS, R., PUNTER, J., WEYER, R., AND SUMM, H. D. Inhibition of 3H glibenclamide binding to sulfonylurea

- receptors by oral antidiabetics. *Arzheim.-Forsch. Drug Res.* 35: 707-712, 1985.
- GILLIS, K. D., GEE, W. M., HAMMOUD, A., MCDANIEL, M. L., FALKE, L. C., AND MISLER, S. Effects of sulfonamides on a metabolite-regulated ATP-sensitive K⁺ channel in rat pancreatic B-cells. *Am. J. Physiol.* 257 (Cell. Physiol. 26): C1119-C1127, 1989.
- GODFRAIND, J. M. AND KRNEVIĆ, K. Tolbutamide suppresses anoxic outward current of hippocampal neurons. *Neurosci. Lett.* 162: 101-104, 1993.
- GRIGG, J. J. AND ANDERSON, E. G. Glucose and sulfonylureas modify different phases of the membrane potential change during hypoxia in rat hippocampal slices. *Brain Res.* 489: 302-310, 1989.
- HANSEN, A. J. Effect of anoxia on ion distribution in the brain. *Physiol. Rev.* 65: 101-148, 1985.
- HANSEN, A. J., HOUNSGAARD, J., AND JAHNSEN, H. Anoxia increases potassium conductance in hippocampal nerve cells. *Acta Physiol. Scand.* 115: 301-310, 1982.
- JIANG, C., SIGWORTH, F. J., AND HADDAD, G. G. Oxygen deprivation activates an ATP-inhibitable K⁺ channel in substantia nigra neurons. *J. Neurosci.* 14: 5590-5602, 1994.
- JIANG, C., XIA, Y., AND HADDAD, G. G. Role of ATP-sensitive K⁺ channels during anoxia: major differences between rat (newborn and adult) and turtle neurones. *J. Physiol. Lond.* 448: 599-612, 1992.
- KAKEI, M., NOMA, A., AND SHIBASAKI, T. Properties of adenosine-triphosphate-regulated potassium channels in guinea-pig ventricular cells. *J. Physiol. Lond.* 363: 441-462, 1985.
- KATCHMAN, A. N. AND HERSHKOWITZ, N. Early anoxia-induced vesicular glutamate release results from mobilization of calcium from intracellular stores. *J. Neurophysiol.* 70: 1-7, 1993.
- KRNEVIĆ, K. AND LEBLOND, J. Changes in membrane currents of hippocampal neurons evoked by brief anoxia. *J. Neurophysiol.* 62: 15-30, 1989.
- KRNEVIĆ, K. AND XU, Y. Z. Dantrolene suppresses the hyperpolarization or outward current observed during anoxia in hippocampal neurons. *Can. J. Physiol. Pharmacol.* 67: 1602-1604, 1989.
- LANCASTER, B. AND NICOLL, R. A. Properties of two calcium-activated hyperpolarizations in rat hippocampal neurones. *J. Physiol. Lond.* 389: 187-203, 1987.
- LEBLOND, J. AND KRNEVIĆ, K. Hypoxic changes in hippocampal neurons. *J. Neurophysiol.* 62: 1-14, 1989.
- LIPTON, P. AND WHITTINGHAM, T. S. Reduced ATP concentration as a basis for synaptic transmission failure during hypoxia in the in vitro guinea-pig hippocampus. *J. Physiol. Lond.* 325: 51-65, 1982.
- MOURRE, C., BEN ARI, Y., BERNARDI, H., FOSSET, M., AND LAZDUNSKI, M. Antidiabetic sulfonylureas: localization of binding sites in the brain and effects on the hyperpolarization induced by anoxia in hippocampal slices. *Brain Res.* 486: 159-164, 1989.
- MURPHY, K. P. S. J. AND GREENFIELD, S. A. ATP-sensitive potassium channels counteract anoxia in neurones of the substantia nigra. *Exp. Brain Res.* 84: 355-358, 1991.
- MURPHY, K. P. S. J. AND GREENFIELD, S. A. Neuronal selectivity of ATP-sensitive potassium channels in guinea-pig substantia nigra revealed by responses to anoxia. *J. Physiol. Lond.* 453: 167-183, 1992.
- NOMA, A. AND SHIBASAKI, T. Membrane current through adenosine-triphosphate-regulated potassium channels in guinea-pig ventricular cells. *J. Physiol. Lond.* 363: 463-480, 1985.
- REINER, P. B., LAYCOCK, A. G., AND DOLL, C. J. A pharmacological model of ischemia in the hippocampal slice. *Neurosci. Lett.* 119: 175-178, 1990.
- RORSMAN, P. AND TRUBE, G. Glucose dependent K⁺ channels in pancreatic β -cells are regulated by intracellular ATP. *Pfluegers Arch.* 405: 305-309, 1985.
- SIESJÖ, B. K. Historical overview. Calcium, ischemia, and death of brain cells. *Ann. NY Acad. Sci.* 522: 638-661, 1988.
- SPRUCE, A. E., STANDEN, N. B., AND STANFIELD, P. R. Studies on the unitary properties of adenosine-5'-triphosphate-regulated potassium channels of frog skeletal muscle. *J. Physiol. Lond.* 382: 213-237, 1987.
- STANDEN, N. B., QUAYLE, J. M., DAVIES, N., BRAYDEN, J. E., HUANG, Y., AND NELSON, M. T. Hyperpolarizing vasodilators activate ATP-sensitive K⁺ channels in arterial smooth muscle. *Science Wash. DC* 245: 177-180, 1989.
- STRUGESS, N. C., KOZLOWSKI, R. Z., CARRINGTON, C. A., HALES, C. N., AND ASHFORD, M. J. L. Effects of sulfonylureas and diazoxide on insulin secretion and nucleotide-sensitive channels in an insulin-secreting cell line. *Br. J. Pharmacol.* 95: 83-94, 1988.
- TRAPP, S. AND BALLANYI, K. K_{ATP} channel mediation of anoxia-induced outward current in rat dorsal vagal neurons in vitro. *J. Physiol. Lond.* 487: 37-50, 1995.
- TRUBE, G. AND HESHELER, J. Inward-rectifying channels in isolated patches of the heart cell membrane: ATP-dependence and comparison with cell-attached patches. *Pfluegers Arch.* 401: 178-184, 1984.
- TRUBE, G., RORSMAN, P., AND OHNO-SHOSAKU, T. Opposite effects of tolbutamide and diazoxide on the ATP-dependent K⁺ channel in mouse pancreatic β -cells. *Pfluegers Arch.* 407: 493-499, 1986.
- WOLL, K. H., LÖNNENDONKER, U., AND NEUMCKE, B. ATP-sensitive potassium channels in adult mouse skeletal muscle: different modes of blockage by internal cations, ATP and tolbutamide. *Pfluegers Arch.* 414: 622-628, 1989.
- XIA, Y., EISENMAN, D., AND HADDAD, G. G. Sulfonylurea receptor expression in rat brain: effect of chronic hypoxia during development. *Pediatr. Res.* 34: 634-641, 1993.
- XIA, Y. AND HADDAD, G. G. Major differences in CNS sulfonylurea receptor distribution between the rat (newborn, adult) and turtle. *J. Comp. Neurol.* 314: 278-289, 1991.
- YAMAMOTO, S., TANAKA, E., AND HIGASHI, H. Mediation by intracellular calcium-dependent signals of hypoxic hyperpolarization in rat hippocampal CA1 neurons in vitro. *J. Neurophysiol.* 77: 386-392, 1997.
- ZHANG, L. AND KRNEVIĆ, K. Whole-cell recording of anoxic effects on hippocampal neurons in slices. *J. Neurophysiol.* 69: 118-127, 1993.
- ZÜNKLER, B. J., LENZEN, S., MÄNNER, K., PANTEN, U., AND TRUBE, G. Concentration-dependent effects of tolbutamide, meglitinide, glipizide, glibenclamide and diazoxide on ATP-regulated K⁺ currents in pancreatic B-cells. *Naunyn-Schmiedeberg's Arch. Pharmacol.* 337: 225-230, 1988.

Review Article

Cardiac potassium currents and channels Part II: Implications for clinical practice and therapy

Jean-Jacques Monsuez*

Department of Internal Medicine, Hôpital Paul Brousse, Paris, France

Received 15 January 1997; accepted 3 July 1997

1. Introduction

The aim of the second part of this review is to consider the mechanisms by which cardiac drugs interact with potassium channels and currents in heart disease.

Implications of K^+ channels as new targets for pharmacological interventions will be reviewed especially with regard to the mechanisms of action of antiarrhythmic agents (old and new class III drugs, proarrhythmia, reverse-use dependence) and $IK_{(ATP)}$ agonists in therapy of myocardial ischemia and preconditioning. Finally, the impairment (and, to a lesser extent, the pharmacological targeting) of K^+ currents in disease, including heart failure, cardiac hypertrophy and the congenital long QT syndrome, will be discussed.

2. Potassium channel blockade in the treatment of arrhythmias

2.1. Classification of antiarrhythmic agents

Advances in our knowledge about the primary molecular structure of several K^+ channels has

provided an opportunity to determine antiarrhythmic drug binding sites. Until now, antiarrhythmic drugs have been classified in groups that were presumed to have common mechanisms of action. Over the past 20 years, the most widely used classification has been that of Vaughan Williams, in which class III includes drugs that prolong action potential duration (APD) without affecting intracardiac conduction [1]. This results in an increase in refractoriness, a well recognized antiarrhythmic effect. Amiodarone, sotalol and clofilium are the most representative agents of this class [1]. One of the mechanisms of action of these compounds is blockade of K^+ channels [2,3], although amiodarone and sotalol also display other activities.

More recently, a new approach to the classification of antiarrhythmic drugs based 'on the molecular targets on which drugs act and on consideration of the mechanisms responsible for arrhythmias', has been suggested [4]. Pure K^+ channel blockers have been discovered and are currently being proposed for clinical use [5]. These include several compounds that interact with IK_r and comprise a methanesulfonamide moiety: dofetilide, almokalant, E4031, sematilide, ambasilide, almokalant and ibutilide [5], the latter also activating a slow inward Na^+ current [6].

One limitation to any attempt to reclassify antiarrhythmic drugs arises from the allocation of any individual drug to only one of the Vaughan Williams

*Corresponding author: Department of Internal Medicine, Hôpital Paul Brousse, 12, Avenue Paul Vaillant Couturier, 94804 Villejuif, Cedex. Tel.: +33 1 45593038; Fax: +33 1 45593788.

classes or to only one of the molecular targets of the revisited classification.

Indeed, several drugs of Vaughan Williams classes I and II also act on K^+ channels, thus displaying class III properties (Table 1). Moreover, class IV drugs (calcium-channel antagonists) may also inhibit calcium-dependent K^+ channels and β -adrenergic blockers may have an effect on the IK_r current by modulation of sympathetic tone (see below). Similarly, 'selective' class III antiarrhythmic drugs D,L-sotalol and E-4031 inhibit not only IK_r current, but also $IK_{(ACh)}$ current, by blocking the atrial muscarinic receptor (D,L-sotalol) or the channel itself (E-4031), thus explaining the efficacy of class III agents in treatment or prevention of recurrences of supraventricular arrhythmias [7].

Although class III antiarrhythmic drugs have been used for almost 20 years, when amiodarone was recognized to control a broad spectrum of cardiac arrhythmias, a renewed clinical interest on these agents has resulted from concerns about the safety of

class I antiarrhythmic drugs raised by the Cardiac Arrhythmia Suppression Trial (CAST) findings [8].

2.1.1. Amiodarone

Amiodarone has been proved to be effective in the treatment of acute supraventricular arrhythmias, including conversion to sinus rhythm with intravenous or oral administration in recent onset atrial tachyarrhythmias or other atrial tachycardias and also in the prevention of recurrences of supraventricular arrhythmias [9]. The drug has been shown to be unusually effective in the treatment of ventricular arrhythmias and prevention of recurrences of ventricular tachycardia or fibrillation [10]. In a dose-ranging study of 273 patients with sustained ventricular tachycardia, intravenous amiodarone (525–2100 mg by continuous infusion over 24 h) was associated with apparent antiarrhythmic response in 40.3% of patients. However, total and cardiac mortality rates were not different among the groups [11].

In the CASCADE study, 228 patients surviving out-of-hospital ventricular fibrillation not associated with a Q-wave infarction were randomly allocated to treat with amiodarone or 'conventional' class I antiarrhythmic therapy. Amiodarone was more effective than class I drugs in preventing recurrences of fatal or life-threatening arrhythmias: survival free of cardiac death, resuscitated cardiac arrest or implanted defibrillator shock rates were 82% and 69% at 2 years, 66% and 52% at 4 years, 53% and 40% at 6 years for amiodarone and conventional class I therapy respectively [12].

Since there was no placebo group, the results of CASCADE should be interpreted bearing in mind the potential deleterious effects of class I drugs demonstrated in the CAST study, even among the patients who received an automatic implanted cardioverter/defibrillator [8].

Several other studies demonstrated a better outcome in post-myocardial infarction patients with ventricular arrhythmias receiving amiodarone compared with controls. Amiodarone reduced the cardiac mortality rate by 61% in the 312 patients included in the Basel antiarrhythmic study of infarct size (BASIS) [13], by 44% in the 613 patients of the Polish amiodarone trial [14] and by 27% in the 1202 patients in the Canadian myocardial infarction arrhythmia trial [15]. Although there was no reduction

Table 1
Blockade of K^+ channels with class I and class III antiarrhythmic drugs

Class	Drug	IK		IK_1	Ito_1 (or Ito)
		IK_r	IK_s		
I _A	Quinidine disopyramide	+	+	+	+
I _b	Lidocaine mexiletine	o	o	o	o
I _c	Flecainide encainide	+	o	o	o
III					
Early class III drugs	Amiodarone	+	o	+	+
	D,L-Sotalol ^a	+	o	+	+
	Clofilium ^b	+	+	o	+
Selective IK_r blockers	E-4031				
	D-Sotalol ^a				
	Dofetilide				
	Sematilide				
	Risotilide	+	o	o	o
	Ambasilide				
	Almokalant				
	Ibutilide				
	Tedisamil	+	o	o	+
	Terikalant ^b	o	o	+	+

^a D,L-Sotalol with and D-sotalol without β -blocking activity. (From [2–7]).

^b Abandoned.

in total cardiac mortality in the 1486 patients (with left-ventricular dysfunction) enrolled in the European myocardial infarction trial (EMIAT), a 35% decrease in arrhythmic death was observed [16].

Patients with congestive heart failure and complex ventricular arrhythmias are at high risk of sudden death. Two trials examined the effects of amiodarone on mortality in patients with congestive heart failure and at least ten ventricular premature beats per hour. In the Grupo de Estudio de la Sobrevida en la Insuficiencia Cardiaca en Argentina (GESICA) study, amiodarone therapy was associated with a 28% reduction in mortality compared with the control group [17]. Conversely, no difference in overall mortality was found among the 674 patients enrolled in the double-blind, placebo-controlled veterans affairs survival trial of antiarrhythmic therapy in congestive heart failure (STAT-CHF), despite a significant suppression of ventricular arrhythmias [18]. One of the potential reasons for these differences is that patients in GESICA had more severe heart failure with a baseline heart rate of 90/min compared with 80 beats/min in STAT-CHF. Indeed, their follow-up showed that amiodarone reduced 2-years mortality only in those with a baseline heart rate above 90 beats/min [19].

Finally, amiodarone trials in post-MI or CHF have shown that the drug is not associated with an increase in mortality or morbidity. However, the electrophysiological reasons for the apparent safety of the drug are less well understood. Whether they are related to the class III antiarrhythmic properties or to a specific effect on one of the K^+ channels on which the drug acts, remains unknown. Indeed, amiodarone exhibits a broad spectrum of electropharmacologic effects including inhibitory actions on sodium channels, calcium channels, α - and β -adrenoreceptors, thyroid hormone receptors, the Na–K ATP-ase and several K^+ channels (IK_r , IK_1 , I_{to1} , IK_{ATP}). It could be overly simplistic — and also less than accurate — to categorize amiodarone simply as a class III antiarrhythmic drug [19].

2.1.2. *D,L Sotalol*

D,L-Sotalol is a non-cardioselective β -adrenergic blocking agent with additional class III antiarrhythmic properties which has been proved to be effective in the treatment of paroxysmal supraventricular ar-

rhythmias (atrial flutter and fibrillation, supraventricular reentrant tachycardias) and ventricular arrhythmias [20–22].

In the 486 patients suffering ventricular tachyarrhythmias enrolled in the electrophysiologic study versus electrocardiographic monitoring (ESVEM) trial, sotalol was shown to be effective in 43% of the 196 tested patients compared with 31% for the other drugs. After a 6.2 year follow-up, the actuarial probability of a recurrence of arrhythmia after a prediction of drug efficacy was less than half (43%) in the 84 patients treated with sotalol than in the 212 patients treated with the other agents [23]. However, the apparent superiority of sotalol over the other agents is difficult to interpret in the absence of a placebo or a conventional β -blocker. In the study by Kühlkamp et al., *D,L*-sotalol was also effective in the suppression of sustained monomorphic ventricular tachycardia inducible by programmed electrical stimulation refractory to class I antiarrhythmic drugs. However, five of the fifty patients enrolled experienced recurrent ventricular tachyarrhythmias and one additional patient died during a 27 months follow-up [24]. The importance of *D,L*-sotalol's β -blocking properties relative to its class III, i.e. IK_r blocking activity, in the suppression of ventricular arrhythmias is not known. Treatment with *D,L*-sotalol is associated with a substantial risk of proarrhythmia, especially torsades de pointes, which is more likely to be due to prolongation of repolarization elicited by the drug rather than to its β -blocking effects.

In the ESVEM study, torsades de pointes occurred in 5.2% of patients receiving sotalol and seven of the ten episodes which were recorded during the follow-up of the 296 patients occurred in patients treated with sotalol [23].

In a study describing the safety profile of sotalol in the first 3257 patients treated for cardiac arrhythmias in double-blind and open-label clinical trials in the US, the overall incidence of proarrhythmia in adults was 4.3%, with a higher incidence of 6.5% of patients treated for life-threatening ventricular arrhythmias [21]. In addition, proarrhythmic events seem to be more common among children, in whom they are detected in about 10% of those receiving sotalol [20].

Thus, as sotalol-related torsades de pointes are promoted by hypokalemia, concomitant diuretic

therapy should be avoided [22]. Also, for the aforementioned reasons, D,L-sotalol should not be considered to be an ordinary β -blocker, but rather a mixed class II (β -blocker) and class III (IK_r blocker) antiarrhythmic drug [22].

2.1.3. D-Sotalol

D-Sotalol, the dextrorotatory isomer of the racemate D,L-sotalol also acts as a class III antiarrhythmic drug by blocking IK_r , but, unlike its racemic counterpart D,L-sotalol, it has only minimal ($1/14^{\text{th}}$ of the racemic sotalol) β -blocking activity [3,5].

The electrophysiological effects of D-sotalol and other new class III antiarrhythmic agents include minimal (D-sotalol) or no (dofetilide, sotalol) bradycardia and prolongation of QT interval and effective refractory periods at atrial and His-Purkinje levels.

The prolongation of APD may be assessed by the monophasic action potential recording from endocardial myocardium. Class III antiarrhythmic drugs increase the effective refractory period directly by prolongation of monophasic APD: $5 \cdot 10^{-9}$ M intravenous dofetilide, 1.5 mg/kg intravenous sotalol and 200 mg amiodarone daily increase the monophasic action potential by 13%, 17–20% and 30% respectively [25].

This results in a prominent antifibrillatory action in both atria and ventricles. This antifibrillatory action of D-sotalol is no longer observed in animal models where an elevated sympathetic activity is associated: however it is conserved with D,L-sotalol which also displays β -adrenergic properties [3,26]. This may result from the role played by the two components of IK_r , IK_{r1} and IK_{r2} . β -adrenergic stimulation increases the magnitude of IK_{r2} which is insensitive to new class III drugs and, in turn, antagonizes the inhibition of IK_{r1} by these drugs [26]. In addition, myocardial ischemia antagonizes the effects of IK_r blockers by activation of IK_{ATP} currents [5].

The survival with oral D-sotalol in patients with left-ventricular dysfunction after myocardial infarction (SWORD) trial was intended to define the role of a selective class III antiarrhythmic agent without β -blocking properties in high risk post-myocardial infarction patients in whom non-selective class III drugs amiodarone and D,L-sotalol have been proved to be useful. Inclusion of 6400 patients with left-ven-

tricular ejection fractions less than 40% after a myocardial infarction was planned, but the trial was stopped at the beginning of 1994 because of a higher mortality in the treatment group [27].

2.1.4. Dofetilide

The most potent selective IK_r blocker currently in development is dofetilide which has no β -blocking activity. Dofetilide prolongs the APD, the effective and functional refractory periods to a similar extent in both atrium and ventricle. Dofetilide produces no change in the relationship of effective refractory period to monophasic APD, thus indicating that the drug prolongs refractoriness solely by virtue of its action on APD [25].

Administration of intravenous dofetilide in 12 patients with coronary artery disease prolonged the QTc by 11%, atrial and ventricular monophasic APD by 31% and 27% respectively and increased the atrial and ventricular effective refractory period by 31% and 20% respectively. These changes were not correlated with modifications of QTc nor with changes in the concentration of dofetilide [25].

Prolongation of APD by dofetilide has been proved useful, by reducing the exitable gap, in terminating or preventing reentrant tachyarrhythmias both in atria and ventricles. Considering that class I antiarrhythmic agents usually fail whereas class III agents are often effective in treatment of type I atrial flutter (which has a reentrant electrophysiological mechanism), Crijns et al. compared the efficacy of a intravenous bolus of dofetilide (8 μ g/kg) with a bolus of flecainide (2 mg/kg) in 20 patients. Seven of the ten patients treated with dofetilide converted to sinus rhythm compared with only one patient treated with flecainide. This study, which was the first to compare the differential effects of class I and class III antiarrhythmic drugs on termination of atrial flutter clearly pointed out that dofetilide was effective despite a small prolongation of the atrial flutter cycle length whereas flecainide resulted in a dose related increase in atrial flutter cycle length but failed to convert the arrhythmia [28].

More recently, a study by Falk et al. showed that intravenous dofetilide restored sinus rhythm with a higher conversion rate in atrial flutter (54%) than in atrial fibrillation 14.5% [29].

Thus, as suggested by Crijns, dofetilide may be a

treatment of choice for patients with atrial flutter, especially when a single infusion is administered in order to avoid potential proarrhythmic effects.

Indeed, proarrhythmia may also be the major limitation of the drug, even when administered in a single infusion in the treatment of supraventricular tachycardias. Bianconi et al. compared dofetilide (8 µg/kg), amiodarone (5 mg/kg) and placebo in 150 patients. Dofetilide was associated with torsades de pointes in 8.3% and with non-sustained ventricular tachycardia in an additional 4.1% of patients [30].

There are only few data currently available on the use of dofetilide in treatment of ventricular arrhythmias. Electrophysiological studies in patients with ventricular tachycardia showed that dofetilide results in an 11–13% prolongation of both atrial and ventricular monophasic APD and an ensuing 10% increase in ventricular effective refractory period which is not affected by stimulation cycle length [31].

In the recent study by Bashir, intravenous dofetilide suppressed or slowed inducible ventricular tachycardia in 17 of 41 patients (41%) whereas in comparable populations sotalol was effective in 35% and class I drugs in 12–26% of cases. Torsades de pointes were observed in only one of the 41 patients but this should not be disregarded in view of the single infusion schedule [32].

The most important conclusions will be provided by the large DIAMOND trial (Danish investigations of arrhythmia and mortality on dofetilide) which consists of two separate, placebo-controlled studies of dofetilide in 3000 patients with heart failure or recent myocardial infarction associated with left-ventricular dysfunction (ejection fraction <35%) [33].

2.1.5. Sematilide

Sematilide hydrochloride, an analogue of procainamide that also blocks IK_r , showed similar efficacy in suppressing the induction of sustained ventricular tachycardia in 41% of patients [34]. In 39 patients with congestive heart failure and a left-ventricular ejection fraction <40%, intravenous sematilide produced dose-dependent increases in corrected QT intervals (4–14%) without any adverse hemodynamic effects on left-ventricular function. However, four patients had QT prolongation >25% from baseline and one of them experienced torsades de pointes [35].

2.1.6. Ibutilide

The investigational antiarrhythmic drug ibutilide prolongs repolarization by blocking IK_r , but also inhibits the slow inward Na^+ current [6]. It has been shown to be effective in treating patients with recent onset atrial flutter or fibrillation. In the study by Ellenbogen et al., where 200 patients with such arrhythmias were randomized to receive a single infusion of placebo or ibutilide, the drug terminated the atrial arrhythmia within 60 min of infusion in 34% of patients (3% after placebo). Nevertheless, polymorphic ventricular tachycardia occurred in 3.6% of patients [36].

2.1.7. Tedisamil

Torsades de pointes has still not been reported with tedisamil, a newly developed bradycardic class III drug that blocks two voltage-dependent K^+ currents in cardiac cells: I_{to} and IK_r . Nevertheless, there are few data available about tedisamil in humans. Tedisamil reduced heart rate and increased the monophasic APD and left-ventricular effective refractory period in a frequency-dependent fashion, thus displaying reverse-use dependence [37]. Further clinical studies are required to assess the efficacy and safety of the drug in humans.

2.2. Proarrhythmia

The common mechanism by which K^+ channel blocking antiarrhythmic agents increase refractoriness, by prolonging repolarization, is also responsible for the well known side-effect of these drugs: 'torsades de pointes' and other increased QT interval-related ventricular arrhythmias [38].

These life-threatening side effects have been reported with class Ia, Ic and class III antiarrhythmic drugs, including newly developed agents such as dofetilide [28–31], almokalant [39], ambasilide [40], E 4031 [41], MK 499 [42], as well as more widely used compounds such as sotalol [22] and, to a lesser extent (0.7–1.3% patients only), amiodarone [10].

Hypokalemia in combination with diuretics or non-sedating antihistamines [44], may also promote proarrhythmic effects.

New insights into the mechanisms underlying antiarrhythmic drug related QT-prolongation and torsades de pointes have recently been suggested by

Antzelevitch and Sicouri [45]. Early after depolarization and triggered activity, which are usually associated with a prolonged repolarization, are also elicited by class Ia and class III antiarrhythmic drugs, hypokalemia and slow heart rates. These phenomena, which are more readily induced in the His-Purkinje network, may also arise from a subset of myocardial cells from the midventricular myocardium. The subpopulation of myocardial cells involved, now known as the M cells, play a key-role in after-depolarization and U-wave genesis by their ability to dramatically prolong APD with slowing stimulation rates. M cell action potential prolongation is enhanced by the blockade of the delayed rectifier currents (I_K) by antiarrhythmic drugs and, conversely, inhibited by K^+ channel agonists such as pinacidil [45].

Faced with these possibly lethal proarrhythmic effects, it has not yet been established whether the selective blockade of K^+ channels by class III agents offers any particular advantage over class I agents, which are also potent inhibitors of sodium channels [2]. Torsades de pointes occur in 1–8% of patients receiving quinidine [38], but may exceed 5% in those receiving sotalol [38]. Conversely, the incidence of proarrhythmia with amiodarone (0.7–1.3% of patients) is lower [2,10,43]. It has been argued that the somewhat greater K^+ channel selectivity of amiodarone compared with sotalol may contribute to a lower tendency for amiodarone to produce torsades de pointes [2,38,43]. However, these considerations remain speculative since amiodarone has also been reported not only to act on several K^+ channels (I_{K_r} , I_{K_1} , I_{to} , and $I_{K_{ATP}}$) but also to possess properties belonging to all four of the Vaughan Williams classes [3,4].

Thus, the relationship between channel selectivity of class III and class I drugs, antiarrhythmic efficacy and proarrhythmia, remains at best unclear.

2.3. Reverse-use dependence

Another controversial feature of selective K^+ blockers such as D-sotalol, E-4031 and dofetilide, is their ability to display 'reverse-use dependence' (reverse rate-dependence of action potential duration). This phenomenon, where the magnitude of the prolongation of repolarization decreases with increased stimulation rates, is explained by the greater

affinity of the drug for the channel in its closed state, thus limiting clinical efficacy in arrhythmias of high ventricular rate [5,46]. Dofetilide has been shown to display apparent reverse-use dependence in several studies. Ventricular pacing in eight patients showed that the drug increased monophasic APD with a greater prolongation at longer than at shorter cycle lengths [47]. Also, QT intervals measured over a wide range of preceding RR intervals by 24-h Holter electrocardiography after oral administration of I_{K_r} blockers showed that the reverse-use dependence was less prominent with D-sotalol than with dofetilide [48].

On the other hand, the conserved drug effect at faster rates (which is a prerequisite for treating tachyarrhythmias) was described in other clinical studies. No reverse-use dependence was observed in treating 50 patients with sustained monomorphic ventricular tachycardia inducible by programmed electrical stimulation receiving dofetilide [30]. During ventricular pacing in humans, the prolongation of APD resulting from dofetilide administration remained unchanged, whatever the stimulation cycle length [30,31].

Finally, at the channel level dofetilide has been shown to be an open channel blocker and thus displays a normal use dependence [31,49,50].

These discrepancies may be explained by several considerations. The apparent reverse-use dependence of selective I_{K_r} blockers may result from the increased contribution of I_{K_s} and I_{K_1} to the net repolarization current at faster heart rates [47]. Accordingly, the use-dependent behaviour of amiodarone may be explained by the concomitant block of I_{K_s} and I_{K_1} by the drug [48]. Indeed, at faster rates, I_{K_s} (on which dofetilide has no effect) is not only incompletely deactivated [31] but also enhanced in the presence of a high sympathetic activity [26]. Vanoli et al. showed that the monophasic APD resulting from administration of D-sotalol in anesthetized dogs is reduced by 40–60% by adrenergic stimulation [26].

A second explanation has been provided by Yuan and Roden who showed that I_{K_r} blockade by dofetilide is strikingly dependent on extracellular potassium: low extracellular K^+ increases the drug block (thus explaining how hypokalemia facilitates drug induced torsades de pointes) and, conversely,

high extracellular K^+ (as promoted by myocardial ischemia or tachycardia) decreases the block, resulting in an apparent reverse-use dependent block [49].

3. Potassium channel agonists

3.1. Vasodilator actions: myocardial ischemia and heart failure

Opening of K^+ channels results in outward currents which polarize the cell membrane. The ensuing hyperpolarization prevents intracellular calcium entry through voltage-gated calcium channels and, in turn, prevents contraction. This results in vascular vasodilatation, a decreased pre- and after-load and, therefore, at cardiac level, in decreased myocardial oxygen demand associated with vasodilatation of coronary arteries.

Most K^+ channel activators available today act by decreasing the affinity of $IK_{(ATP)}$ channels for ATP, thus increasing the probability of channel opening. Accordingly, their efficacy is enhanced during ischemia.

To date, several compounds have been developed, including nicorandil, cromakalim and the related bimakalim, aprikalim and pinacidil. Minoxidil, a conventional antihypertensive drug used for over a decade, and diazoxide, which is also well known for its antihypertensive and hyperglycemic effects, also act by opening $IK_{(ATP)}$ channels.

Nicorandil, a nicotinamide-derived vasodilator that acts as a K^+ agonist and also contains a nitrate moiety, reduces both cardiac afterload and preload via vascular smooth muscle cell relaxation.

The acute hemodynamic effects at rest of orally administered nicorandil in patients with heart failure include decreases in systemic systolic and diastolic blood pressure, pulmonary capillary wedge pressure, right atrial pressure pulmonary artery pressure, systemic and pulmonary resistances [51], and an increase in resting cardiac output [52].

Until recently, the mechanism of the hemodynamic effects of nicorandil in congestive heart failure was thought to be due to the nitrate behavior of the drug. Tsutamoto et al., using the plasma arteriovenous cyclic guanosine monophosphate (cGMP) difference

as an indicator of nitrate tolerance in patients with heart failure, showed that the absence of hemodynamic tolerance of nicorandil is likely to be due to its action as a K_{ATP}^+ channel opener and not to its nitrate activity [53].

Despite some controversy raised from a recent report [53], nicorandil has been proved to be useful in treating myocardial ischemia [54,55]. Orally administered nicorandil increased duration of exercise to onset of angina and, to a lesser extent, exercise capacity in patients with stable coronary heart disease [55]. Also, in 37 patients with stable angina pectoris, the compound has been shown to produce similar improvements in exercise duration as atenolol [56].

3.2. Preconditioning and cardioprotective effects

In addition to their potent vasodilator effects on coronary vasculature, it has been suggested that potassium channels openers exert a protective effect in the ischemic-hypoxic myocardium by opening myocyte K_{ATP} channels. As a result, they are believed to play a role in preconditioning, since their administration has also been shown both to reduce infarct size and to accelerate recovery from stunning in several experimental models [57,58] during which a short period of reversible ischemia (2–10 min) followed by an intervening reperfusion (<2 h) protects the myocardium from a second ischemic insult by preventing the decrease in contractile function ('myocardial stunning') observed during a sustained reperfusion period [59].

The preconditioning stimulus elicits a cascade of intracellular events leading to protein kinase C-dependent activation of K_{ATP}^+ channels resulting in an outward K^+ current that shortens the action potential and limits ATP depletion and Ca^{2+} influx. This in turn results in myocardial protection by slowing cell metabolism and decreasing ATP consumption [60].

Administration of K^+ channel agonists prior to ischemia results in a similar cardioprotective effect. In several models of transient reversible ischemia, K^+ channel openers such as nicorandil, pinacidil, aprikalim, bimakalim, cromakalim decreased myocardial stunning during sustained reperfusion, with segmental shortening at the end of reperfusion being improved from 20% to 75% of its pre-ischemic control value [59,63]. In a large number of animal

studies K_{ATP}^+ channel openers have also been proved to be able to slow the progression of an ischemic injury, thus resulting in a significant reduction in myocardial infarct size, provided the drug is administered before ischemia (review in [61]). These two cardioprotective effects result from K_{ATP}^+ channel activation because they are antagonized by glibenclamide, a selective K_{ATP}^+ channel blocker [57–61].

In a recent animal study, where changes in coronary blood flow (CBF) and APD were used as indexes of coronary vascular and myocyte K_{ATP} channel activity respectively, Yao et al. demonstrated that intracoronary administration of either low or high doses of the potassium channel opener bimakalim markedly reduced myocardial infarction size to a similar extent, whatever the dose administered [62]. This protective effect of bimakalim, which occurred without systemic hemodynamic and CBF effects, was parallel to its effect on shortening APD, suggesting that potassium channel openers may exert part of their cardioprotective properties through the activation of myocardial rather than coronary vascular K_{ATP} channels. However, the precise mechanism by which potassium channel openers reduce infarct size is not fully understood, since the lowest doses of intracoronary bimakalim used by Yao resulted in a similar infarct size reduction as was obtained by higher doses, but failed to shorten the APD.

Thus, any conclusions suggesting that the cardioprotective effects of potassium channel openers could be supported by APD shortening and, in turn, by the resulting decreased intracellular calcium overload only, remain uncertain. Finally, as emphasized by Hearse, a conceptual framework has been developed to explain, mostly with theoretical and experimental arguments, the cardioprotective effects of K_{ATP}^+ openers [61].

Nonetheless, there is a growing body of evidence that preconditioning can also be induced in humans. Studies performed during angioplasty procedures have shown that signs of myocardial ischemia are less severe during repeat balloon inflations than during the first inflation. In the study of Tomai et al., where the balloon catheter was successively inflated for 2 min, deflated for at least 5 min and inflated again for 2 min, ST-segment shifts during the second inflation were less than during the first inflation, but were similar when glibenclamide was administered

prior to the first inflation. Although some controversy has risen from the very short (2 min) preconditioning stimulus, these data suggest that angioplasty-related preconditioning is also mediated by K_{ATP}^+ channels [63]. Moreover, pretreatment with intracoronary adenosine prior to the first inflation resulted in similar ST-segment shifts during both inflations in the study by Kerensky et al. [64]. This also supports the hypothesis that adenosine is the endogenous mediator of myocardial protection in humans.

Finally, preconditioning during coronary artery bypass surgery has also been demonstrated. Two sequences of 3 min cross-clamping before 10 min global ischemia performed by Yellon et al., resulted in preservation of intracellular ATP levels [65].

Thus, the new concepts of myocardial protection and preconditioning play a role in several clinical settings.

3.3. Arrhythmogenesis

Despite their potential benefits in ischemic heart disease K_{ATP}^+ openers, by inducing myocardial K^+ efflux and shortening the action potential, may also be deleterious by promoting arrhythmias [66–68]. Although they prevent or reduce early and delayed after-depolarizations (by counteracting the responsible inward current) and abnormal automaticity (which arises at reduced resting potential and represents the substrate of the arrhythmias occurring in the acute phase of myocardial infarction), they enhance re-entry (due to the shortened action potential) [66]. Moreover, as re-entry plays a key-role in myocardial ischemia related ventricular arrhythmias, K_{ATP}^+ agonists may adversely affect the outcome of patients with coronary artery disease. Finally, the occurrence of heterogeneity in slowed conduction, decreased refractoriness and increased extracellular K^+ levels may worsen these effects [66]. Conversely, the arrhythmogenic effects of K_{ATP}^+ openers may be attenuated by their cardioprotective effects which may delay and/or postpone the consequences of ischemia [61,66]. Also, the clinical relevance of this controversy remains uncertain. The small size studies which have been performed have not documented adverse proarrhythmic effects. Larger scale prospective trials are required.

4. Impairment of potassium currents in disease

4.1. Heart failure

Several K^+ currents are impaired in heart failure, resulting in changes in both resting potential and APD.

Electrophysiological studies performed in explanted failing hearts have demonstrated a decreased resting membrane potential recorded from isolated atrial myocytes. This diastolic depolarization has been shown to be caused by the impairment of both IK_1 and $IK_{(ACh)}$ currents, thus decreasing the whole K^+ conductance. Two different mechanisms were suggested by Koumi et al., including a diminished IK_1 and $IK_{(ACh)}$ channel density in atrial cells associated with a decreased sensitivity of $IK_{(ACh)}$ channels to Gi-mediated ACh-stimulation of M_2 -receptors [69]. More recently, an increased I_f current has also been described in human ventricular myocytes from three patients with heart failure [70]. Although I_f density in ventricular myocytes of hypertrophied and failing hearts from animals has been correlated with the severity of heart failure, the clinical relevance of these changes in humans remains unknown [70].

Prolongation of the APD is the second major electrophysiological feature of heart failure [71]. It has been shown to result from reduction in the transient outward current I_{to} , which has been documented in failing ventricular myocytes both in experimental models and in humans [75]. This abnormality, which is more pronounced in middle ventricular myocytes (M cells) may also result in enhanced spatial inhomogeneities of repolarization which has been regarded as one of the main underlying mechanisms of sudden death in heart failure, by promoting after depolarization and triggered activity.

The arrhythmogenic consequences of action potential prolongation, including increased duration, spatial and temporal dispersion of QT have extensively been reviewed by Tomaselli et al. [71].

4.2. Long QT syndrome

Mutations in HERG, the gene that encodes the major subunit of the cardiac IK_r channel, cause chromosome 7-linked (7q35) congenital long QT (LQT2) syndrome, that is inherited as an autosomal

dominant trait and is associated with torsades de pointes and sudden death. Several missense mutations, including one in the pore region (G628S, the most severe), of HERG have been identified and cause a loss of HERG [72,73].

In addition, mutations causing the long QT-syndrome have been identified in two other genes: $KVLQT_1$ (11p15.5), a newly cloned gene encoding for a still not unidentified K^+ channel ($KVLQT_1$ mutations account for more than 50% of congenital LQTS) and $SCN5A$, the gene encoding for the cardiac sodium channel α -subunit (LQT₃ syndrome) [73].

A mechanistic link between inherited and acquired LQT2 syndrome has been established since hypokalemia also results in a decreased HERG current and, in turn, in prolonged repolarization. Also, it has recently been shown that class III antiarrhythmic drugs block the HERG channel, thus confirming the link between acquired (drug-induced) and congenital long QT syndrome [49,74].

5. Side-effects of non-cardiac drugs

Cardiac arrhythmias have been reported in patients who ingested overdoses of non-sedating antihistamines. These proarrhythmic effects were also seen in patients treated with terfenadine or astemizole, who had liver failure or co-treatment with other drugs competing for the same hepatic cytochrome *P*-450 system, such as ketoconazole and erythromycin [75].

The underlying mechanism of this rare but potentially life-threatening proarrhythmic effect of non-sedating antihistamines has recently been shown to be potassium channel blockade [44]. In contrast to class III antiarrhythmic drugs that act predominantly via inhibition of the delayed outward K^+ current, IK_r , terfenadine and astemizole cause a voltage-dependent blockade of the inward rectifier, IK_1 , and to a lesser extent, of the transient outward I_{to} . Conversely, terfenadine has only a small effect on IK_r . As mentioned by Berul and Morad, blockade of IK_1 and I_{to} results in prolongation of the APD and QT prolongation. These effects occur only at high drug concentrations and, therefore, are 'consistent with the scarcity of clinical reports of arrhythmia and sudden

death, despite the widespread use of these agents' [44]. Also, they may arise under conditions when repolarization is already compromised such as the congenital long QT syndrome. More recently, terfenadine has been shown to block HERG, whereas terfenadine carboxylate, its major metabolite does not. This may explain why ketoconazole may promote arrhythmias in patients treated with terfenadine [76].

The clearance of cisapride, a peristaltic drug, is also decreased by ketoconazole. Two cases of torsades de pointes have been reported with the combined therapy [77].

The adverse effects of erythromycin, another drug which may prolong APD and promote early after-depolarizations and torsades de pointes has been recently recognized as the IK_r channel of M cells [78,79].

Finally, torsades de pointes may be promoted by several other drugs, especially antimicrobial agents such as quinine, chloroquine, halofantrine, pentamidine, spiramycin, trimethoprim–sulfamethoxazole, but the precise mechanisms by which the arrhythmias are induced at channel level require further investigation.

6. Conclusion

The role played by cardiac K^+ currents and channels in pharmacological interventions in heart disease has increasingly been recognized.

IK_r blockers have antiarrhythmic properties but their use is limited by a substantial risk of proarrhythmic effects. New insights into the electrophysiological mechanisms by which life-threatening ventricular arrhythmias compromise survival of patients with heart failure and/or antiarrhythmic drug therapy suggest that these adverse effects result from the impairment of one or several K^+ currents. Accurate identification of the K^+ channels involved could help to define targeted therapeutic approaches.

In addition, the new concepts of the role of K_{ATP}^+ channels in myocardial ischemia and cardioprotection resulting from preconditioning are also expected to generate a broad spectrum of clinical applications.

Acknowledgments

We are indebted to Dr. John Evans for careful manuscript revision and to Pascale Granger for secretarial assistance.

References

- [1] Vaughan Williams EM. A classification of antiarrhythmic actions reassessed after a decade of new drugs. *J Clin Pharmacol* 1984;24:129–47.
- [2] Colatsky TJ, Follmer CH, Starmer CF. Channel specificity in antiarrhythmic drug action: mechanism of potassium channel block and its role in suppressing and aggravating cardiac arrhythmias. *Circulation* 1990;92:2235–42.
- [3] Singh BN. Arrhythmia control by prolonging repolarization: the concept and its potential therapeutic impact. *Eur Heart J* 1993;14(suppl H):14–23.
- [4] The Sicilian Gambit. Task Force of the Working Group on arrhythmias of the European Society of Cardiology. A new approach to the classification of antiarrhythmic drugs based on their actions on arrhythmogenic mechanisms. *Circulation* 1991, 84: 1831–51.
- [5] Katristis D, Camm AJ. New class III antiarrhythmic drugs. *Eur Heart J* 1993;14(suppl H):93–9.
- [6] Yang T, Snyders DJ, Roden DM. Ibutilide, a methanesulfonamide antiarrhythmic is a potent blocker of the rapidly activating delayed rectifier K^+ current (IK_r) in AT-1 cells. *Circulation* 1995;91:1799–806.
- [7] Mori K, Hara Y, Saito T, Masuda Y, Nakaya H. Anticholinergic effects of class III antiarrhythmic drugs in guinea pig atrial cells. *Circulation* 1995;91:2834–43.
- [8] The Cardiac Arrhythmia Suppression Trial (CAST) Investigators preliminary report: effect of encainide and flecainide on mortality in a randomized trial of arrhythmia suppression after myocardial infarction. *N Engl J Med* 1989, 321: 406–412.
- [9] Mason JW. Amiodarone. *N Engl J Med* 1987;316:455–65.
- [10] Kowey PR, Marinchak RA, Rials SJ, Filart R. Intravenous amiodarone. *J Am Coll Cardiol* 1997;29:1190–8.
- [11] Levine JM, Massumi A, Scheinman MS et al. Intravenous amiodarone for recurrent sustained hypotensive ventricular tachyarrhythmias. *J Am Coll Cardiol* 1996;27:67–75.
- [12] The CASCADE investigators randomized antiarrhythmic drug therapy in survivors of cardiac arrest (CASCADE study). *Am J Cardiol* 1993, 72: 280–287.
- [13] Burkart F, Pfisterer M, Kiowski W, Follath F, Burckhardt D. Effects of antiarrhythmic on mortality in survivors of myocardial infarction with asymptomatic complex ventricular arrhythmias: Basel Antiarrhythmic Study of Infarct Survival (BASIS). *J Am Coll Cardiol* 1990;16:1711–8.
- [14] Ceremuzynski F, Kleczar E, Kreminska-Pakula M et al. Effects of amiodarone on mortality after myocardial infarction: a double blind, placebo-controlled, pilot study. *J Am Coll Cardiol* 1992;20:1051–62.
- [15] Cairns JA, Connolly SJ, Roberts R, Gent M. Randomised trial of outcome after myocardial infarction in patients with frequent or repetitive ventricular premature depolarizations: CAMIAT. *Lancet* 1997;349:675–82.

- [16] Julian DG, Camm AJ, Frangin G, Janse MJ, Munoz A, Schwartz PJ, Simon P. Randomised trial of effect of amiodarone on mortality in patients with left-ventricular dysfunction after recent myocardial infarction: EMIAT. *Lancet* 1997;349:667–74.
- [17] Doval HC, Nul DR, Grancelli HO, Perrone SV, Bortman GR, Curiel L. Randomized trial of low-dose amiodarone in patients with severe congestive heart failure. *Lancet* 1994;344:493–8.
- [18] Singh SN, Fletcher RD, GrossFisher S et al. Amiodarone in patients with congestive heart failure and asymptomatic ventricular arrhythmias. *N Engl J Med* 1995;333:77–82.
- [19] Nul DR, Doval HC, Grancelli HO et al. Heart rate is a marker of amiodarone mortality reduction in severe heart failure. *J Am Coll Cardiol* 1997;29:1199–205.
- [20] Pfammatter JP, Paul T, Lehmann C, Kallfelz HC. Efficacy and proarrhythmia of oral sotalol in pediatric patients. *J Am Coll Cardiol* 1995;26:1002–7.
- [21] MacNeil DJ, Davies RO, Deitchman D. Clinical safety profile of sotalol in the treatment of arrhythmias. *Am J Cardiol* 1993;72:44A–50A.
- [22] Barlow JB, Obel IWP, Pocock WA, McKibbin JK. Sotalol: a unique class III antiarrhythmic agent. *Am J Cardiol* 1994;73:932–3.
- [23] Mason JW. for the Electrophysiologic study versus electrocardiographic monitoring (ESVEM) investigators. A comparison of seven antiarrhythmic drugs in patients with ventricular tachyarrhythmias. *N Engl J Med* 1993;329:445–51.
- [24] Kühlkamp V, Mermi J, Mewis C, Braun U, Seipel L. Long-term efficacy of D,L-sotalol in patients with sustained ventricular tachycardia refractory to class I. antiarrhythmic drugs. *Eur Heart J* 1995;16:1625–31.
- [25] Sedgwick ML, Dalrymple I, Rae AP, Cobbe SM. Effects of the new class III dofetilide on the atrial and ventricular intracardiac monophasic action potential in patients with angina pectoris. *Eur Heart J* 1995;16:1641–6.
- [26] Vanoli E, Priori S, Nakagawa H, Hirao K, Napolitano C, Diehl L, Lazzara R, Schwartz PJ. Sympathetic activation, ventricular repolarization and IK₁ blockade: implications for the antifibrillatory efficacy of potassium channel blocking agents. *J Am Coll Cardiol* 1995;25:1609–14.
- [27] Waldo AL, Camm AJ, deRuyter H et al. Survival with oral D-sotalol in patients with left ventricular dysfunction after myocardial infarction: rationale, design and methods (the SWORD trial). *Am J Cardiol* 1995;75:1023–7.
- [28] Crijns HJ, WanGelder IC, Kingma JH, Dunsenman PH, Gosselink ATM, Lie KI. A trial flutter can be terminated by a class III antiarrhythmic drug but not by class Ic drug. *Eur Heart J* 1994;15:1403–8.
- [29] Falk RH, Pollak A, Singh SN, Friedrich T. Intravenous dofetilide, a class III antiarrhythmic agent, for the termination of sustained atrial fibrillation or flutter. *J Am Coll Cardiol* 1997;29:385–90.
- [30] Bianconi L, Dinelli M, Pappalardo A, Richiardi E, Castro A, Alboni P, Santini M, Dalrymple HW, Radula D. Comparison of intravenously-administered dofetilide-versus amiodarone in the acute termination of atrial fibrillation and flutter. *Circulation* 1995;92(Suppl I):I-774.
- [31] Yuan S, Wohlfart B, Rasmussen HS, Olsson S, Blomstrom-Lundqvist C. Effect of dofetilide on cardiac repolarization in patients with ventricular tachycardia. *Eur Heart J* 1994;15:514–22.
- [32] Bashir Y, Thomsen PE, Kinema JH et al. Electrophysiologic profile and efficacy of intravenous dofetilide, a new class III antiarrhythmic drug, in patients with sustained monomorphic ventricular tachycardia. *Am J Cardiol* 1995;76:1040–4.
- [33] Moller M. Diamond antiarrhythmic trials. *Lancet* 1996;348:1597–8.
- [34] Sager PT, Nedemane K, Antimisariar M et al. Antiarrhythmic effects of selective prolongation of refractoriness. Electrophysiologic actions of sotalol HCl in humans. *Circulation* 1993;88:1072–82.
- [35] Stambler BS, Gottlieb SS, Singh BN, Ramanathan KB, Ogilby JD, Ellenbogen KE. Hemodynamic effects of intravenous sotalol in patients with congestive heart failure: a class III antiarrhythmic agent without cardiodepressant effects. *J Am Coll Cardiol* 1995;26:1679–84.
- [36] Ellenbogen KA, Stambler BS, Wood MA et al. Efficacy of intravenous ibutilide for rapid termination of atrial fibrillation and atrial flutter. *J Am Coll Cardiol* 1996;28:130–6.
- [37] Bargheer K, Bode F, Klein HU, Trappe HJ, Franz MR, Lichtlen PR. Prolongation of monophasic action potential duration and the refractory period in the human heart by tedisamil, a new potassium-blocking agent. *Eur Heart J* 1994;15:1409–14.
- [38] Roden DM. Risks and benefits of antiarrhythmic therapy. *N Engl J Med* 1994;331:785–91.
- [39] Wiesfeld ACP, Crijns HJG, Bergstrand RH, Almgren O, Hillege BE, Lie KI. Torsades de pointes with Almokalant a new class III antiarrhythmic drug. *Am Heart J* 1993;126:1008–11.
- [40] Napolitano C, Diehl L, Schwartz PL, Priori SG. Modulation of the electrophysiologic effects of amasilide induced by β -adrenergic stimulation in isolated ventricular myocytes. *J Am Coll Cardiol* 1994;23:444A.
- [41] Isomoto S, Shimizu A, Konoe A et al. Electrophysiologic effects of E-4031, a new class III antiarrhythmic agent, in patients with supraventricular tachyarrhythmias. *Am J Cardiol* 1993;71:1464–7.
- [42] Singh BN, Ellenbogen KA, Zoble RG et al. Electrocardiographic effects of oral MK-499, a new class III antiarrhythmic agent in patients with coronary disease. *J Am Coll Cardiol* 1994;23:92A.
- [43] Hohnloser SH, Klingenhoben T, Singh BN. Amiodarone — associated proarrhythmic effect — A review with special reference to torsade de pointes tachycardia. *Ann Intern Med* 1994;121:529–35.
- [44] Berul CI, Morad M. Regulation of potassium channels by non-sedating antihistamines. *Circulation* 1995;91:2220–5.
- [45] Antzelevitch C, Sicouri S. Clinical relevance in the generation of U waves, triggered activity and torsades de pointes. *J Am Coll Cardiol* 1994;23:259–77.
- [46] Hondeghem LM, Snyders DJ. Class III antiarrhythmic agents have a lot of potential but a long way to go: reduced effectiveness and dangers of reverse-use dependence. *Circulation* 1990;81:686–90.
- [47] Sager PT. Frequency-dependent electrophysiologic effects of dofetilide in humans. *Circulation* 1995;92(Suppl I):I-774.
- [48] Okada Y, Ogawa S, Sadanaga T, Mitamura H. Assessment of reserve-use dependent blocking actions of class III antiarrhythmic drugs by 24-hour holter electrocardiography. *J Am Coll Cardiol* 1996;27:84–9.
- [49] Yang T, Roden DM. Extracellular potassium modulation of drug block of I_{Kr}. *Circulation* 1996;93:407–11.
- [50] Spector PS, Curran ME, Keating MT, Sanguinetti MC. Class III antiarrhythmic drugs block HERG, a human cardiac delayed rectifier K⁺ channel. *Circ Res* 1996;78:499–503.
- [51] Tice FD, Binkley PF, Cody RJ, Moeschberger ML, Mohrland JS, Wolf DL, Leier CV. Hemodynamic effect of oral nicorandil in congestive heart failure. *Am J Cardiol* 1990;65:1361–7.
- [52] Galie N, Varani E, Maiello L, Boriani G, Boschi S, Binetti G, Magnani B. Usefulness of nicorandil in congestive heart failure. *Am J Cardiol* 1990;65:343–8.

- [53] Tsutamoto T, Kinoshita M, Hisanaga T, Maeda Y, Maeda K, Wada A, Fukai D, Yoshida S. Comparison of hemodynamic effects and plasma cyclic guanosin monophosphate of nicorandil and nitroglycerin in patients with congestive heart failure. *Am J Cardiol* 1995;75:1162–5.
- [54] Thadani U, Strauss W, Glasser SP, Frishman W, Burger AJ, Locker J, Mohrland JS. Evaluation of antianginal and antiischemic efficacy of nicorandil: results of a multicenter study. *J Am Coll Cardiol* 1994;23:267A.
- [55] Camm JA, Maltz MB. A controlled single-dose study of the efficacy, dose response and duration of action of nicorandil in angina pectoris. *Am J Cardiol* 1989;63:61J–5J.
- [56] Hugues LO, Rose EL, Lahiri A, Raftery EB. Comparison of nicorandil and atenolol in stable angina pectoris. *Am J Cardiol* 1990;66:679–82.
- [57] Auchampach JA, Maruyana M, Caverio I, Gross GJ. Pharmacological evidence for a role of ATP dependent potassium channels in myocardial stunning. *Circulation* 1992;86:311–9.
- [58] Yao Z, Caverio I, Gross GJ. Activation of cardiac K_{ATP} channels: an endogenous protective mechanism during repetitive ischemia. *Am J Physiol* 1993;264:H495–504.
- [59] Verdouw PD, Gho BCG, Dunker DJ. Ischaemic preconditioning: is it clinically relevant?. *Eur Heart J* 1995;16:1169–76.
- [60] Speechly-Dick ME, Grover GJ, Yellon DM. Does ischemic preconditioning in the human involve protein kinase C and the ATP-dependent K^+ channel?. *Circ Res* 1995;77:1030–5.
- [61] Hearse DJ. Activation of ATP-sensitive potassium channels: a novel pharmacological approach to myocardial protection?. *Cardiovasc Res* 1995;30:1–17.
- [62] Yao Z, Garrett J, Gross GJ. Effects of the K_{ATP} channel opener Bimakalim on coronary blood flow, monophasic action potential duration and infarct size in dogs. *Circulation* 1994;89:1769–75.
- [63] Tomai F, Crea F, Gaspardone A, Versaci FDE, Paulis R, Penta DE, Peppo A, Chiariello L, Gioffre PA. Ischemic preconditioning during angioplasty is prevented by glibenclamide, a selective ATP-sensitive K^+ channel blocker. *Circulation* 1994;90:700–5.
- [64] Kerensky RA, Kutcher MA, Braden GA, Applegate RJ, Solis GA, Little WC. The effect of intracoronary adenosine on preconditioning during PTCA. *Circulation* 1993;88:1–588.
- [65] Yellon DM, Alkhulaifi AM, Pugsley WB. Preconditioning the human myocardium. *Lancet* 1993;342:276–7.
- [66] Wilde AM, Janse MJ. Electrophysiological effects of ATP sensitive potassium channel modulation: implications for arrhythmogenesis. *Cardiovasc Res* 1994;28:16–24.
- [67] Siegel P. Blockers of ATP sensitive potassium current are of potential benefit in ischaemic heart disease. *Cardiovasc Res* 1994;28:31–2.
- [68] Caverio I, Premmereur J. ATP sensitive potassium channel openers are of potential benefit in ischaemic heart disease. *Cardiovasc Res* 1994;28:32–3.
- [69] Koumi SI, Arentzen CE, Backer CL, Wasserstrom A. Alterations in muscarinic K^+ channel response to acetylcholine and to G protein-mediated activation in atrial myocytes isolated from failing human hearts. *Circulation* 1994;90:2213–24.
- [70] Cerbai E, Pino R, Porciatti F et al. Characterization of the hyperpolarization-activated current, I_p , in ventricular myocytes from human failing hearts. *Circulation* 1997;95:568–71.
- [71] Tomaselli GF, Beuckelmann DJ, Calgins HG, Berger RD, Kessler PD, Lawrence JH, Kass D, Feldman AM, Marban E. Sudden cardiac death in heart failure; The role of abnormal repolarization. *Circulation* 1994;90:2534–9.
- [72] Benson DW, MacRae CA, Vesely MR et al. Missense mutation in the pore region of HERG causes familial long QT syndrome. *Circulation* 1996;93:1791–5.
- [73] Roden DM, Lazzara R, Rosen M, Schwartz PJ, Towbin J, Vincent M. Multiple mechanisms in the long QT syndrome. *Circulation* 1996;94:1996–2012.
- [74] Kiehn J, Lacerda AE, Wible B, Brown AM. Molecular physiology and pharmacology of HERG. *Circulation* 1996;94:2572–9.
- [75] Woosley RL, Chen Y, Freiman JP, Gillis RA. Mechanisms of the cardiotoxic actions of terfenadine. *J Am Med Assoc* 1993;269:1352–6.
- [76] Roy ML, Dumaine R, Brown AM. HERG, a primary human ventricular target of the non-sedating antihistamine terfenadine. *Circulation* 1996;94:817–23.
- [77] Wolfe SM, Ahmad SR. Cisapride and torsades de pointes. *Lancet* 1995;345:508.
- [78] Daleau P, Turgeon J. Prolongation of QT interval induced by erythromycin may be explained by an inhibition of the rapid component of the delayed rectifier potassium IK_r . *Circulation* 1994;90:1–248.
- [79] Antzelevitch C, Sun ZQ, Zhang ZQ, Yan GX. Cellular and ionic mechanisms underlying erythromycin-induced long QT intervals and torsade de pointes. *J Am Coll Cardiol* 1996;28:1836–48.

An ATP-sensitive potassium channel activator reduces infarct volume in focal cerebral ischemia in rats

HITONORI TAKABA, TETSUHIKO NAGAO, HIROSHI YAO,
TAKANARI KITAZONO, SETSURO IBAYASHI, AND MASATOSHI FUJISHIMA
Second Department of Internal Medicine, Faculty of Medicine,
Kyushu University, Fukuoka 812-82, Japan

Takaba, Hitonori, Tetsuhiko Nagao, Hiroshi Yao, Takanari Kitazono, Setsuro Ibayashi, and Masatoshi Fujishima. An ATP-sensitive potassium channel activator reduces infarct volume in focal cerebral ischemia in rats. *Am. J. Physiol.* 273 (Regulatory Integrative Comp. Physiol. 42): R583-R586, 1997.—ATP-sensitive potassium channels are activated under hypoxic or ischemic conditions. The effects of ATP-sensitive potassium channel activators on cerebrovasculature and cerebral blood flow (CBF) are not well understood. We examined the effect of the ATP-sensitive potassium channel activator Y-26763 on focal cerebral ischemia in rats. In 24 spontaneously hypertensive rats, either Y-26763 (24 $\mu\text{g/kg}$) or vehicle was given by intracarotid infusion over 60 min, starting 30 min before photochemically induced thrombotic occlusion of the middle cerebral artery. CBF was measured by laser-Doppler flowmetry in the peri-ischemic penumbral cortex. Although Y-26763 lowered systemic blood pressure by 13 mmHg, the infarct volume assessed 3 days after the occlusion was significantly smaller in the Y-26763-treated group ($n = 12$, $71.2 \pm 22.0 \text{ mm}^3$) than in the control group ($n = 12$, $94.7 \pm 20.4 \text{ mm}^3$, $P = 0.013$). Y-26763 did not affect CBF before or after occlusion compared with CBF values of the control group. The results are consistent with the view that the activation of the ATP-sensitive potassium channel is neuroprotective in focal cerebral ischemia.

cerebral blood flow; photothrombosis

SYNTHETIC ACTIVATORS of ATP-sensitive potassium (K_{ATP}) channels hyperpolarize the membrane, block voltage-dependent Ca^{2+} influx, and thereby cause relaxation of vascular muscle (7, 22). Previous studies from our own (14, 15, 20) and other laboratories (9) confirmed that K_{ATP} channels are present and functional in cerebral blood vessels. Because K_{ATP} channels are activated under hypoxic or ischemic conditions (6, 17), activators of K_{ATP} channels may increase cerebral blood flow (CBF), particularly in the ischemic and/or peri-ischemic region.

K_{ATP} channels are also present in neurons (2, 11–13). Thus K_{ATP} channels may protect neurons against ischemia through their membrane-stabilizing action (inhibition of excessive neuronal excitation through membrane hyperpolarization) rather than by their circulatory improvements. Indeed, some activators of K_{ATP} channels exert beneficial effects in global ischemia when administered into cerebral ventricles (8). However, it remains to be elucidated whether activators of K_{ATP} channels are capable of reducing neuronal damages in focal cerebral ischemia, which is clinically more relevant to human brain infarction. The purpose of this study was to examine whether the intracarotid infusion of the K_{ATP} channel activator Y-26763 (16) reduces

infarct volume produced by photochemically induced thrombotic middle cerebral artery (MCA) occlusion in spontaneously hypertensive rats (SHR).

METHODS

Twenty-four male SHR (4–5 mo old, 300–375 g) were anesthetized with halothane (4% for induction, 1.5% during the surgical preparation with a face mask, 0.75% after intubation, and 0.5% for maintenance) in a mixture of 70% nitrous oxide and 30% oxygen. The right femoral artery and vein were cannulated with PE-50 tubing. Another catheter was inserted into the right common carotid artery for infusion of Y-26763 or vehicle. The proximal right common carotid artery was then ligated. The rats were endotracheally intubated with PE-240 tubing. The rats were mechanically ventilated after immobilization with pancronium bromide (an initial dose of 0.3 mg iv followed by 0.1 mg every 30 min). Arterial blood gases were monitored and maintained within normal limits throughout the experiments. Rectal and head temperatures were maintained at 37.5 and 36.0–36.5°C, respectively, by means of a heating pad and a warming lamp. Rats were placed on a stereotaxic head holder in the sphinx position and a 2-cm incision was made vertically midway between the right orbit and the right external auditory canal. The temporalis muscle was separated and retracted, and a burr hole (3 mm in diameter) was made 1 mm rostral to the anterior junction of the zygoma and squamosal bones under an operating microscope, revealing the distal segment of the MCA above the rhinal fissure.

After the MCA was exposed, thrombotic occlusion of the distal MCA was produced photochemically according to the method of Yao and colleagues (21, 23). Briefly, a krypton laser operating at 568 nm (Innova 301, Coherent) was used to irradiate the distal MCA at a power of 20 mW. The laser beam was focused with a cylindrical lens and positioned with a mirror on the distal MCA. The corresponding energy at the focal plane was $\sim 64 \text{ mW/mm}^2$. The photosensitizing dye rose bengal (15 mg/ml in 0.9% saline; Wako Pure Chemical Industries) was administered intravenously to a body dose of 20 mg/kg over 90 s starting simultaneously with 4 min of laser irradiation.

Regional CBF was measured by laser-Doppler flowmetry (5) as previously described (20). A laser-Doppler probe was placed close above the dura mater 3 mm posterior and 3 mm lateral to the bregma. This probe was connected to a perfusion monitor (ALF 21D, Advance). Because visible light interferes with laser-Doppler flowmetry, the heating lamp was temporarily turned off during measurements of CBF. Changes in CBF were expressed as a percentage of the average of two baseline values.

Intracarotid infusion of Y-26763 ($0.1\text{--}1.6 \mu\text{g}\cdot\text{kg}^{-1}\cdot\text{min}^{-1}$ for 1 min) transiently increased CBF without affecting systemic blood pressure (20). In contrast, intravenous infusion of Y-26763 ($0.6 \mu\text{g}\cdot\text{kg}^{-1}\cdot\text{min}^{-1}$ for 60 min) effectively lowered arterial pressure (unpublished observation). On the basis of these previous data, we infused Y-26763 ($0.4 \mu\text{g}\cdot\text{kg}^{-1}\cdot\text{min}^{-1}$

for 60 min) into the common carotid artery in this study, expecting this compound to reach the brain as much as possible without changing systemic blood pressure considerably. Y-26763 (total dose 24 $\mu\text{g/kg}$), dissolved in dimethyl sulfoxide (DMSO) or the same volume of DMSO as a vehicle, was injected into the right common carotid artery using a constant infusion pump (EP-60, Eicom) over 60 min starting 30 min before the distal MCA occlusion.

Two hours after distal MCA occlusion, the head wound was closed and the catheters were removed. The rats were carefully weaned from the respirator and returned to the home cage after regaining the ability to breathe independently.

After 3 days, the rats were decapitated under amobarbital anesthesia (100 mg/kg ip), and the brains were rapidly removed. The entire brains were cooled in ice-cold saline for 10 min and cut into 2-mm-thick coronal sections in a cutting block, and the brain slices were then immersed in 2% 2,3,5-triphenyltetrazolium chloride (Wako Pure Chemical Industries) at 37°C for 30 min in the dark (3). The posterior surface of each section was photographed, and the infarct area, indicated by the lack of staining, was calculated by means of National Institutes of Health Image software (version 1.56). The infarct volume of each rat was calculated as the product of the infarct area times the 2-mm thickness of each section.

All values are expressed as means \pm SD. Physiological variables and infarct volumes were compared between the control and the Y-26763-treated groups by means of an unpaired *t*-test. Mann-Whitney *U* test was used for comparisons of CBF. *P* values less than 0.05 were considered to be statistically significant.

RESULTS

Mean arterial blood pressure in the Y-26763-treated group was significantly lower than that in the control group before and after distal MCA occlusion. No significant differences were observed in arterial blood gases or hematocrits between the two groups throughout the experiment (Table 1). CBF was measured in five rats of

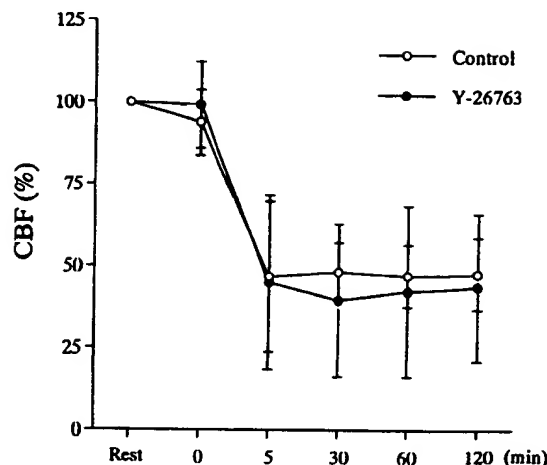


Fig. 1. Changes in cerebral blood flow (CBF) in control ($n = 5$) and Y-26763-treated ($n = 5$) groups. Bars represent means \pm SD.

each group. Y-26763 did not affect CBF before and after the occlusion (Fig. 1).

The area of infarction that was limited to the neocortex with a sharply margined infarct rim was reduced in most sections in the Y-26763-treated group compared with the control group (Fig. 2, A and B). However, the difference did not reach statistical significance. The infarct volume was significantly smaller in the Y-26763-treated group ($71.2 \pm 22.0 \text{ mm}^3$) than in the control group ($94.7 \pm 20.4 \text{ mm}^3$, $P = 0.013$, Fig. 3).

DISCUSSION

The present study revealed that the intracarotid infusion of the K_{ATP} channel activator Y-26763 reduced infarct volume when given 30 min before photochemically induced thrombotic MCA occlusion in rats. Thus the activation of the K_{ATP} channel appears to be neuro-

Table 1. Physiological variables

	Rest	Distal MCA Occlusion			
		0 min	5 min	30 min	120 min
Control ($n = 12$)					
MABP, mmHg	164 \pm 10	162 \pm 10	182 \pm 14	175 \pm 14	161 \pm 14
PCO ₂ , mmHg	36 \pm 2	36 \pm 3			36 \pm 4
PO ₂ , mmHg	132 \pm 24	132 \pm 23			133 \pm 27
pH	7.42 \pm 0.03	7.41 \pm 0.03			7.41 \pm 0.03
Hematocrit, %	42 \pm 3	41 \pm 3			42 \pm 2
Glucose, mg/dl	109 \pm 20	112 \pm 12			121 \pm 18
Temperature, °C					
Rectum	37.2 \pm 0.1	37.1 \pm 0.1	37.1 \pm 0.2	37.1 \pm 0.1	37.1 \pm 0.1
Head	36.2 \pm 0.5	36.2 \pm 0.5	36.2 \pm 0.5	36.2 \pm 0.5	36.4 \pm 0.5
Y-26763 ($n = 12$)					
MABP, mmHg	163 \pm 9	149 \pm 9*	174 \pm 16	154 \pm 20*	144 \pm 13*
PCO ₂ , mmHg	37 \pm 4	37 \pm 5			36 \pm 2
PO ₂ , mmHg	131 \pm 27	133 \pm 26			127 \pm 18
pH	7.40 \pm 0.03	7.39 \pm 0.04			7.40 \pm 0.02
Hematocrit, %	42 \pm 3	41 \pm 3			41 \pm 2
Glucose, mg/dl	111 \pm 16	104 \pm 18			112 \pm 13
Temperature, °C					
Rectum	37.2 \pm 0.1	37.1 \pm 0.1	37.2 \pm 0.1	37.1 \pm 0.1	37.1 \pm 0.1
Head	36.3 \pm 0.4	36.3 \pm 0.4	36.2 \pm 0.4	36.2 \pm 0.4	36.2 \pm 0.4

Values are means \pm SD ($n = 12$). * $P < 0.01$ vs. control by unpaired *t*-test. MCA, middle cerebral artery; MABP, mean arterial blood pressure.

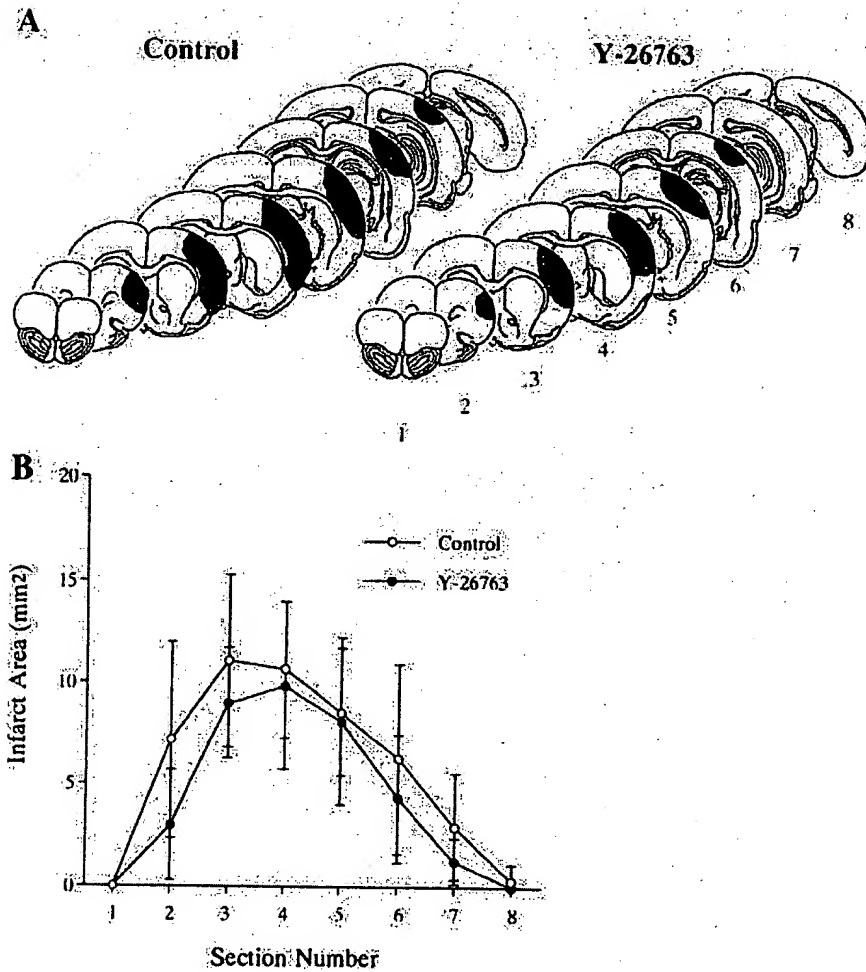


Fig. 2. A: schematic representation of infarct areas in each coronal section in a control and a Y-26763-treated rat. Infarct was limited to the neocortex with a sharply marginated infarct rim (shaded areas). B: infarct areas (shaded areas) in each coronal section in control ($n = 12$) and the Y-26763-treated ($n = 12$) groups. Bars represent means \pm SD.

protective in focal cerebral ischemia. Cerebrovascular response to a potassium channel opener is diminished in hypertensive rats, as shown in our previous study (20). Thus it may be ideal to use normotensive Wistar-Kyoto (WKY) rats. However, several previous studies showed that the infarct size induced by occlusion of the MCA in WKY rats is small and of great variation compared with that in SHR. Such characteristics of

WKY rats would not be suitable for the evaluation of the efficacy of pharmacological substances in cerebral ischemia. Hence, we used SHR rather than WKY rats in the present study.

Y-26763 did not change CBF in the peri-ischemic penumbral region before or during ischemia. Thus the beneficial effect of Y-26763 is thought to be mediated by its direct action on neurons rather than by its vasodilatory effect, as far as the present study is concerned. However, systemic blood pressure in the Y-26763-treated group was lower than that in the control group before and after distal MCA occlusion. In the peri-ischemic penumbral region, CBF changes depending on perfusion pressure as a result of autoregulatory failure. Hence, Y-26763 may be capable of improving blood supply to peri-ischemic tissues under a fixed pressure level. In support of this, we observed that Y-26763 preserved CBF during hemorrhagic hypotension (unpublished observation). Thus we cannot rule out the possibility that Y-26763 exerts a neuroprotective effect via its vasodilatory effect.

The benefit of K_{ATP} channel activation during cerebral ischemia will be further strengthened if the effect of Y-26763 is counteracted by a specific blocker of the channel. It is also of great interest to know whether K_{ATP} channels are activated during cerebral ischemia by an intrinsic mechanism. These questions can be

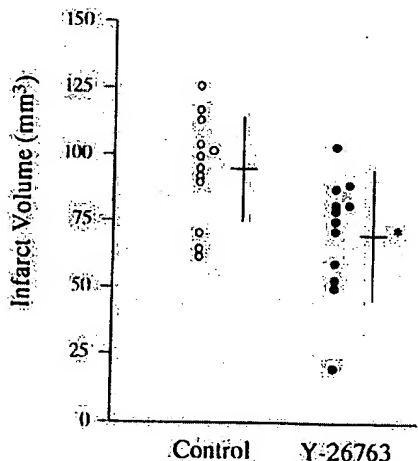


Fig. 3. Infarct volumes in control ($n = 12$) and Y-26763-treated ($n = 12$) groups. Bars represent means \pm SD. * $P = 0.013$ vs. control by unpaired t -test.

answered by comparing infarct volumes in rats treated by the specific inhibitor glibenclamide and its vehicle. Inhibition of the effect of Y-26763 and the identification of an intrinsic mechanism using glibenclamide warrant further experimentation.

Perspectives

Although the precise mechanism underlying the neuroprotective effect of Y-26763 is not clear, it may be explained from the viewpoint of glutamate-mediated excitotoxicity, which is now accepted as a major contributing factor to ischemic neuronal damage (4, 10, 18, 19). Two beneficial properties can be expected from Y-26763. First, it is possible that Y-26763 prevents Ca^{2+} entry by hyperpolarizing presynaptic nerve terminals and consequently inhibits glutamate release. In rat hippocampus, K_{ATP} channels densely distributed in mossy fibers, which are associated with glutamate release (13). Second, Y-26763 may hyperpolarize postsynaptic neurons and confer resistance to the depolarization induced by the stimulation of glutamate receptors. In support of this notion, K_{ATP} channels are present in the postsynaptic neurons of the rat hippocampus (13), and the K_{ATP} channel activators cromakalim and diazoxide abolish excitotoxicity in cultured hippocampal pyramidal neurons (1).

In this study, our primary aim was to examine whether or not the activation of K_{ATP} channels protects against focal cerebral ischemia by intracarotid administration. Therefore, the drug was given before the introduction of ischemia to get the maximal effect. In clinical settings, a drug must be neuroprotective even if it is given after the onset of stroke. On the basis of the current results, it would be necessary to push our experiments forward with therapeutic considerations.

In conclusion, intracarotid infusion of Y-26763 reduced ischemic neuronal damage in the photothrombotic focal ischemia model in rats. The mechanism underlying the neuroprotective effect of the K_{ATP} channel activator may be stabilization of the neuronal membrane.

Y-26763 was kindly provided by Yoshitomi Pharmaceutical, Fukuoka, Japan.

Address for reprint requests: H. Takaba, Second Dept. of Internal Medicine, Faculty of Medicine, Kyushu Univ., Maidashi 3-1-1, Higashi-ku, Fukuoka 812-82, Japan.

Received 5 February 1997; accepted in final form 4 April 1997.

REFERENCES

1. Abele, A. E., and R. J. Miller. Potassium channel activators abolish excitotoxicity in cultured hippocampal pyramidal neurons. *Neurosci. Lett.* 115: 195-200, 1990.
2. Ashford, M. L. J., N. C. Sturgess, N. J. Trout, N. J. Gardner, and C. N. Hales. Adenosine 5'-triphosphate-sensitive ion channels in neonatal rat cultured central neurons. *Pflügers Arch.* 412: 297-304, 1988.
3. Bederson, J. B., L. H. Pitts, S. M. Germano, M. C. Nishimura, R. L. Davis, and H. M. Bartkowski. Evaluation of 2,3,5-triphenyltetrazolium chloride as a stain for detection and quantification of experimental cerebral infarction in rats. *Stroke* 17: 1304-1308, 1986.
4. Choi, D. W. Glutamate neurotoxicity and diseases of the nervous system. *Neuron* 1: 623-634, 1988.
5. Dirnagl, U., B. Kaplan, M. Jacewicz, and W. Pulsinelli. Continuous measurement of cerebral cortical blood flow by laser-Doppler flowmetry in a rat stroke model. *J. Cereb. Blood Flow Metab.* 9: 589-596, 1989.
6. Edwards, G., and A. H. Weston. The pharmacology of ATP-sensitive potassium channels. *Annu. Rev. Pharmacol. Toxicol.* 33: 597-637, 1993.
7. Hamilton, T. C., S. W. Weir, and A. H. Weston. Comparison of the effects of BRL34915 and verapamil on electrical and mechanical activity in rat portal vein. *Br. J. Pharmacol.* 88: 103-111, 1986.
8. Heurteaux, C., V. Bertina, C. Widmann, and M. Lazdunski. K^{+} channel activators prevent global ischemia-induced expression of c-fos, c-jun, heat shock protein, and amyloid β -protein precursor genes and neuronal death in rat hippocampus. *Proc. Natl. Acad. Sci. USA* 90: 9431-9435, 1993.
9. Kitazono, T., F. M. Faraci, H. Taguchi, and D. D. Heistad. Role of potassium channels in cerebral blood vessels. *Stroke* 26: 1713-1723, 1995.
10. Meldrum, B. Excitotoxicity in ischemia: an overview. In: *Cerebrovascular Diseases: Sixteenth Research (Princeton) Conference*, edited by M. D. Ginsberg and W. D. Dietrich. NY: Raven, 1989, p. 47-60.
11. Mourre, C., Y. Ben Ari, H. Bernardi, M. Fosset, and M. Lazdunski. Antidiabetic sulfonylureas: localization of binding sites in the brain and effects on the hyperpolarization induced by anoxia in the hippocampal slices. *Brain Res.* 486: 159-164, 1989.
12. Mourre, C., C. Widmann, and M. Lazdunski. Sulfonylurea binding sites associated with ATP-regulated K^{+} channels in the central nervous system: autoradiographic analysis of their distribution and ontogenesis, and of their localization in mutant mice cerebellum. *Brain Res.* 519: 29-43, 1990.
13. Mourre, C., C. Widmann, and M. Lazdunski. Specific hippocampal lesions indicate the presence of sulfonylurea binding sites associated to ATP-sensitive K^{+} channels both postsynaptically and on mossy fibers. *Brain Res.* 540: 340-344, 1991.
14. Nagao, T., S. Ibayashi, S. Sadoshima, K. Fujii, K. Fujii, Y. Ohya, and M. Fujishima. Distribution and physiological roles of ATP-sensitive K^{+} channels in the vertebralbasilar system of the rabbit. *Circ. Res.* 78: 238-243, 1996.
15. Nagao, T., S. Sadoshima, M. Kamouchi, and M. Fujishima. Cromakalim dilates rat cerebral arteries in vitro. *Stroke* 22: 221-224, 1991.
16. Nakajima, T. Y-27152: a long-acting K^{+} channel activator with less incidence of tachycardia. *Cardiovasc. Drugs Ther.* 9: 372-384, 1991.
17. Nelson, M. T., J. B. Patlak, J. F. Worley, and N. B. Standen. Calcium channels, potassium channels, and voltage dependence of arterial smooth muscle tone. *Am. J. Physiol.* 259 (Cell Physiol. 28): C3-C18, 1990.
18. Rothman, S. M., and J. W. Olney. Glutamate and the pathophysiology of hypoxic-ischemic brain damage. *Ann. Neurol.* 19: 105-111, 1986.
19. Siesjö, B. K., and F. Bengtsson. Calcium fluxes, calcium antagonists, and calcium-related pathology in brain ischemia, hypoglycemia, and spreading depression: an unifying hypothesis. *J. Cereb. Blood Flow Metab.* 9: 127-140, 1989.
20. Takaba, H., T. Nagao, S. Ibayashi, T. Kitazono, K. Fujii, and M. Fujishima. Altered cerebrovascular response to a potassium channel activator in hypertensive rats. *Hypertension* 28: 143-146, 1996.
21. Watson, B. D., W. D. Dietrich, R. Prado, H. Nakayama, H. Kanemitsu, N. N. Futrell, H. Yao, C. G. Markgraf, and P. Wester. Concepts and techniques of experimental stroke induced by cerebrovascular photothrombosis. In: *Central Nervous System Trauma: Laboratory Techniques and Recent Advancement*, edited by S. T. Ohnishi and T. Ohnishi. Boca Raton, FL: CRC, 1995, p. 169-194.
22. Weir, S. W., and S. H. Weston. The effect of BRL34915 and nicorandil on electrical and mechanical activity and on ^{86}Rb efflux in rat blood vessels. *Br. J. Pharmacol.* 88: 121-128, 1986.
23. Yao, H., S. Ibayashi, H. Sugimori, K. Fujii, and M. Fujishima. Simplified model of Krypton laser-induced thrombotic distal middle cerebral artery occlusion in spontaneously hypertensive rats. *Stroke* 27: 333-336, 1996.

Ionic Mechanisms Underlying Depolarizing Responses of an Identified Insect Motor Neuron to Short Periods of Hypoxia

HERVÉ LE CORRONC,¹ BERNARD HUE,¹ AND ROBERT M. PITMAN²

¹Laboratory of Neurophysiology, University of Angers, F-49045 Angers Cedex, France; and ²School of Biomedical Sciences, Gatty Marine Laboratory, University of St. Andrews, Fife KY16 8LB, Scotland

Le Corronc, Hervé, Bernard Hue, and Robert M. Pitman. Ionic mechanisms underlying depolarizing responses of an identified insect motor neuron to short periods of hypoxia. *J. Neurophysiol.* 81: 307–318, 1999. Hypoxia can dramatically disrupt neural processing because energy-dependent homeostatic mechanisms are necessary to support normal neuronal function. In a human context, the long-term effects of such disruption may become all too apparent after a “stroke,” in which blood-flow to part of the brain is compromised. We used an insect preparation to investigate the effects of hypoxia on neuron membrane properties. The preparation is particularly suitable for such studies because insects respond rapidly to hypoxia, but can recover when they are restored to normoxic conditions, whereas many of their neurons are large, identifiable, and robust. Experiments were performed on the “fast” coxal depressor motoneuron (D_f) of cockroach (*Periplaneta americana*). Five-minute periods of hypoxia caused reversible multiphasic depolarizations (10–25 mV; $n = 88$), consisting of an initial transient depolarization followed by a partial repolarization and then a slower phase of further depolarization. During the initial depolarizing phase, spontaneous plateau potentials normally occurred, and inhibitory postsynaptic potential frequency increased considerably; 2–3 min after the onset of hypoxia all electrical activity ceased and membrane resistance was depressed. On reoxygenation, the membrane potential began to repolarize almost immediately, becoming briefly more negative than the normal resting potential. All phases of the hypoxia response declined with repeated periods of hypoxia. Blockade of ATP-dependent Na/K pump by 30 μ M ouabain suppressed only the initial transient depolarization and the reoxygenation-induced hyperpolarization. Reduction of aerobic metabolism between hypoxic periods (produced by bubbling air through the chamber instead of oxygen) had a similar effect to that of ouabain. Although the depolarization seen during hypoxia was not reduced by tetrodotoxin (TTX; 2 μ M), lowering extracellular Na^+ concentration or addition of 500 μ M Cd^{2+} greatly reduced all phases of the hypoxia-induced response, suggesting that Na influx occurs through a TTX-insensitive Cd^{2+} -sensitive channel. Exposure to 20 mM tetraethylammonium and 1 mM 3,4-diaminopyridine increased the amplitude of the hypoxia-induced depolarization, suggesting that activation of K channels may normally limit the amplitude of the hypoxia response. In conclusion we suggest that the slow hypoxia-induced depolarization on motoneuron D_f is mainly carried by a TTX-resistant, Cd^{2+} -sensitive sodium influx. Ca^{2+} entry may also make a direct or indirect contribution to the hypoxia response. The fast transient depolarization appears to result from block of the Na/K pump, whereas the reoxygenation-induced hyperpolarization is largely caused by its subsequent reactivation.

INTRODUCTION

The ability of a neuron to transmit signals is highly dependent on its ability to regulate its transmembrane ionic gradi-

ents and resting potential. Because such ionic gradients are maintained by energy-dependent ion pumps, suppression of ATP synthesis can have serious consequences. It is well known that mammalian central neurons cannot incur an oxygen (O_2) debt and, as a consequence, are particularly susceptible to hypoxia (reduction of O_2 supply to tissues below physiological levels) or ischemia (Fujiwara et al. 1987; Glötzner 1967; Godfraind et al. 1971; Grossman and Williams 1971; Hansen et al. 1982; Misgeld and Frotscher 1982; Negishi and Svætichin 1966; Speckmann et al. 1970). A brief fall in O_2 tension can cause a rapid and complete loss of excitability, which is fully reversible; longer periods of hypoxia, however, rapidly cause cell death (Farooqui et al. 1994; Haddad and Jiang 1993a; Kristián and Siesjö 1997; Somjen et al. 1993).

By studying the effects of hypoxia in a variety of species including those that have developed protective mechanisms to resist the effects of hypoxia, a more profound understanding of the role of metabolism in maintenance of normal electrical activity can be gained. This approach may lead to clinical strategies to limit the impact of hypoxia on the human CNS. Certain species of turtle and carp have the capacity to survive periods of anoxia (total lack of O_2) lasting days or weeks. Survival of these anoxia-tolerant animals depends on their ability to maintain ATP levels at or near normal levels through glycolysis, the only energy source during anoxia (Lutz et al. 1996; Lutz and Nilsson 1997; Sick et al. 1993). The energy consumption of the brain is reduced by increasing the level of inhibitory neurotransmitters such as γ -aminobutyric acid and adenosine (Buck and Bickler 1995; Nilsson and Lutz 1993; Pérez-Pinzón et al. 1993). In turtle, Na^+ channels are also down-regulated (Pérez-Pinzón et al. 1992), and excitatory synaptic transmission is reduced (Nilsson and Lutz 1993).

Adult insects are tolerant to low levels of O_2 , but they appear to have developed a survival strategy that differs from those of the anoxia-tolerant vertebrates discussed previously. Within 2 min of being placed in an atmosphere of 100% nitrogen (N_2) or 100% carbon dioxide (CO_2), insects such as cockroaches convulse and then become paralyzed because they are unable to maintain normal levels of ATP under these conditions, but they can recover fully from periods of hypoxia lasting several hours (Pitman 1988; Wegener 1993). Biochemical and electrophysiological approaches were used to understand the response of insect tissues to acute O_2 deprivation and subsequent reoxygenation. Insects have a level of aerobic metabolism that, for a given mass

of tissue, exceeds that of mammals but have an extremely low capability for anaerobic metabolism. Thus it was found that insect flight muscles (Wegener 1993, 1996; Wegener et al. 1996) and drone retina (Coles and Tsacopoulos 1987) do not produce detectable concentrations of lactate. To support this high rate of aerobic metabolism, gaseous air is carried extremely close to cells through a network of ducts (tracheae). Hypoxia blocks virtually all energy-generating metabolic pathways and depletes the intracellular content of ATP in <10 min (Brazitikos and Tsacopoulos 1991; Walter and Nelson 1975; Wegener 1993). Hypoxia causes a depolarization of neurons of the cockroach nerve cord that is initially associated with an increase in electrical activity (Walter and Nelson 1975) and cholinergic synaptic transmission (Mony et al. 1986); after a few minutes, however, both decrease and finally cease for the remainder of the period of hypoxia (Mony et al. 1986). Hypoxia also depolarizes neurons of the drone retina (Dimitracos and Tsacopoulos 1985) and blocks impulses in mechanosensory neurons (Hamon and Guillet 1996; Hamon et al. 1988). During reoxygenation, the ATP stores are rapidly resynthesized and return to normal (Brazitikos and Tsacopoulos 1991; Walter and Nelson 1975; Wegener 1993). At the same time synaptic transmission, cellular membrane potential, and impulse thresholds return to control values with no apparent long-term alteration (Hamon et al. 1988; Mony et al. 1986). Although the electrical activity of the insect nervous system rapidly returns to normal after periods of hypoxia lasting a few minutes, longer anoxia periods can have chronic effects on excitability; between 10 h and 5 days after a 1- to 3-h period in CO_2 or N_2 , the soma of the metathoracic fast coxal depressor motoneuron (D_f) of cockroach can generate fast sodium action potentials (Pitman 1988) in place of calcium-dependent action potentials or plateau potentials that are normally recorded from this preparation (Hancox and Pitman 1991). The reasons for such long-term alterations are still not clear. However, they may reflect a widespread phenomenon because similar changes in excitability and expression of ion channels were reported after axotomy in neurons of a number of invertebrates (Kuwada and Wine 1981; Pellegrino et al. 1984; Pitman et al. 1972) and vertebrates (Kuno and Llinas 1970; Titmus and Faber 1986; Waxman et al. 1994).

Although there is a considerable body of knowledge about the metabolic strategies used by different animals to minimize the effects of hypoxia, little is known about the electrical changes that occur in individual neurons of such animals during and after periods of hypoxia. The aim of the work presented here is to use an identified insect neuron, the properties of which are known in detail, to characterize its response to brief periods of hypoxia. A brief preliminary report of some of this work was already published (Le Corronc et al. 1997).

METHODS

Preparation

All experiments were performed at room temperature (20–23°C) on adult male cockroaches (*Periplaneta americana*) reared at 28°C in the laboratory. The cockroaches were dissected ventrally, and the three thoracic ganglia and the first part of the abdominal

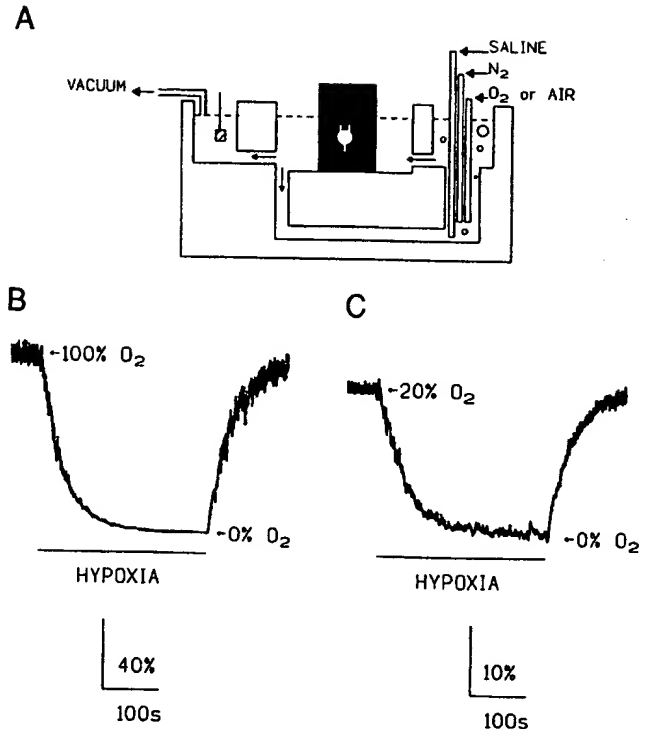


FIG. 1. A: schematic drawing of the experimental chamber. The metathoracic ganglion (white) is shown on the black piece of Perspex. Tubes in the right chamber carry saline, N_2 and O_2 or air. Small arrows in the chamber indicate the movement of saline. The hatched square on the left represents the agar bridge, which makes connection with the reference electrode. The dashed line represents the surfaces of the saline. B and C: variation of percentage of O_2 in the chamber during a 5-min period of hypoxia (horizontal bar). B: when 100% O_2 is replaced by N_2 , the percentage of O_2 drops from 100% to close to 0%. C: in the presence of air, the oxygen level is ~20–21% and decreases to a value to ~0% in N_2 . On the vertical axis the range of PO_2 is different for oxygen and air.

nerve cord were isolated. The preparation was placed in the following saline (in mM): 210 NaCl, 3.1 KCl, 9 CaCl_2 , 60 sucrose, 10 N-tris[hydroxymethyl]methyl-2-aminoethanesulfonic acid; pH was adjusted to 7.2 with NaOH. The preparation was set up as described previously (Pitman 1988). The bathing solution superfused at a rate of 0.3 ml/min and was gassed continuously with 100% O_2 at a rate of ~60 ml/min through a vertical column connected to the chamber containing the isolated metathoracic ganglion. As shown in Fig. 1A the experimental chamber was designed to allow fast recirculation. Excess liquid was removed by a vacuum pump.

Intracellular recordings

One of the paired D_f motoneurons was visually located, and its membrane potential was recorded with microelectrodes pulled from borosilicate glass capillary tubes (GC150F-15, Clark Electromedical Instruments, Reading, UK). Microelectrodes were filled with 1 M K-acetate and had a resistance of 15–20 M Ω . Recordings were made with an Axoclamp-2B intracellular amplifier (Axon instruments, Foster City, CA), the output of which was passed to a digital oscilloscope and a chart recorder. Data were digitized via an IEEE connection to an A/D converting interface (HO-79, Hamag, Frankfurt, Germany) and stored on a personal computer with software developed in our own laboratory.

Induction of hypoxia

Hypoxia was induced by switching from 100% O₂ to 100% N₂ (~60 ml/min) for 5 min once every 30 min, allowing 25 min of oxygenation in between episodes. These gases were introduced by bubbling them into the chamber via separate plastic tubes (Fig. 1A). O₂ rather than air was bubbled through the saline because the PO₂ level attained with air was judged too low and because Hamon and Guillet (1986) previously demonstrated that the electrical activity of oxygenated cockroach nerve cords recorded *in vitro* is similar to that recorded *in situ*. To determine both the steady-state PO₂ values when either 100% O₂ or 100% N₂ were bubbled into the saline and the rate of change that occurred after switch-over, a polarimetric method was used. The microsensor (Chemical Microsensor 1201, Diamond Electro-Tech, Ann Harbor, MI) was first calibrated with O₂ (100% O₂) and N₂ (0% O₂) in a small tube with saline, as recommended, and then moved to the chamber. Under the conditions of our physiological experiments, the steady-state O₂ level in the chamber indicated 100% when O₂ was bubbled, and, during 5-min periods in which 100% N₂ was bubbled, the percentage of O₂ quickly decreased to a value closed to 0% (Fig. 1B). The PO₂ drop was rapidly reversed when O₂ was reintroduced. In some experiments air rather than 100% O₂ was bubbled through the chamber. Under these circumstances, the microsensor registered a PO₂ value of 20–21%, as might be expected if complete equilibration with the saline occurred. When air was replaced by N₂ for 5 min the PO₂ rapidly and reversibly dropped to a value closed to 0% (Fig. 1C).

Solutions and drugs

In experiments carried out in low-Na⁺ (50 mM) saline, tris(hydroxymethyl)aminomethane (Tris) was substituted at equal molarity (pH was adjusted to 7.2 with HCl) (cf. Pitman 1975, 1979). For 20 mM tetraethylammonium chloride (TEA) plus 1 mM 3,4-diaminopyridine (3,4-DAP) saline, an equal molarity of sucrose was removed from the normal saline and pH adjusted to 7.2. Low Ca²⁺–high Mg²⁺ saline had the same composition as normal saline except that it contained 0.3 mM Ca²⁺ and 12 mM Mg²⁺. Nominally zero calcium solution contained 1 mM ethylene glycol-bis(β -aminoethyl ether)-*N,N,N',N'*-tetraacetic acid, and 12 mM Mg²⁺. Ouabain, Ni²⁺, tetrodotoxin (TTX), and Cd²⁺ were added to normal saline at concentration used. Verapamil hydrochloride was first dissolved in 200 μ l of dimethyl sulfoxide. The stock solution (50 mM) was diluted in saline to final concentration of 100 μ M. All compounds were purchased from Sigma Chemicals.

Statistical data are expressed as means \pm 1 SE. On graphs, error bars are shown when larger than symbols. When necessary, statistical significance is assessed with analysis of variance in which a *P* value < 0.05 (Dunnett test) was regarded as significant.

RESULTS

Effects of hypoxia

Figure 2 shows a typical response of motoneuron D_r to a 5-minute period of hypoxia, consisting of a multiphasic membrane depolarization (10–25 mV) from the resting membrane potential of -78.2 ± 0.4 mV ($n = 88$). The depolarization started 45–75 s after the interruption of oxygenation and consisted of an initial transient depolarization (Fig. 2Ab) followed by partial repolarization (Fig. 2Ac). This, in turn, gave way to a slower phase of further depolarization (Fig. 2Ad). Early in the initial phase of the hypoxia-induced depolarization, spontaneous plateau potentials were produced (Fig. 2Ab), and the frequency of inhibitory post-

synaptic potentials increased considerably beyond control levels (cf. Fig. 2, Aa and Ac). The second phase of depolarization developed more slowly than the first and was marked by the absence of plateau potentials or postsynaptic potentials (Fig. 2Ad). On reoxygenation the membrane potential began to repolarize almost immediately and reached a value more negative than the normal resting potential. In 58% ($n = 51$) of neurons, this hyperpolarization was followed by a transient depolarization (3–7 mV) before the membrane potential settled to a steady level (Fig. 2, A and B). In some instances, the late depolarization was sufficiently large to evoke plateau potentials (Fig. 2B), but this was not always the case (Fig. 2A); 42% ($n = 37$) of cells lacked the late depolarizing phase of recovery from hypoxia (Fig. 2C). We were unable to establish any characteristic of neurons that would predict whether they would show the late depolarizing phase during their recovery from hypoxia.

Membrane resistance was determined by measuring the amplitude of membrane potential excursions produced by applying regular hyperpolarizing current pulses (–1.1- to –1.7-nA intensity; 500-ms duration) through the recording electrode. Hypoxia produced a fall in membrane resistance, the magnitude of which varied during the course of the hypoxic period (Fig. 3A). Membrane resistance dropped to $70 \pm 3\%$ (5.63 ± 0.62 M Ω ; $n = 4$) of its control value (100%; 8.16 ± 0.80 M Ω ; $n = 4$) during the initial rapid phase of depolarization and continued to fall throughout the period of hypoxia, reaching $50 \pm 5\%$ (4.06 ± 0.60 M Ω ; $n = 4$) of control when maximal depolarization was attained. During reoxygenation the membrane resistance increased beyond the control value during the late transient depolarizing phase ($115 \pm 6\%$; 9.35 ± 1.35 M Ω ; $n = 4$) before returning to normal (Fig. 3A). The previously described changes in membrane resistance suggest that ionic conductances are increased during hypoxia but can fall below control values during the transient depolarizing phase of recovery.

Motoneuron D_r is able to generate calcium-dependent plateau potentials when long depolarizing current pulses are applied to the soma (Hancox and Pitman 1991). To investigate the effect of hypoxia on the excitable properties of motoneuron D_r, regular depolarizing current pulses were delivered through the intracellular recording microelectrode (Fig. 3B). As shown in Fig. 3Ba, plateau potentials are prolonged depolarizing events, which can trigger (presumably Na⁺-dependent) axonal action potentials that appear in soma recordings as attenuated deflections superimposed on plateau potential (Fig. 3, Ba, Bb, and Bd–Bf). Near the beginning of the hypoxia response, the plateau potential developed more rapidly after the onset of each depolarizing pulse (Fig. 3Bb) than under control conditions. During the slow sustained depolarizing phase of the hypoxia response the ability to generate plateau potentials was lost and was not restored when the membrane potential was returned to its original level by hyperpolarizing current (Fig. 3Bc). Approximately 4 min after reoxygenation, cells regained the ability to generate plateau potentials (Fig. 3Bd). During the late transient depolarizing recovery phase, plateau potential duration was increased beyond that observed under control conditions (Fig. 3Be). This increase probably resulted from the fall in membrane conductance, which occurs at this time. This would both enhance the excitability of the neuron and

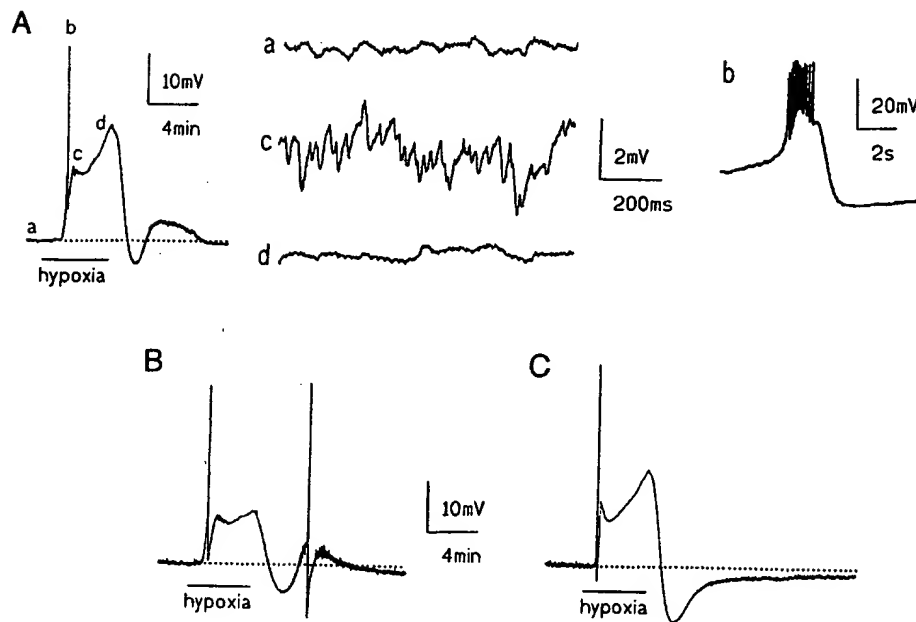


FIG. 2. Effects of hypoxia on membrane potential of motoneuron D_f . *A, left*: 5-min period of hypoxia causes a multiphasic depolarization. The activity seen during the phases of the response marked *a-d* are shown in more detail in the correspondingly lettered panels. During the early phase of depolarization, plateau potentials were produced (*b*). Because the chart recorder had slow response characteristics, the amplitude of plateau potentials is attenuated. This does not apply to detailed panels *a-d* because they provided from the digital interface. Inhibitory postsynaptic potentials were also evoked during the first phase of hypoxia (*c*) but, like plateau potentials, were absent during the slow depolarizing phase (*d*). The resting membrane potential is shown by dotted lines. During reoxygenation a transient hyperpolarization appeared, which was followed by a transient depolarization in some preparations (traces *A* and *B*) but not in others (*C*). When present, this depolarizing phase was sometimes sufficiently large to evoke plateau potentials (*B*). Traces *B* and *C* are both shown on the same scale.

increase the depolarization evoked by applied current pulses of fixed magnitude. Eventually, the characteristics of plateau potentials returned to those observed before the period of hypoxia (Fig. 3*Bf*).

Effects of repetitive periods of hypoxia

When motoneuron D_f was exposed to five successive periods of hypoxia, each separated by a 25-min recovery interval, all phases of the hypoxia response underwent a progressive decline. Figure 4 shows responses to the first, the third, and the fifth hypoxia periods in one preparation that exhibited a late transient depolarization after reintroduction of oxygen (Fig. 4*A*) and another that did not (Fig. 4*B*). The

magnitudes of the sustained depolarizing phase of successive hypoxia responses (measured relative to the resting membrane potential of the neuron, dotted line), showed a decline, the extent of which was similar from one neuron to another; this was also true for the hyperpolarization seen during recovery. The beginning of the first hypoxia period served as the reference time zero, and the amplitudes of depolarizing (filled star in Fig. 4, *A* and *B*) and hyperpolarizing phases (open star in *A* and *B*) of this first hypoxia response were taken as 100%. Data points on the graphs in Fig. 4*C* represent average values taken from successive hypoxia responses recorded from different neurons. Graphs combine data from responses similar to those shown in both Fig. 4, *A* and *B*. During the fifth hypoxia period, the magnitude of the sus-

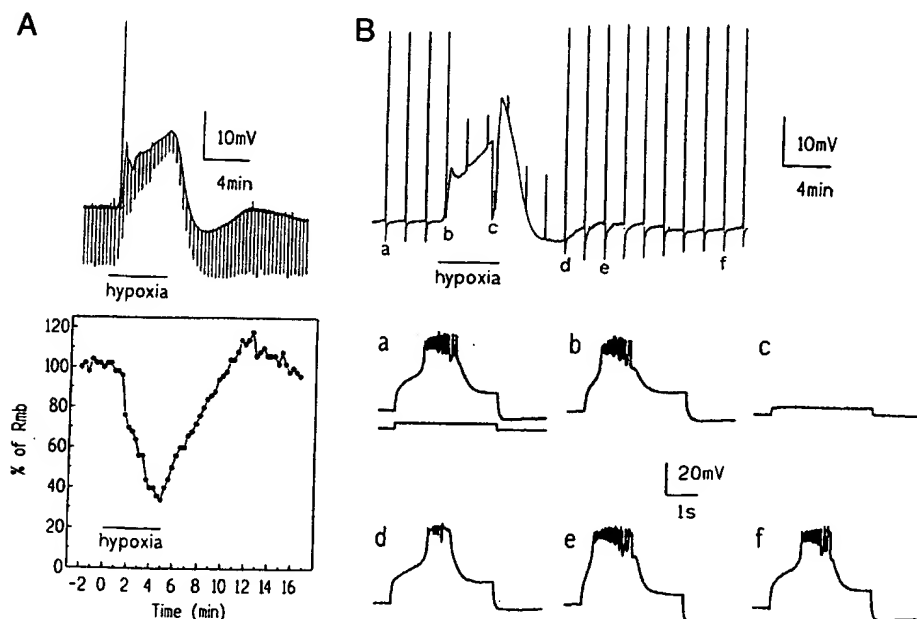


FIG. 3. Membrane resistance and excitability of motoneuron D_f during hypoxia. *A*: voltage responses produced by hyperpolarizing current pulses (-1.7 nA; 500-ms duration) were reversibly reduced during hypoxia, indicating a fall in membrane resistance. The lower box was the percentage change in membrane resistance (% of R_{mb}) taken from the record shown in the top panel. Hypoxia began at 0 min. *B*: plateau potentials evoked by depolarizing current pulses (3.6 nA; 3-s duration) applied during those phases of the hypoxia response lettered *a-f* are shown on an expanded time scale in the correspondingly lettered panels. Plateau potentials developed with less delay (*b*) during the initial phase of hypoxia compared with control (*a*). Plateau potentials could not be evoked during the second phase of depolarization even if the cell was manually clamped to its original resting potential (*c*). During reoxygenation, plateau potentials were restored (*d*) and were longer (*e*) during a time corresponding to the transient depolarization. The lower trace on the expanded scale of *a* shows the timing of the depolarizing current pulse.

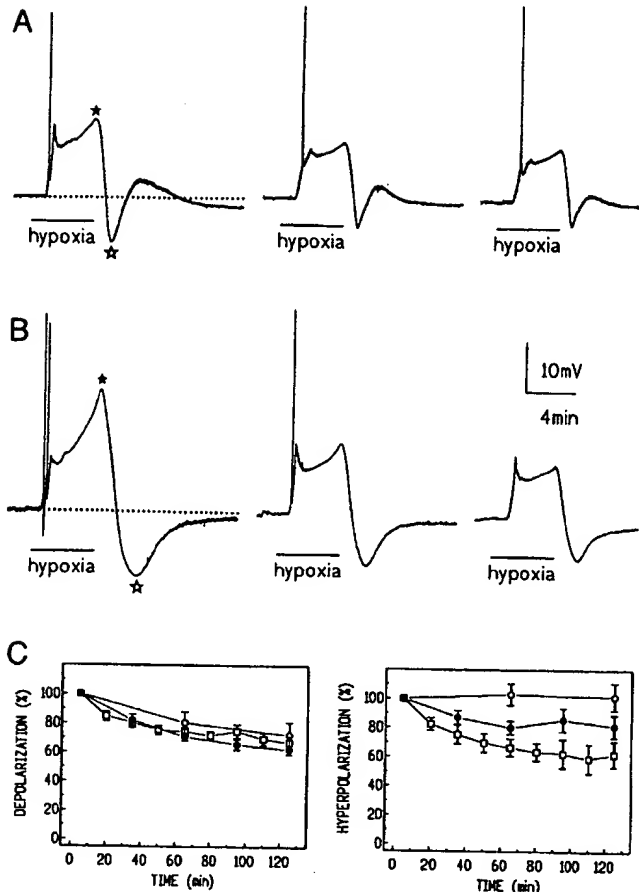


FIG. 4. Effects of repeated periods of hypoxia. *A* and *B*: all phases of the hypoxia-induced response progressively declined when 5 hypoxia periods (5-min duration) were repeated every 30 min. Only alternate responses (first, third, and fifth) are shown. Responses with (*A*) and without (*B*) reoxygenation-induced transient depolarizing phases are shown. The dotted line indicated the resting potential. *C*: effect of interval between successive hypoxia periods (5 min each) on the decline in size of the slow depolarization evoked during hypoxia (filled star in *A* and *B*; left box in *C*) and the hyperpolarization after reoxygenation (open star in *A* and *B*; right box in *C*). Values are expressed as percentages of the amplitudes of these components in the first hypoxia response. The first hypoxia period began at 0 min. Filled circles represent the normal experimental protocol (i.e., hypoxia periods repeated every 30 min; $n = 8$); open circles ($n = 3$) show the decline seen when hypoxia was administered every 60 min, and open squares ($n = 9$) that when hypoxia was repeated every 15 min.

tained depolarization was reduced to $62 \pm 3\%$ ($n = 8$) of that in this first response, whereas the reoxygenation-induced hyperpolarization stabilized at $81 \pm 8\%$ ($n = 8$) of the first response. To establish whether the sustained depolarization and the reoxygenation-induced hyperpolarization had similar rates of recovery, the effect on these components of increasing the recovery interval between hypoxia periods from the normal 25–55 min or decreasing it to 10 min was investigated. With extended intervals the decline of hyperpolarization (open circles in Fig. 4*C*) no longer occurred; by using short intervals, on the other hand, the hyperpolarization (open squares in Fig. 4*C*) showed a greater decline. In contrast, the rate of decline in the slow depolarization was similar for all three recovery intervals (Fig. 4*C*). The decline in slow depolarization could only be prevented by lowering

the Ca^{2+} concentration in the saline. The chronic changes responsible for the decline in the response to hypoxia are not entirely clear but may involve changes in intracellular Ca^{2+} . The regime of 5-min periods of hypoxia separated by 25-min recovery intervals was used in all experiments because this provides the best compromise; shortening the recovery intervals would cause successive responses to decline too rapidly. Increasing their duration, on the other hand, while reducing the extent to which hypoxia responses decline, would prolong experiments to such an extent that the effects of drugs would be difficult to investigate. All drugs were applied between the first and second hypoxia responses recorded from any preparation. Administrations were made sufficiently early to allow an interval of ≥ 15 min before the onset of the second hypoxia period. This protocol allowed the first response to serve as a standard. Because the amplitude of successive responses to hypoxia declined, statistical analysis was achieved by comparing features of hypoxia responses recorded from different preparations at corresponding times in the experimental protocol.

Effects of ouabain and low oxygen level

To study whether an interruption of Na-K pump (or the Na^+/K^+ ATPase) activity contributes to the cellular response to hypoxia, we performed experiments with ouabain, a blocker of this pump. Bath application of $30 \mu\text{M}$ ouabain blocked the fast transient depolarization and the reoxygenation-induced hyperpolarization (Fig. 5*A*) but had little effect on the amplitude of the slow depolarization (which, even in the absence of ouabain, declines with successive periods of hypoxia). After reintroduction of oxygen, the cell repolarized more slowly than under control conditions. Although ouabain initially had little effect on the resting potential, after 25–30 min, the membrane potential gradually depolarized irreversibly to a new stable level 10–15 mV more positive than the normal resting potential.

An alternative strategy we used to investigate the role of metabolism in the maintenance of the electrochemical gradient was to reduce O_2 in the chamber by switching from pure O_2 ($\text{Po}_2 = 100\%$) to air ($\text{Po}_2 = 20\%$, low aerobic metabolism protocol) as used by Coles et al. (1996) on drone retina. Equilibration with air caused a small (5–10 mV), transient membrane depolarization, followed a return to its initial value (Fig. 5*B*). When the gas bubbling through the experimental chamber was switched from air to nitrogen, a hypoxia response was evoked that closely resembled that observed in the presence of ouabain but had the advantage that it was not complicated by a background membrane depolarization (Fig. 5*B*). After recovery from this type of response, reintroduction of O_2 caused an immediate hyperpolarization (7.8 ± 1.9 mV; $n = 4$). This is consistent with a transient increase of metabolism beyond the maximum level obtainable when the preparation is equilibrated with air. In two of four experiments in which O_2 was reintroduced after a period of exposure to air, cells produced spontaneous plateau potentials (Fig. 5*B*). All preparations in which the effects of equilibration with air were studied showed normal hypoxia responses, once they were subsequently equilibrated with O_2 before a period of hypoxia (Fig. 5*B*).

The previous results suggest that blockade of the sodium

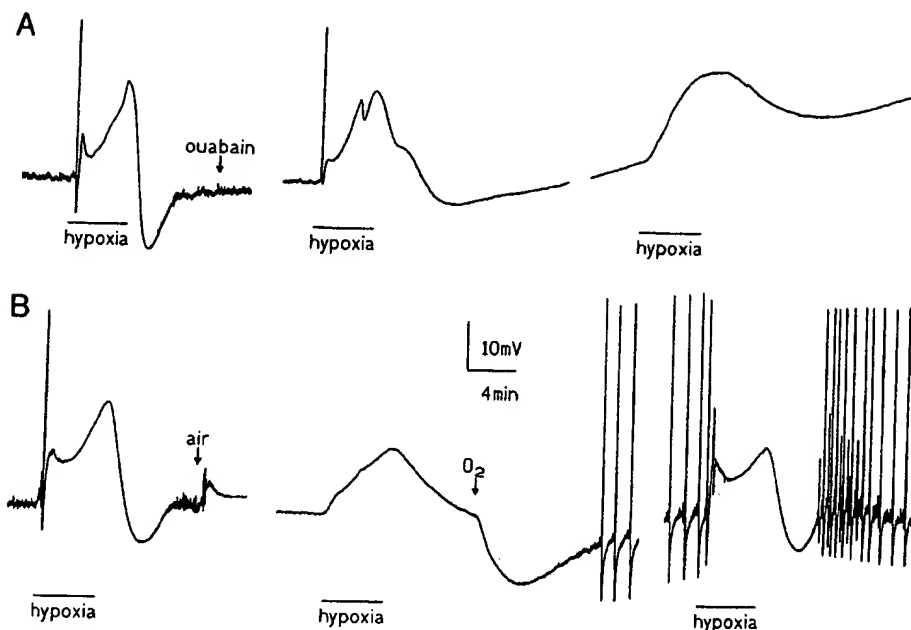


FIG. 5. Effect on the hypoxia response of ouabain and gassing the preparation with air in place of oxygen. *A*: 30 μ M ouabain blocked only the fast transient depolarization and the reoxygenation-induced hyperpolarization. The first (control), second, and third hypoxia responses are shown. The ouabain effect developed slowly. Ouabain caused a slow, progressive depolarization when applied on D_f even in the presence of oxygen. Because the resting potential declines, the effect on the hypoxia responses may be indirect. The amplitude of the slow depolarization declines with successive periods of hypoxia even in the absence of ouabain, so the amplitude of the slow depolarization is no smaller than control. *B*: when O_2 was replaced by air bubbling in the saline, a small transient depolarization occurred then the resting potential returned to its previous value. The first, the third, and the fourth hypoxia periods were shown. When air was switched to N_2 , the third evoked-hypoxia response was similar to those observed in the presence of ouabain. Reintroduction of O_2 caused an immediate transient hyperpolarization, after which the neuron began to generate spontaneous plateau potentials. The multiphasic characteristic of the hypoxia response was also restored after reintroduction of O_2 .

pump is probably not primarily responsible for the hypoxia-induced slow depolarization because this component of the response was not blocked by ouabain or low aerobic metabolism. In contrast the initial phase of depolarization and the rapid repolarization and subsequent hyperpolarization observed when O_2 is reintroduced may well, at least in part, respectively result from inhibition and reactivation of the Na-K pump. A net increase in transmembrane Na^+ and Ca^{2+} influx and K^+ efflux through cationic channels could therefore contribute to the depolarization. Ionic channel blockers and solutions of altered ionic composition were applied to characterize the ionic dependence of the hypoxia-induced depolarization.

Effect of verapamil, Ni^{2+} and low and zero Ca^{2+} solutions

In these experiments we tested the hypothesis that membrane potential alterations seen during hypoxia resulted from an influx of Ca^{2+} through the surface membrane. In a medium containing 100 μ M verapamil ($n = 6$), the hypoxia response and the hyperpolarization seen on reoxygenation were unaffected (not shown); 600 μ M Ni^{2+} ($n = 6$) had no effect on the response to hypoxia but completely blocked the hyperpolarization seen on reintroduction of oxygen (Fig. 6, *A* and *C*). After treatment with Ni^{2+} , the progressive decline in the amplitude of the hypoxia depolarization that occurs in control conditions was reversed. In most preparations, Ni^{2+} at the concentrations used caused the threshold

for plateau potentials to become less negative to such an extent that these events occurred spontaneously (Fig. 6*A*). In the presence of a low Ca^{2+} (0.3 mM) and high Mg^{2+} (12 mM) saline, the only effect observed was a significant reduction in the rate of decline in the hypoxia-induced depolarization (Fig. 6*C*; $n = 3$; $P < 0.05$ for data measured 65 min from the start of the experiment). In a solution containing 2 mM Ca^{2+} and 7 mM Mg^{2+} ($n = 5$) (not shown) the results obtained were the same as those described for 0.3 mM Ca^{2+} and 12 mM Mg^{2+} . In nominally zero Ca^{2+} saline ($n = 4$), the amplitude of plateau potentials at the start of the hypoxia response was reduced, whereas the slow phase of the response was augmented ($P < 0.01$ at 65 min). This bathing solution reduced the amplitude of the hyperpolarization seen on reoxygenation (Fig. 6, *B* and *C*; $P < 0.01$ at 65 min). The results obtained in low or zero Ca^{2+} salines indicated that there is a complex relationship between $[Ca^{2+}]_o$ and its effect on the slow phase of the hypoxia response.

Because Ca^{2+} channel blockers did not depress either phase of depolarization during hypoxia, it appears that Ca^{2+} channels do not play a major role in the response of the neuron to reduced oxygen tension. It appears, however, that Ca^{2+} may play a modulatory role because low Ca^{2+} solutions enhance rather than reduce the slow depolarizing phase of the response. The involvement of Ca^{2+} in the posthypoxia hyperpolarization remains enigmatic because it is blocked by Ni^{2+} but not in nominally zero Ca^{2+} bathing solution or by verapamil.

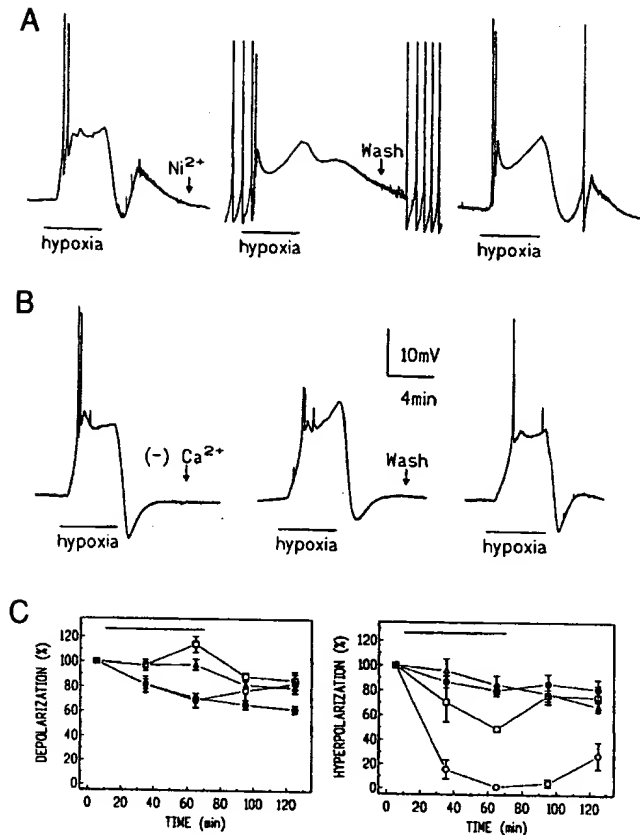


FIG. 6. Effect of Ni^{2+} and low and zero Ca^{2+} . *A*: $600 \mu\text{M}$ Ni^{2+} had little or no effect on the response to hypoxia but blocked the hyperpolarization induced by reoxygenation. At the concentration used, Ni^{2+} caused the neuron to generate spontaneous plateau potentials. After washing out the blocker, the normal response was restored. *B*: when motoneuron D_1 was incubated in a nominally zero Ca^{2+} saline, the amplitude of plateau potentials was reduced and the slow phase of the response was increased. The amplitude of the hyperpolarization seen on reoxygenation was reduced. In *A* and *B* the first, the third, and the fifth hypoxia responses were shown. *C*: graphs show the amplitude of the slow phase of the response (*left panel*) and hyperpolarization (*right panel*) in the presence of Ni^{2+} and low and zero Ca^{2+} as a percentage of those phases of the first hypoxia response recorded from the neuron. \bullet : control ($n = 8$); \circ : $600 \mu\text{M}$ Ni^{2+} ($n = 6$); Δ : 0.3 mM Ca^{2+} plus 12 mM Mg^{2+} ($n = 3$); \square : nominally 0 mM Ca^{2+} , 1 mM ethylene glycol-bis(β -aminoethyl ether)- N,N,N',N' -tetraacetic acid and 12 mM Mg^{2+} ($n = 4$). The period over which solutions of altered composition were applied is indicated by the horizontal bars.

Effect of TTX and low Na^+ -containing solution

In the presence of $2 \mu\text{M}$ TTX ($n = 4$), the depolarizing phase of the hypoxia response was not significantly altered (Fig. 7, *A* and *C*; $P > 0.05$ at 65 min). It appears that this dose was effective in blocking Na^+ channels because both spontaneous postsynaptic potentials (not shown) and Na^+ -dependent action potentials normally superimposed on plateau potentials were abolished (not illustrated). TTX, however, did cause a delayed and long-term reduction in the hyperpolarization seen on reoxygenation (Fig. 7*C*). To investigate the possibility that a TTX-resistant Na^+ influx is involved in the hypoxia response, the preparation was exposed to low- Na^+ (23% of normal) solution. After changing to low- Na^+ saline, the resting potential of the neuron hyper-

polarized (by ~ 10 – 15 mV) and then gradually returned to its original value over a period of ~ 30 – 40 min . As a consequence, the membrane potential would have been more negative during the second hypoxia response than at the start of the experiment; to compensate for this the membrane was artificially returned to its starting value by passing current through the recording microelectrode. In such experiments ($n = 3$), all phases of the hypoxia response were greatly reduced (Fig. 7, *B* and *C*; $P < 0.01$ at 65 min). In low- Na^+ solution, return of the membrane potential to the resting level on reoxygenation was much faster than in normal saline. Hypoxia responses recorded after returning the preparation to normal saline solution showed that, although the slow phase of depolarization recovered, neither the early transient depolarizing phase nor the posthypoxia hyperpolarization reappeared (Fig. 7*B*).

The previous results combined with those presented in the previous section strongly support the conclusion that the depolarizing phase of the hypoxia response results from an influx of Na^+ through TTX-insensitive Na^+ channels.

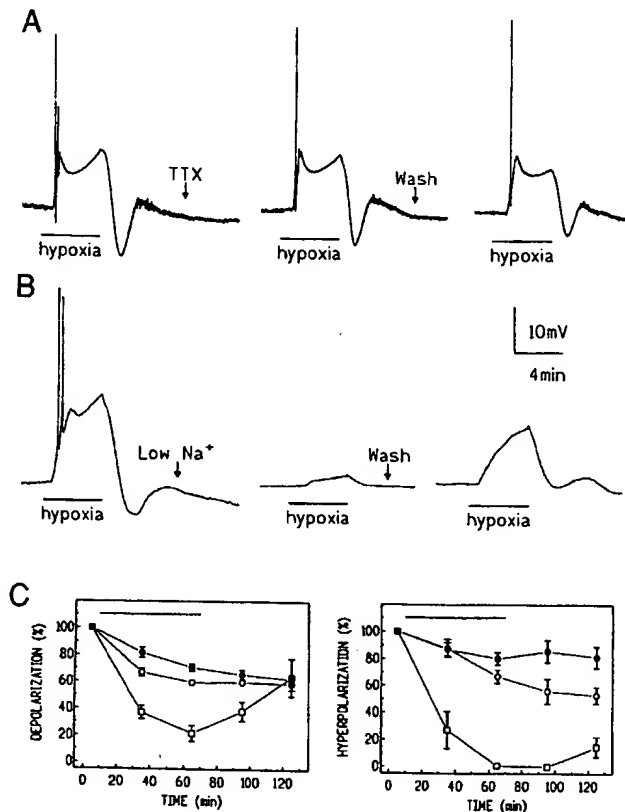


FIG. 7. Effect of tetrodotoxin (TTX) and low Na^+ -containing solution. *A*: $2 \mu\text{M}$ TTX had no effect on the hypoxia-induced electrical response. *B*: Low Na^+ -containing solution (23% of normal Na^+) reduced all phases of the hypoxia response. After the washout of the low Na^+ -containing solution, the slow depolarizing phase recovered, but neither the early transient depolarizing phase nor the posthypoxia hyperpolarization were restored. In *A* and *B* the first, the third, and the fifth hypoxia responses were shown. *C*: graphs summarize the results obtained in TTX and in low Na^+ -containing solution on the slow depolarization and on the reoxygenation-induced hyperpolarization. \bullet : control ($n = 8$); \circ : $2 \mu\text{M}$ TTX ($n = 4$); \square : low Na^+ -containing solution ($n = 3$). The period over which TTX and low Na^+ were applied is indicated by the horizontal bars.

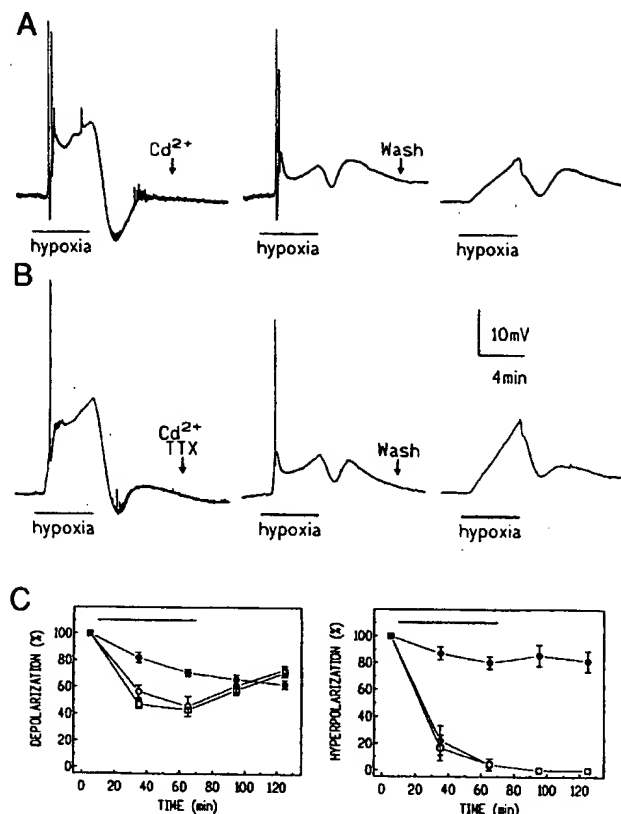


FIG. 8. Effect of Cd^{2+} on the hypoxia response. Bath application of $500 \mu\text{M}$ Cd^{2+} (A) and $500 \mu\text{M}$ Cd^{2+} plus $2 \mu\text{M}$ TTX (B) reduced by the same percentage (C) the slow depolarizing phase and the hyperpolarization induced by reoxygenation. TTX and Cd^{2+} are applied simultaneously to demonstrate Cd^{2+} -sensitive TTX-resistant conductance. The rapid transient depolarizing phase of the response persisted during application of drugs but was lost after washing the drugs from the preparation. Only the slow depolarization recovered. In C the horizontal bar indicates the period over which drugs were applied to the bath. \bullet : control ($n = 8$); \circ : $500 \mu\text{M}$ Cd^{2+} ($n = 3$); \square : $500 \mu\text{M}$ Cd^{2+} plus $2 \mu\text{M}$ TTX ($n = 4$).

Effect of Cd^{2+} on the response to hypoxia

Because Cd^{2+} -sensitive, TTX-resistant Na^+ channels were observed in the amphibian nervous system (Bowers 1985), the possibility was tested that such a current is responsible for the hypoxia response of the neuron under investigation here. Figure 8A shows the effects of $500 \mu\text{M}$ Cd^{2+} on the hypoxia response. The depolarizing phase of the response and the hyperpolarization after hypoxia were attenuated ($P < 0.05$ and $P < 0.01$ respectively at 65 min; $n = 3$), whereas a transient depolarizing component to recovery became apparent. In those preparations that initially possessed a transient depolarizing recovery phase (cf. Fig. 2, A and B), this was augmented by Cd^{2+} . After washing Cd^{2+} from the preparation, the rapid phase of depolarization underwent further decline, the slow depolarization recovered ($73 \pm 3\%$ at 125 min; $n = 3$), and the hyperpolarizing and depolarizing phases of recovery showed little change.

To check whether TTX and Cd^{2+} are operating on the same conductance, both drugs were applied simultaneously. An additive effect would indicate that the two agents operate via different mechanisms. In the presence of $2 \mu\text{M}$ TTX and $500 \mu\text{M}$ Cd^{2+} ($n = 4$; Fig. 8, B and C) the hypoxia responses

were indistinguishable from those obtained in Cd^{2+} alone. This provides evidence that Na^+ influx occurs via a Cd^{2+} -sensitive, TTX-resistant channel of a type not previously described in insect neurons.

Effect of K^+ channel blockers

To test the hypothesis that the hypoxic response involved a K^+ efflux, experiments were performed in the presence of the K^+ channel blockers TEA (20 mM) and 3,4-DAP (1 mM). Under these conditions the hypoxia-induced depolarization was significantly increased ($P < 0.01$ at 65 min; $n = 3$), and the hyperpolarization after reoxygenation was significantly reduced ($P < 0.01$ at 65 min; $n = 3$; Fig. 9, A and B). A dramatic increase in the electrical activity of the neuron was also observed. Because of the powerful effect of K^+ channel blockers, the period of exposure to these agents was restricted to one period of hypoxia (rather than two for all other drugs) to minimize damage to the neuron. When these drugs were washed from the preparation, the reoxygenation hyperpolarization reappeared and reached a greater amplitude than normal. Abolition of the hyperpolarizing phase of recovery was not a consequence of the high level of spontaneous activity in the neuron because this persisted during the wash at a time when the hyperpolarizing phase had reappeared.

DISCUSSION

We have shown that brief periods of hypoxia cause a multiphasic response in the soma of the fast coxal depressor

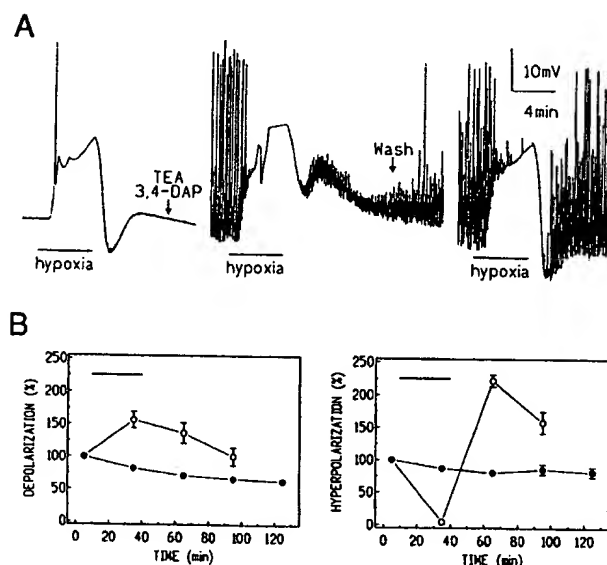


FIG. 9. In the presence of both 20 mM tetraethylammonium chloride (TEA) and 1 mM 3,4-DAP the amplitude of the hypoxia-induced depolarization was increased, whereas the hyperpolarization was reduced (A). These effects were probably not initiated by the large increase of electrical activity evoked by potassium blockers because this persisted during the wash at a time when the hyperpolarizing phase had reappeared. To minimize damage to motoneuron D_1 , K^+ channel blockers were applied during only one hypoxia period then washed off (other drugs and altered solutions remained on the preparation during 2 hypoxia responses). The first, the second, and the fourth hypoxia response were shown. B: plots show the quantitative effects of drugs (horizontal bar) on the slow depolarization (left panel) and on hyperpolarization (right panel). \bullet : control ($n = 8$); \circ : 20 mM TEA plus 1 mM 3,4-diaminopyridine ($n = 3$).

motoneuron (D_f) of the cockroach. Our results demonstrate for the first time in an insect neuron that the different phases response to hypoxia are produced by different mechanisms

Features of the response to hypoxia

Our observations clearly show that motoneuron D_f is highly sensitive to hypoxia to which it responds with a multiphasic membrane depolarization; initially spontaneous synaptic activity and excitability are increased, and then there is a fall in membrane resistance accompanied by a loss of excitability. Reoxygenation induces a fast hyperpolarization that is sometimes followed by a transient depolarization. During this latter phase, membrane resistance and excitability are higher than normal. Similar responses were seen in the cell bodies of some other identified cockroach neurons (personal observations), including giant interneurons (Mony et al. 1986). Our results are also generally comparable with observations on the effects of oxygen deprivation on some mammalian neurons; striatal (Calabresi et al. 1995), hypoglossal (Donnelly et al. 1992; Haddad and Donnelly 1990; Haddad and Jiang 1993b), vagal (Donnelly et al. 1992; Haddad and Jiang 1993b), and neocortical (O'Reilly et al. 1995; Rosen and Morris 1993) neurons depolarize, and their membrane resistance drops during hypoxia. Initially, the frequency of evoked action potentials in these neurons increases, but a few minutes later such activity is completely abolished. Hypoglossal neurons undergo a transient increase in presumed synaptic potentials in the early phase of hypoxia (Haddad and Donnelly 1990). When reoxygenated, striatal, hypoglossal, vagal, and neocortical neurons, unlike D_f , only slowly repolarize to their normal resting potential and do not undergo any transient hyperpolarization (Calabresi et al. 1995; Donnelly et al. 1992; Haddad and Jiang 1993b; O'Reilly et al. 1995; Rosen and Morris 1993). During recovery from hypoxia, the membrane resistance of both vagal motoneurons and neocortical neurons, like that of D_f , increases above normal (O'Reilly et al. 1995), presumably accounting for the period of hyperexcitability. If the period of hypoxia to which CA1 hippocampal (Fujiwara et al. 1987; Krnjevic and Leblond 1989; Leblond and Krnjevic 1989) or substantia nigra pars compacta (Mercuri et al. 1994) neurons are exposed is sufficiently brief, only membrane hyperpolarization is observed; if the preparation is reoxygenated at this point, an immediate transient further hyperpolarization occurs before the membrane potential returns to its normal value. This response may have a basis similar to that observed when D_f is reoxygenated.

ATP-dependent processes

Both the initial fast transient-depolarization of the hypoxia response and the hyperpolarization seen on reoxygenation were blocked when the preparation was treated with ouabain. These components of the hypoxia response were also suppressed if the preparation was perfused with solution with a lowered PO_2 in the intervals between periods of hypoxia (This was done by equilibrating the preparation with air instead of O_2 in the intervals between administration of 100% N_2 , a low aerobic metabolism protocol). Block of the reoxygenation-induced hyperpolarization in D_f by ouabain

was similar to that seen in both CA1 (Fujiwara et al. 1987) and in nigral neurons (Mercuri et al. 1994). These observations indicate that the ATP-dependent "Na pump" (Na^+ - K^+ ATPase) makes a direct contribution to the membrane potential changes observed during and after brief periods of hypoxia. Further support for this hypothesis is provided by the fact that the onset of the first transient depolarization occurred without the reduction in the membrane resistance that might be expected if it resulted from opening of ion channels (see Fig. 3A).

The resting potential of motoneuron D_f has an electrogenic Na^+ - K^+ pump component, which is sensitive to oxygen tension, ouabain, extracellular K^+ concentration, Na^+ injection, and low temperature (David and Sattelle 1990). Because hypoxia is known to rapidly deplete intracellular ATP in insects (Brazitikos and Tsacopoulos 1991; Walter and Nelson 1975; Wegener 1993), we suggest that this slows ion pumping by the Na^+ - K^+ ATPase, so disrupting both ionic homeostasis and neuronal function. ATP is thought to be restored rapidly when tissues are reoxygenated; therefore, the posthypoxic repolarization could be brought about by reactivation of the electrogenic Na^+ pump and reestablishment of ionic gradients. That hyperpolarization is seen when O_2 is reintroduced suggests that the pump transiently operates at a higher rate than normal. Because the slow depolarizing phase of the hypoxia response is not affected by ouabain and is accompanied by a large increase in membrane conductance, it is likely to be produced primarily by opening of ion channels caused either by redistribution of ions or by the resultant membrane potential depolarization.

Ionic dependence of hypoxia

Both the initial transient ouabain-sensitive and the slow depolarizing components of the hypoxia response are suppressed by a reduction in the external Na^+ concentration, suggesting that both are caused by an influx of this ion. Because TTX has no effect, while Cd^{2+} mimics the action of low Na^+ saline, it is likely that the depolarization induced by hypoxia is mainly caused by flow of Na^+ ions through a TTX-resistant Cd^{2+} -sensitive Na^+ channel. That the effects of low Na^+ and Cd^{2+} on both the first transient depolarization and the hyperpolarization induced by reoxygenation are irreversible suggests that they may be acting at the same site, although this cannot be considered certain because the cause of this irreversibility is unknown. Although Cd^{2+} blocks voltage-dependent Ca^{2+} currents in motoneuron D_f (Mills and Pitman 1997), it would be difficult to attribute the effects reported here to such an action. If this were the case, the effects of Cd^{2+} should be mimicked by low or zero Ca^{2+} saline but not by those of low Na^+ solutions. However, the effect of Cd^{2+} was similar to that of low Na^+ but different from that of low or zero Ca^{2+} saline. We suggest therefore that hypoxia activates a TTX-resistant Cd^{2+} -sensitive Na^+ influx in D_f . Our findings are similar to those obtained with brain stem neurons (Haddad and Donnelly 1990; Haddad and Jiang 1993b) and in striatal neurons (Calabresi et al. 1995) in which membrane depolarization is reduced by lowering external Na^+ concentration but not application of TTX. With the exception of somatically recorded axon spikes the normal electrical activity in D_f was TTX insensi-

tive (Hancox and Pitman 1991). Although we conclude that a Na^+ influx is the major cause of the slow membrane depolarization seen during hypoxia, we cannot exclude the possibility that a small Ca^{2+} influx does make some contribution to the hypoxia response. The delay in the effect of Cd^{2+} on the first transient depolarizing phase of the hypoxia response could result from a relatively low sensitivity to this agent. However, it is more likely to occur because this phase of the hypoxia response is generated in a site within the ganglionic neuropile that is relatively inaccessible to Cd^{2+} because this phase of the response continued to decline after Cd^{2+} had been washed from the experimental chamber. To investigate this, Cd^{2+} was applied during three hypoxia periods rather than two. In such experiments, the initial transient depolarization of the third response was blocked (not shown), supporting the conclusion that Cd^{2+} does have a site of action that is relatively inaccessible.

In low and nominally zero Ca^{2+} solutions, the amplitude of the hypoxia-induced depolarization was increased. Calabresi et al. (1995) found a similar enhancement in the amplitude of the hypoxia-induced depolarization recorded from nigral neurons bathed in a medium containing low Ca^{2+} (0.5 mM) plus high Mg^{2+} (10 mM). We suggest the following mechanism for this enhancement: normally, sufficient Ca^{2+} influx occurs during hypoxia to activate a Ca^{2+} -dependent (gK_{Ca}) K conductance. In motoneuron D_r , this conductance has been shown to be considerably larger than the inward Ca currents that generated them (David and Pitman 1995a,b; Mills and Pitman 1997; Thomas 1984). The effect of this current therefore would be to limit the size of the hypoxia-induced depolarization. When the preparation is bathed in low or nominally zero Ca^{2+} saline, I_{Ca} and hence I_{KCa} will fall, so increasing the overall amplitude of the hypoxia-induced depolarization. Ca influx may not be the only mechanism by which K currents are activated; activation and modulation of gK_{Ca} in D_r may be brought about by a rise in $[\text{Ca}^{2+}]_i$ resulting not only from influx across the surface membrane but also by release from intracellular stores (David and Pitman 1995a,b, 1996). Both mechanisms may contribute to any rise in $[\text{Ca}^{2+}]_i$ that occurs during hypoxia. Enhancement of the hypoxia-induced depolarization by K channel blockers (TEA plus 3,4-DAP) provides further support for the role of K current activation during hypoxia. It appears that K channels are also activated in other preparations; in drone retina and in mammalian neurons it was found that hypoxia increases the extracellular K^+ concentration (Dimitracos and Tsacopoulos 1985; Donnelly et al. 1992), whereas K^+ blockers augment the hypoxia response in mammalian neurons (Jiang and Haddad 1991). In mammalian neurons, gK_{Ca} (Leblond and Krnjevic 1989; Yamamoto et al. 1997) and ATP-sensitive K^+ channels (gK_{ATP}) (Fujimura et al. 1997; Jiang and Haddad 1991) are the main route by which intracellular K^+ is lost during hypoxia. In D_r , depolarization caused by Na^+ influx, a rise in intracellular Ca^{2+} and a fall in ATP could all contribute, in principle, to activation of gK and limitation in amplitude of the hypoxia-induced depolarization. The contribution of gK_{ATP} to the hypoxia response in D_r is not clear, however, because glibenclamide has little or no effect on hypoxia response (Pitman, personal observations).

Although we indicated previously that reactivation of

Na^+/K^+ pump appears to be the primary cause of the post-hypoxic hyperpolarization, it appears that other processes also may be involved because this component is depressed by K^+ channel blockers, TTX, or by bathing the preparation in nominally zero Ca^{2+} saline. One contributor may be $\text{Na}^+/\text{Ca}^{2+}$ exchange because the posthypoxic hyperpolarization is blocked by Ni^{2+} (600 μM), which was used to selectively block $\text{Na}^+/\text{Ca}^{2+}$ exchange in guinea-pig ventricular myocytes (Kimura et al. 1987). It has been shown previously that Ni^{2+} does not block voltage-dependent Ca^{2+} currents in D_r (Mills and Pitman 1997).

The reoxygenation-induced hyperpolarization was sometimes followed by a transient depolarization. Although we have not elucidated the mechanism of this latter phase, the associated decrease in membrane conductance suggests that closure of ion channels may be involved. In hippocampal CA1 neurons, the duration of the reoxygenation-induced hyperpolarization is longer at potentials close to the K^+ equilibrium potential (Fujiwara et al. 1987). These observations were attributed to a block of voltage-independent K^+ currents occurring concurrently with the reoxygenation-induced hyperpolarization at the resting membrane potential. We suggest that a similar reduction in K conductance may account for the appearance of the late depolarizing component recorded from D_r when it is reoxygenated. This could account for the increase of membrane resistance and excitability seen during this phase.

Repetitive hypoxia

Under our experimental conditions, there was a progressive decline in all phases of responses to successive periods of hypoxia. This was not caused by a deterioration in preparations caused by loss of microelectrode impalement or by washout of some vital factor from the environment of the neuron because the decline was decreased by increasing the interval between hypoxia. Moreover, between periods of hypoxia, neurons regained normal electrical characteristics (e.g., resting potential, input resistance, and excitability), indicating they were undamaged. A reduction in extracellular Ca^{2+} concentration specifically blocks the decline of the depolarizing phase but not the transient hyperpolarization seen on reoxygenation. However, the relationship between the extracellular Ca^{2+} concentration and the decline is complex. We suggest that, in D_r , the progressive decline of the reoxygenation-induced hyperpolarization is related to metabolism. Support for this suggestion comes from work on the drone retina, in which long recovery intervals between successive hypoxia periods are needed to replenish the stores of energy-rich substrates and to enable identical hypoxia responses to occur (Dimitracos and Tsacopoulos 1985).

This study is the first report of the acute effect of hypoxia on an insect motoneuron, showing that the response of this preparation has similarities with those of mammalian neurons. We conclude that, in this insect neuron, as in some mammalian neurons, hypoxia causes an increase in Na^+ and Ca^{2+} influx and a K^+ efflux associated with block of the Na-K pump, caused by a fall in intracellular ATP. In many studies on the irreversible damage to the mammalian brain induced by O_2 deprivation, the main goal is a deeper understanding of events that lead to cell death. Increases in intra-

cellular Ca^{2+} and Na^{+} are the two main hypothetical causes of hypoxia-induced injury (Farooqui et al. 1994; Friedman and Haddad 1993, 1994; Haddad and Jiang 1993a). It is thought that these ions may trigger a cascade of cellular events, the final outcome of which is the neuronal death. Unlike mammals, insects recover from hypoxia, showing that irreversible anoxic damage is not an inevitable consequence of metabolic block and loss ionic homeostasis. Because we already provided evidence that the hypoxia response is associated with an Na^{+} influx in D_1 , we need to determine whether $[\text{Ca}^{2+}]_i$ also changes and makes a significant contribution. If both these cations are greatly increased in D_1 during hypoxia, it is important to establish why they do not trigger irreversible neuronal injury or death.

We thank M. Fuentes for typing the manuscript.

H. Le Corrionc was partly supported by a postdoctoral fellowship from the Royal Society and the Centre National de la Recherche Scientifique.

Address for reprint requests: H. Le Corrionc, Laboratory of Neurophysiology, UPRES EA 2647 University of Angers, rue Haute de Reculée, F-49045 Angers Cedex, France.

Received 24 December 1997; accepted in final form 16 September 1998.

REFERENCES

- BOWERS, C. W. A cadmium-sensitive, tetrodotoxin-resistant sodium channel in bullfrog autonomic axons. *Brain Res.* 340: 143–147, 1985.
- BRAZITIKOS, P. D. AND TSACOPOULOS, M. Metabolic signaling between photoreceptors and glial cells in the retina of the drone (*Apis mellifera*). *Brain Res.* 567: 33–41, 1991.
- BUCK, L. T. AND BICKLER, P. E. Role of adenosine in NMDA receptor modulation in the cerebral cortex of an anoxia-tolerant turtle (*Chrysemys picta bellii*). *J. Exp. Biol.* 198: 1621–1628, 1995.
- CALABRESI, P., PISANI, A., MERCURI, N. B., AND BERNARDI, G. On the mechanisms underlying hypoxia-induced membrane depolarization in striatal neurons. *Brain* 118: 1027–1038, 1995.
- COLES, J. A., MARCAGGI, P., VÉGA, C., AND COTILLON, N. Effects of photoreceptor metabolism on interstitial and glial cell pH in bee retina: evidence of a role for NH_4^+ . *J. Physiol. (Lond.)* 495: 305–318, 1996.
- COLES, J. A. AND TSACOPOULOS, M. Aspects of carbohydrate metabolism in photoreceptors and glial cells in the retina of the drone, *Apis mellifera*. In: *Functions of Neuroglia*, edited by A. I. Roitbak. Tbilisi, Georgia: Metsniereba, 1987, p. 155–161.
- DAVID, J. A. AND PITMAN, R. M. Muscarinic agonists modulate calcium-dependent outward currents in an identified insect motoneurone. *Brain Res.* 669: 153–156, 1995a.
- DAVID, J. A. AND PITMAN, R. M. Calcium and potassium currents in the fast coxal depressor motor neuron of the cockroach *Periplaneta americana*. *J. Neurophysiol.* 74: 2043–2050, 1995b.
- DAVID, J. A. AND PITMAN, R. M. Modulation of Ca^{2+} and K^{+} conductances in an identified insect neurone by the activation of an α -bungarotoxin-resistant cholinergic receptor. *J. Exp. Biol.* 199: 1921–1930, 1996.
- DAVID, J. A. AND SATTELLE, D. B. Ionic basis of membrane potential and of acetylcholine-induced currents in the cell body of the cockroach fast coxal depressor motor neurone. *J. Exp. Biol.* 151: 21–39, 1990.
- DIMITRACOS, S. A. AND TSACOPOULOS, M. The recovery from a transient inhibition of the oxidative metabolism of the photoreceptors of the drone (*Apis mellifera*). *J. Exp. Biol.* 119: 165–181, 1985.
- DONNELLY, D. F., JIANG, C., AND HADDAD, G. G. Comparative responses of brain stem and hippocampal neurons to O_2 deprivation: in vitro intracellular studies. *Am. J. Physiol.* 262 (Lung Cell. Mol. Physiol. 6): L549–L554, 1992.
- FAROOQUI, A. A., HAUN, S. E., AND HORROCKS, L. A. Ischemia and hypoxia. In: *Basic Neurochemistry: Molecular, Cellular and Medical Aspects*, edited by G. J. Siegel. New York: Raven, 1994, p. 867–883.
- FRIEDMAN, J. E. AND HADDAD, G. G. Major differences in Ca_i^{2+} response to anoxia between neonatal and adult rat CA1 neurons: role of Ca_s^{2+} and Na_s^{+} . *J. Neurosci.* 13: 63–72, 1993.
- FRIEDMAN, J. E. AND HADDAD, G. G. Removal of extracellular sodium prevents anoxia-induced injury in freshly dissociated rat CA1 hippocampal neurons. *Brain Res.* 641: 57–64, 1994.
- FUJIMURA, N., HIGASHI, H., SHIMOJI, K., AND YOSHIMURA, M. Effects of hypoxia on rat hippocampal CA1 neurons in vitro. *J. Neurophysiol.* 77: 378–385, 1997.
- FUJIMURA, N., HIGASHI, H., SHIMOJI, K., AND YOSHIMURA, M. Effects of hypoxia on rat hippocampal neurones in vitro. *J. Physiol. (Lond.)* 384: 131–151, 1987.
- GLÖTZNER, F. Intracelluläre Potentiale, Eeg und corticale. Gleichspannung an der sensomotorischen Rinde der Katze bei akuter Hypoxie. *Arch. Psychiatr. Nervenkr.* 210: 274–296, 1967.
- GODFRAND, J. M., KAWAMURA, H., KRNEVIC, K., AND PUMAIN, R. Actions of dinitrophenol and some other metabolic inhibitors on cortical neurones. *J. Physiol. (Lond.)* 215: 199–222, 1971.
- GROSSMAN, R. G. AND WILLIAMS, V. F. Electrical activity and ultrastructure of cortical neurons and synapses in ischemia. In: *Brain Hypoxia*, edited by J. B. Brierly and B. S. Meldrum. London: Heinemann, 1971, p. 61–75.
- HADDAD, G. G. AND DONNELLY, D. F. O_2 deprivation induces a major depolarization in brain stem neurons in the adult but not in the neonatal rat. *J. Physiol. (Lond.)* 429: 411–428, 1990.
- HADDAD, G. G. AND JIANG, C. O_2 deprivation in the central nervous system: on mechanisms of neuronal response, differential sensitivity and injury. *Prog. Neurobiol.* 40: 277–318, 1993a.
- HADDAD, G. G. AND JIANG, C. Mechanisms of anoxia-induced depolarization in brainstem neurons: in vitro current and voltage clamp studies in the adult rat. *Brain Res.* 625: 261–268, 1993b.
- HAMON, A. AND GUILLET, J. C. Effects of oxygen on the cercal receptors of the cockroach *Periplaneta americana*. *Comp. Biochem. Physiol. A Physiol.* 83: 427–431, 1986.
- HAMON, A. AND GUILLET, J. C. Location and dynamic properties of the spike generator in an insect mechanosensory neuron. *J. Comp. Physiol. [A]* 179: 235–243, 1996.
- HAMON, A., GUILLET, J. C., AND CALLEC, J. J. Initiation and conduction of impulses in mechanosensory neurons: effects of hypoxia. *Comp. Biochem. Physiol. A Physiol.* 91: 797–805, 1988.
- HANCOX, J. G. AND PITMAN, R. M. Plateau potentials drive axonal impulse burst in insect motoneurons. *Proc. R. Soc. Lond. B Biol. Sci.* 244: 33–38, 1991.
- HANSEN, A. J., HOUNSGAARD, J., AND JAHNSEN, H. Anoxia increases potassium conductance in hippocampal nerve cells. *Acta Physiol. Scand.* 115: 301–310, 1982.
- JIANG, C. AND HADDAD, G. G. Effect of anoxia on intracellular and extracellular potassium activity in hypoglossal neurons in vitro. *J. Neurophysiol.* 66: 103–111, 1991.
- KIMURA, J., MIYAMAE, S., AND NOMA, A. Identification of sodium-calcium exchange current in single ventricular cells of guinea-pig. *J. Physiol. (Lond.)* 384: 199–222, 1987.
- KRISTIAN, T. AND SIESJÖ, B. K. Changes in ionic fluxes during cerebral ischaemia. In: *Neuroprotective Agents and Cerebral Ischaemia*, edited by A. R. Green and A. J. Cross. San Diego, CA: Academic, 1997, p. 24–45.
- KRNEVIC, K. AND LEBLOND, J. Changes in membrane currents of hippocampal neurons evoked by brief anoxia. *J. Neurophysiol.* 62: 15–30, 1989.
- KUNO, M. AND LLINAS, R. Enhancement of synaptic transmission by dendritic potentials in chromatolysed motoneurons of the cat. *J. Physiol. (Lond.)* 210: 807–821, 1970.
- KUWADA, J. Y. AND WINE, J. J. Transient, axotomy-induced changes in the membrane properties of crayfish central neurones. *J. Physiol. (Lond.)* 317: 435–461, 1981.
- LEBLOND, J. AND KRNEVIC, K. Hypoxic changes in hippocampal neurons. *J. Neurophysiol.* 62: 1–14, 1989.
- LE CORRIONC, H., HUE, B., AND PITMAN, R. M. Hypoxia causes rapid multiphasic depolarization of an identified cockroach (*Periplaneta americana*) motoneurone. *J. Physiol. (Lond.)* 504P: 27P, 1997.
- LUTZ, P. L., NILSSON, G. E., AND PÉREZ-PINZÓN, M. A. Anoxia tolerant animals from a neurobiological perspective. *Comp. Biochem. Physiol. B Biochem. Mol. Biol.* 113: 3–13, 1996.
- LUTZ, P. L. AND NILSSON, G. E. Contrasting strategies for anoxic brain survival—glycolysis up or down. *J. Exp. Biol.* 200: 411–419, 1997.
- MERCURI, N. B., BONCI, A., CALABRESI, P., STRATTA, F., AND BERNARDI, G. Responses of rat mesencephalic dopaminergic neurons to a prolonged period of oxygen deprivation. *Neuroscience* 63: 757–764, 1994.

- MILLS, J. D. AND PITMAN, R. M. Electrical properties of a cockroach motor neuron soma depend on different characteristics of individual Ca components. *J. Neurophysiol.* 78: 2455–2466, 1997.
- MISGELD, U. AND FROTSCHER, M. Dependence of the viability of neurons in hippocampal slices on oxygen supply. *Brain Res. Bull.* 8: 95–100, 1982.
- MONY, L., HUE, B., AND CALLEC, J. J. Effects of hypoxia on resting potential and transmitter release at cercal afferent, giant interneurone synapses in the cockroach, *Periplaneta americana* L. *Comp. Biochem. Physiol. A Physiol.* 83: 751–753, 1986.
- NEGISHI, K. AND SYAETICHIN, G. Effects of anoxia, CO₂ and NH₃ on S-potential producing cells and on neurons. *Pflügers Arch.* 292: 177–205, 1966.
- NILSSON, G. E. AND LUTZ, P. L. Role of GABA in hypoxia tolerance, metabolic depression and hibernation—possible links to neurotransmitter evolution. *Comp. Biochem. Physiol. C Pharmacol. Toxicol.* 105: 329–336, 1993.
- O'REILLY, J. P., JIANG, C., AND HADDAD, G. G. Major differences in response to graded hypoxia between hypoglossal and neocortical neurons. *Brain Res.* 683: 179–186, 1995.
- PELLEGRINO, M., NENCIONI, B., AND MATTEOLI, M. Response to axotomy of an identified leech neuron, in vivo and in culture. *Brain Res.* 298: 347–352, 1984.
- PÉREZ-PINZÓN, M. A., LUTZ, P. L., SICK, T. J., AND ROSENTHAL, M. Adenosine, a "retaliatory" metabolite, promotes anoxia tolerance in turtle brain. *J. Cereb. Blood Flow Metab.* 13: 728–732, 1993.
- PÉREZ-PINZÓN, M. A., ROSENTHAL, M., SICK, T. J., LUTZ, P. L., PABLO, J., AND MASH, D. Downregulation of sodium channels during anoxia: a putative survival strategy of turtle brain. *Am. J. Physiol.* 262 (Regulatory Integrative Comp. Physiol. 31): R712–R715, 1992.
- PITMAN, R. M. The ionic dependence of action potentials induced by colchicine in an insect motoneurone cell body. *J. Physiol. (Lond.)* 247: 511–520, 1975.
- PITMAN, R. M. Intracellular citrate or externally applied tetraethylammonium ions produce calcium-dependent action potentials in an insect neurone cell body. *J. Physiol. (Lond.)* 291: 327–337, 1979.
- PITMAN, R. M. Delayed effects of anoxia upon the electrical properties of an identified cockroach motoneurone. *J. Exp. Biol.* 135: 95–108, 1988.
- PITMAN, R. M., TWÉEDLE, C. D., AND COHEN, M. J. Electrical responses of insect central neurons: augmentation by nerve section or colchicine. *Science* 178: 507–509, 1972.
- ROSEN, A. S. AND MORRIS, M. E. Anoxic depression of excitatory and inhibitory postsynaptic potentials in rat neocortical slices. *J. Neurophysiol.* 69: 109–117, 1993.
- SICK, T. J., PÉREZ-PINZÓN, M., LUTZ, P. L., AND ROSENTHAL, M. Maintaining coupled metabolism and membrane function in anoxic brain: a comparison between the turtle and rat. In: *Surviving Hypoxia*, edited by P. W. Hochachka, P. L. Lutz, T. Sick, M. Rosenthal, and G. van den Thillart. Boca Raton, FL: CRC, 1993, p. 351–363.
- SOMJEN, G. G., AITKEN, P. G., CZÉH, G., JING, J., AND YOUNG, J. N. Cellular physiology of hypoxia of the mammalian central nervous system. In: *Molecular and Cellular Approaches to the Treatment of Neurological Disease*, edited by S. G. Waxman. New York: Raven, 1993, p. 51–65.
- SPECKMANN, E.-J., CASPERS, J., AND SOKOLOV, H. Aktivitätsänderungen spinaler Neurone während einer Asphyxie. *Pflügers Arch.* 319: 122–138, 1970.
- THOMAS, M. V. Voltage-clamp analysis of a calcium-mediated potassium conductance in cockroach (*Periplaneta americana*) central neurones. *J. Physiol. (Lond.)* 350: 159–178, 1984.
- TITMUS, M. J. AND FABER, D. S. Axotomy-induced alterations in the electrophysiological characteristics of neurons. *Prog. Neurobiol.* 35: 1–51, 1990.
- WALTER, D. C. AND NELSON, S. R. Energy metabolism and nerve function in cockroaches (*Periplaneta americana*). *Brain Res.* 94: 485–490, 1975.
- WAXMAN, S. G., KOCIS, J. D., AND BLACK, J. A. Type III sodium channel mRNA is expressed in embryonic but not adult spinal sensory neurons, and is reexpressed following axotomy. *J. Neurophysiol.* 72: 466–470, 1994.
- WEGENER, G. Hypoxia and posthypoxic recovery in insects: physiological and metabolic aspects. In: *Surviving Hypoxia*, edited by P. W. Hochachka, P. L. Lutz, T. Sick, M. Rosenthal, and G. van den Thillart. Boca Raton, FL: CRC, 1993, p. 417–434.
- WEGENER, G. Flying insects: model systems in exercise physiology. *Experientia* 52: 404–412, 1996.
- WEGENER, G., KRAUSE, U., AND NEWSHOLME, E. A. Metabolic regulation—physiological and medical aspects. *Experientia* 52: 391–395, 1996.
- YAMAMOTO, S., TANAKA, E., AND HIGASHI, H. Mediation by intracellular calcium-dependent signals of hypoxic hyperpolarization in rat hippocampal CA1 neurons in vitro. *J. Neurophysiol.* 77: 386–392, 1997.

Hypoxic Depolarization of Cerebellar Granule Neurons by Specific Inhibition of TASK-1

Leigh D. Plant, BSc; Paul J. Kemp, DPhil; Chris Peers, PhD;
Zaineb Henderson, PhD; Hugh A. Pearson, PhD

Background and Purpose—The mechanisms underlying neuronal excitotoxicity during hypoxic/ischemic episodes are not fully understood. One feature of such insults is a rapid and transient depolarization of central neurons. TASK-1, an open rectifying K⁺ leak channel, is significant in setting the resting membrane potential of rat cerebellar granule neurons by mediating a standing outward K⁺ current. In this study we investigate the theory that the transient neuronal depolarization seen during hypoxia is due to the inhibition of TASK-1.

Methods—Activity of TASK-1 in primary cultures of rat cerebellar granule neurons was investigated by the whole-cell patch-clamp technique. Discriminating pharmacological and electrophysiological maneuvers were used to isolate the specific channel types underlying acute hypoxic depolarizations.

Results—Exposure of cells to acute hypoxia resulted in a reversible and highly reproducible mean membrane depolarization of 14.2 ± 2.6 mV ($n=5$; $P<0.01$). Two recognized means of inhibiting TASK-1 (decreasing extracellular pH to 6.4 or exposure to the TASK-1-selective inhibitor anandamide) abolished both the hypoxic depolarization and the hypoxic depression of a standing outward current, identifying TASK-1 as the channel mediating this effect.

Conclusions—Our data provide compelling evidence that hypoxia depolarizes central neurons by specific inhibition of TASK-1. Since this hypoxic depolarization may be an early, contributory factor in the response of central neurons to hypoxic/ischemic episodes, TASK-1 may provide a potential therapeutic target in the treatment of stroke. (*Stroke*. 2002; 33:2324-2328.)

Key Words: brain ■ ion channels ■ ischemia ■ potassium channels

Hypoxic/ischemic episodes, such as those that occur during stroke, can cause depolarization of the resting membrane potential in nervous tissue.^{1,2} The resting membrane potential is controlled primarily by a selective permeability to K⁺. An emergent family of proteins known as the 2-P domain K⁺ (K_{2P}) channels has been shown to contribute significantly to this resting K⁺ permeability. K_{2P} channels are “leak” channels that lack voltage dependence and therefore are active across a wide range of potentials.³ They are expressed in a wide range of tissues and can be modulated by a variety of mechanisms, including membrane stretch, extracellular Na⁺, protein kinases A and C, local anesthetics, general anesthetics, and long-chain fatty acids.³ Within the K_{2P} channel family are a group of channels that are sensitive to inhibition by H⁺, at or near physiological pH; these are known collectively as TASK (TWIK-related, Acid-Sensitive K_{2P} channels) and individually as TASK-1⁴ (KCNK3), TASK-2⁵ (KCNK5), and TASK-3⁶ (KCNK9). On the basis of structural correlates, 2 additional members of this group have been recently described: TASK-4⁷ and TASK-5/KT3.3.^{8,9}

TASK-1 has recently been shown to have a functional role in the central nervous system, where it sets the resting

membrane potential and input conductance of cerebellar granule neurons in both primary culture and in slice preparations.^{10,11} Flow of K⁺ through channels formed by TASK gives rise to the standing outward current that can be measured in these cells at depolarized holding potentials.¹⁰ This current can be inhibited by extracellular acidification and activation of Gαq-coupled receptors such as the M₃ muscarinic receptor.¹⁰

Hypoxia is known to modulate the activity of a wide range of ion channels in central neurons and other tissues (reviewed by Lopez-Barneo et al¹²), and native TASKs of both carotid body glomus cells¹³ and a human cell line¹⁴ and recombinant TASK-1 have recently been shown to be inhibited by acute hypoxia.¹⁵ Since experimentally induced hypoxia in nervous tissue not only causes depolarization but can also result in acidosis and neurotransmitter release, and since similar effects are seen in clinical conditions that result in hypoxia, such as stroke,^{1,2} we hypothesized that the underlying mechanism for this response is hypoxic inhibition of TASK-1. The aim of this study, therefore, was to determine the functional consequences of hypoxia in a neuron known to express TASK-1 and to determine whether this response is a result of hypoxic inhibition of native TASK-1 channels.

Received October 29, 2001; final revision received April 24, 2002; accepted May 8, 2002.

From the School of Biomedical Sciences and Institute for Cardiovascular Research (C.P.), University of Leeds, Leeds, UK.

Correspondence to Dr H.A. Pearson, School of Biomedical Sciences, University of Leeds, Leeds LS2 9JT, UK. E-mail h.a.pearson@leeds.ac.uk

© 2002 American Heart Association, Inc.

Stroke is available at <http://www.strokeaha.org>

DOI: 10.1161/01.STR.0000027440.68031.B0

Materials and Methods

Culturing of Rat Central Neurons

All experiments were performed with the use of primary cultures of rat cerebellar granule neurons. Cells were obtained by enzymatic and mechanical dissociation, as previously described.^{16,17} Briefly, tissue was removed from 6- to 8-day-old rat pups and triturated after a 15-minute trypsin digestion (EC 4.4.21.4, 2.5 mg · mL⁻¹ in PBS), which was halted by the addition of PBS containing soybean trypsin inhibitor (0.1 mg · mL⁻¹). Cells were pelleted by centrifugation (1 minute at 100g) and resuspended in minimum essential medium supplemented with 10% fetal calf serum, 2.5% chick embryo extract, 26 mmol/L glucose, 19 mmol/L KCl, 2 mmol/L L-glutamine, and penicillin/streptomycin (50 IU · mL⁻¹/50 µg · mL⁻¹). The cells were seeded at a density of 0.25×10^6 cells per well on circular 13-mm-diameter poly-L-lysine-coated coverslips. Multiwells were incubated in a humidified atmosphere containing 5% CO₂/95% air at 37°C. After 48 hours, the culture medium was exchanged for one consisting of minimum essential medium supplemented with 10% horse serum, 2.5% chick embryo extract, 26 mmol/L glucose, 19 mmol/L KCl, 2 mmol/L L-glutamine, penicillin/streptomycin (50 IU · mL⁻¹/50 µg · mL⁻¹), and 80 µmol/L fluorodeoxyuridine to prevent proliferation of nonneuronal cells. Culture medium was exchanged every 3 days, and all recordings were made from cells between days 5 to 12 in culture.

Electrophysiology

K⁺ currents were recorded from cells at room temperature (measured in all experiments as 22°C) with the use of either the amphotericin B perforated patch-clamp technique for TASK or the conventional whole-cell patch-clamp technique for measurement of voltage-gated currents. Glass micropipettes (2 to 4 MΩ) were fabricated from borosilicate glass and filled with solution containing (in mmol/L): KCl 140, CaCl₂ 0.5, EGTA 5, HEPES 10, K₂ATP 2, MgCl₂ 1; pH was adjusted to 7.2 with KOH. Patch perforation was achieved by including amphotericin B (240 µg · mL⁻¹) in the pipette solution. The external solution with which cells were continually perfused comprised the following (in mmol/L): NaCl 120, KCl 2.5, MgCl₂ 2, CaCl₂ 0.5, glucose 10, HEPES 10. pH was adjusted to 7.4 or 6.4 with NaOH, as appropriate. Cells were made hypoxic by perfusion with an external solution that had been bubbled with nitrogen for at least 30 minutes before perfusion. Oxygen tension was measured at the cell with the use of a polarized carbon fiber electrode and was ~30 mm Hg in all experiments reported herein. This degree of hypoxia was reached within 1 minute of switching perfusion. For all electrophysiological measurements, series resistance and capacitance transients were electronically compensated. For measurement of voltage-gated currents, linear leak and residual transients were removed offline with a P/5 leak subtraction protocol.

To evoke K⁺ currents, a voltage protocol modified from Millar et al¹⁰ was used. Cells were held at -20 mV, and the membrane potential was ramped to -100 mV over a period of 800 ms before reduction to -20 mV (Figure 2, inset). Ramp hyperpolarizations were repeated every 20 seconds. Voltage-gated K⁺ currents were evoked as described by Ramsden et al¹⁷ by depolarizing from a prepulse potential of -140 mV to test potentials ranging from -70 mV to +90 mV. Membrane potential was measured in current clamp (I=0 pA), with the use of the same solutions as those used in voltage-clamp experiments.

Currents were recorded and analyzed with the use of the Patch v6.0 program by Cambridge Electronic Design. Further analyses were performed with the use of Microsoft Excel 97 and Microcal Origin version 6.1. Student's *t* tests (paired and unpaired, as appropriate) were used to determine the significance of differences between the means, with probability values of <0.05 considered significant.

Materials

Standard reagents were obtained from Sigma-Aldrich or BDH. All culture reagents were obtained from Gibco BRL. Anandamide was purchased from Tocris Cookson Ltd.

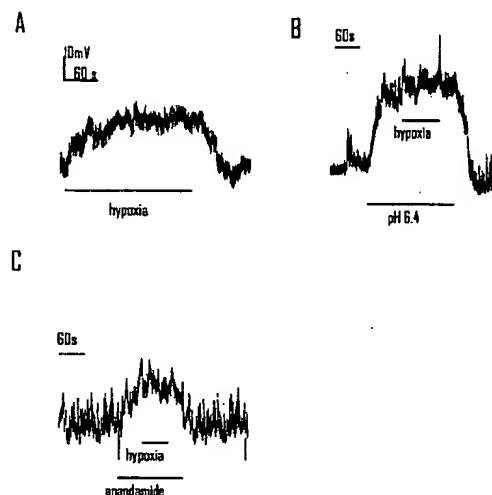


Figure 1. Modulation of hypoxic depolarization and excitability. A, Sample recording of membrane potential under current-clamp conditions. For the period represented by the horizontal bar, perfusate PO₂ was reduced from 150 to ~30 mm Hg. B and C, Similar to A, except that hypoxia was applied in the continued presence of either pH 6.4 (B) or 1 µmol/L anandamide (C). Scale bar shown in A applies also to B and C. Each experiment was repeated at least 5 times with similar results.

Results

Acute Hypoxia Depolarizes Cerebellar Granule Neurons

Exposure of cells to acute hypoxia resulted in a reversible and highly reproducible depolarization (mean value, 14.2 ± 2.6 mV; *n*=5; *P*<0.01), as exemplified in Figure 1A (see also the Table). Such a depolarization is consistent with an inhibitory effect of hypoxia on channels that set the resting membrane

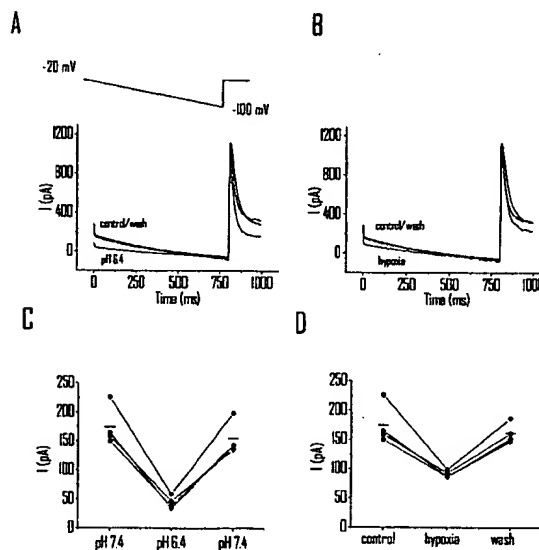


Figure 2. Effect of acidosis or hypoxia on standing outward current. A and B, Sample tracings recorded during the voltage-clamp protocol shown in the inset before, during, and after application of perfusate at pH 6.4 (A) or hypoxic perfusate (B). C and D, Current amplitudes measured at -20 mV before, during, and after application of perfusate at pH 6.4 (C) or hypoxic perfusate (D). Mean values (*n*=4) are indicated by the horizontal bars.

Membrane Potential and Input Resistance Values of Cerebellar Granule Neurons

	Control	Hypoxia	pH 6.4	Anandamide	pH 6.4 +Hypoxia	Anandamide +Hypoxia
Membrane potential, mV	-73.5±1.4 (15)	-60.7±1.7 (5)	-37.2±4.9 (5)	-56.4±2.0 (5)	-36.7±4.9 (5)	-54.9±1.6 (5)
Input resistance, MΩ	328±24 (15)	467±12 (5)	558±21 (5)	475±24 (5)	570±24 (5)	489±21 (5)

Values are mean±SEM, with number of cells shown in parentheses. Input resistance was calculated from the slope of current ramps (approximated to a straight line) evoked between 10 mV positive to and 10 mV negative to the resting membrane potential. Statistical differences (see text) were determined by paired *t* tests. For these, each experimental group had its own control values, and these are shown pooled in the table.

potential. Since it has been proposed that one member of the TASK channel family underlies the standing outward current in these cells¹⁰ and that recombinant TASK-1 is inhibited by hypoxia,¹⁵ we hypothesized that modulation of TASK-1 activity by hypoxia would explain this observation. Therefore, we used maneuvers designed to modulate selectively TASK-1 activity and investigated the effect of these on hypoxia-evoked depolarization. The effects of hypoxia on the membrane potential were mimicked by extracellular acidification (Figure 1B and Table). Thus, reducing extracellular pH from 7.4 to 6.4 (which inhibits recombinant TASK-1 channels by >80%¹⁵) produced a significant depolarization of 35±4 mV (*n*=5; *P*<0.001; Figure 1B and Table). Importantly, when hypoxia was applied to cells already depolarized at a pH of 6.4, no further significant effect on membrane potential was observed (Figure 1B and Table). Similarly, subjecting cells to a discriminating concentration (1 μmol/L) of the selective TASK-1 blocker anandamide¹⁸ also resulted in marked depolarization (16.7±4 mV; *n*=5; *P*<0.001) and prevented further significant depolarization by acute hypoxia (Figure 1C and Table). These data show clearly that an acid- and anandamide-sensitive current is inhibited by hypoxia and strongly suggest that TASK-1 is the channel underlying this conductance. To confirm this hypothesis and identify definitively the nature of this hypoxia-sensitive current, we studied hypoxic modulation of the standing outward current using voltage clamp.

Standing Outward Current Is Hypoxia Sensitive

In confirmation of previous suggestions that the standing outward current is the acid-sensitive TASK-1,^{10,11} Figures 2 and 4 demonstrate that either reducing extracellular pH to 6.4 or application of anandamide causes significant current depression. Thus, at physiological pH of 7.4, cerebellar granule neurons, held at -20 mV, had mean outward current and current density of 218±13 pA and 97.7±0.1 pA/pF, respectively (*n*=34). The effect of extracellular acidification on this standing outward current is shown in the sample tracing of Figure 2A. Reducing pH from 7.4 to 6.4 resulted in a substantial and reversible decrease in the current (Figure 2A and 2C) but was without significant effect on the voltage-gated currents that were activated on return of the membrane potential to -20 mV after the hyperpolarizing ramp (Figure 2A). This current was also sensitive to inhibition by the muscarinic receptor agonist carbachol (100 μmol/L), which gave rise to a 55±1% decrease in the standing outward current (*n*=4; *P*<0.001; data not shown). When cells were exposed to hypoxia, a similar inhibition of the standing outward current was seen (Figure 2B and 2D). This suggests that the TASK-1 currents are O₂ sensitive in these neurons. To ensure that noninactivating voltage-gated K⁺ channel currents (eg, delayed rectifier) did not contribute to the O₂-sensitive component of the standing outward current,

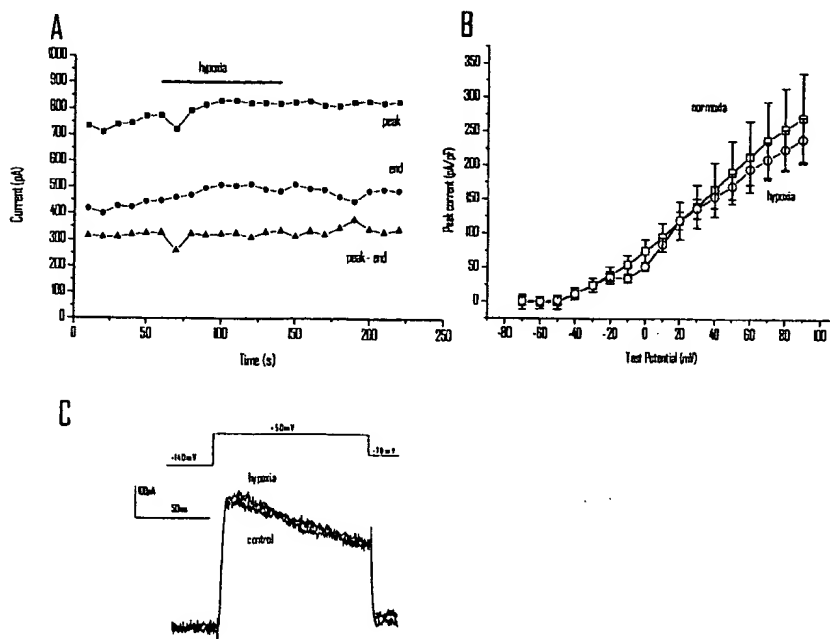


Figure 3. Lack of effect of hypoxia on voltage-gated K⁺ currents. **A**, Typical time course of current amplitudes measured on depolarization to +50 mV. Cells were held at -70 mV and, after a 5-minute waiting period to allow for run-down of the TASK current, prepulsed to -140 mV before test depolarizations. **B**, Mean current-voltage relationships for the peak current measured in 9 cells before (open squares) and during (open circles) application of hypoxia. **C**, Mean leak subtracted K⁺ currents activated by depolarization to +50 mV before and during application of hypoxia. Current tracings were averaged from the same 9 cells used in **B**. The voltage protocol is shown above.

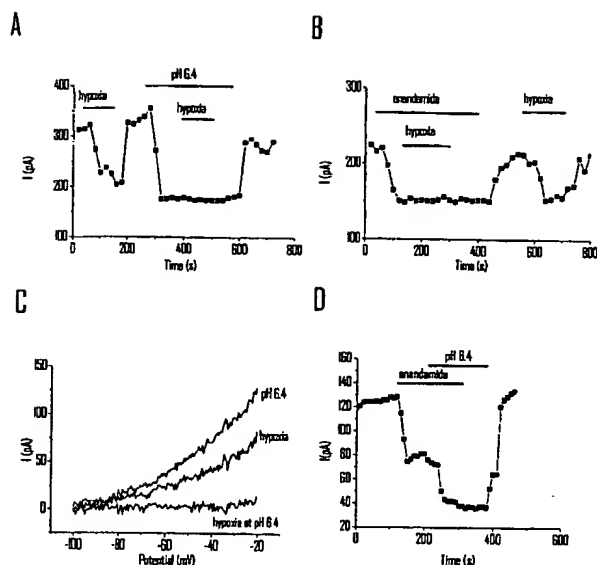


Figure 4. Acid and anandamide occlusion of hypoxic inhibition. **A** and **B**, Typical time courses of current amplitudes measured at -20 mV, showing hypoxic inhibition and its modulation in the presence of pH 6.4 (**A**) or $1 \mu\text{mol/L}$ anandamide (**B**). Periods of application are shown by horizontal bars. **C**, Mean subtracted current-voltage relationships showing the hypoxic and acid-sensitive currents ($n=4$). Also shown is the minimal residual O_2 -sensitive current in the presence of pH 6.4. **D**, Typical time course of current amplitude measured at -20 mV, showing anandamide inhibition and its modulation in the presence of pH 6.4. **A**, **B**, and **D** are representative of 5 repeated experiments in each case.

voltage-gated currents were activated by repetitive depolarizations to $+50$ mV from a prepulse potential of -140 mV with the use of conventional ruptured patch (as opposed to perforated patch) whole cell. Under these conditions, TASK currents are minimal because of "run-down" of the channel.¹⁹ No inhibition of voltage-gated currents was observed on application of hypoxia (Figure 3A and 3C). Current-voltage relationships were constructed before and during perfusion with hypoxic solutions (Figure 3B). No effect of hypoxia was seen on voltage-gated currents at any of the potentials tested. Thus, the inhibitory effect of hypoxia on K^+ channels in these cells appears to be specific for TASK and does not involve inhibition of voltage-gated channels.

To substantiate the claim that the O_2 - and acid-sensitive currents were one and the same, we investigated the effect of hypoxia in the presence of extracellular acidosis. Plotted in Figure 4A is a sample time course of the amplitude of the standing outward current during these maneuvers. Thus, exposing cells to hypoxia resulted in a rapid and reversible decrease in the current amplitude by $47 \pm 3\%$ ($n=6$; $P<0.001$). Subtraction of the ramp current recorded in hypoxia from the ramp current recorded in normoxia resulted in the difference (ie, O_2 -sensitive) current exemplified in Figure 4C. When the perfusing solution was switched from a pH of 7.4 to 6.4, a more substantial decrease in the standing current at -20 mV was observed ($75 \pm 2\%$; Figure 4A); the subtracted acid-sensitive current is shown in Figure 4C. It is noteworthy that, apart from absolute magnitude, the O_2 - and acid-sensitive current-voltage relationships appear similar (ie,

follow Goldman-Hodgkin-Katz rectification), which suggests that these currents are flowing through open rectifying K^+ channels. Importantly, exposure of cells to hypoxia at pH 6.4 produced no further significant inhibition (Figure 4A); this is seen clearly in the third tracing of Figure 4C, which plots the negligible O_2 -sensitive current at pH of 6.4.

Further evidence for the involvement of TASK-1 in the hypoxic inhibition of the standing outward current is provided by the data shown in Figure 4B. Anandamide ($1 \mu\text{mol/L}$) inhibited the standing outward current by $46 \pm 3\%$ ($n=4$). This effect was maximal because a higher concentration of anandamide ($3 \mu\text{mol/L}$) produced no further blocking effect ($n=4$; data not shown). In the presence of this discriminating concentration of anandamide ($1 \mu\text{mol/L}$), hypoxia was no longer effective (Figure 4B). The ability of anandamide to inhibit the current was absent in hypoxia. Under this condition, application of anandamide resulted in a further inhibition of only $2 \pm 1\%$ of the original current ($n=4$). Consistent with these findings for anandamide and for low pH and hypoxia were changes in cell input resistance (Table). These were calculated by approximating currents to straight lines for 10 mV positive to and 10 mV negative to the cell resting potential (Table). Thus, significant increases in input resistance were found for hypoxia ($P<0.05$), pH 6.4 ($P<0.001$), and anandamide ($P<0.01$). Furthermore, at pH 6.4 or in the presence of anandamide, no further significant increase in cell input resistance to hypoxia was observed (Table).

Even though the degree of current inhibition by low pH was much greater than the inhibition seen with anandamide, both completely occluded the effect of hypoxia. This suggests that the standing outward current in these cells is composed of more than one channel type, with only one (the anandamide-sensitive TASK-1) being inhibited by hypoxia. To address this possibility we applied anandamide and low pH to the same cell. An example of the time course for this effect is shown in Figure 4D. Extracellular acidification blocked an additional component of the standing outward current when applied in the presence of anandamide (inhibition by anandamide, $42 \pm 1\%$; inhibition by anandamide and pH 6.4, $77 \pm 4\%$; $n=4$). Furthermore, when anandamide was removed from the acidified extracellular medium, no recovery could be observed (inhibition by pH 6.4 alone, $78 \pm 3\%$; eg, Figure 4D), clearly indicating that low pH blocked the anandamide-sensitive component of current. Thus, there appear to be 2 components of the acid-sensitive standing outward current in these cells: one that is inhibited by anandamide and one that is anandamide insensitive. A recent study by Talley and coworkers²⁰ indicates that both TASK-1 and TASK-3 are highly expressed in the granule cell layer of the cerebellum, suggesting that the anandamide-insensitive current that we observe is carried by TASK-3. If such a suggestion is true, this would indicate that TASK-3 is also hypoxia insensitive in these cells.

Discussion

The standing outward current observed in cerebellar granule neurons held at a potential of -20 mV is thought to be a consequence of TASK expression. The current is sensitive to muscarinic inhibition and modulation by pH,¹⁰ and previous

studies have claimed that TASK-1 is the specific channel involved. However, these previous claims were based on positive immunoreactivity with the use of a commercially available antibody raised against TASK-1 and sensitivity to pH, a characteristic common to all expressed TASK-like channels. In this study we confirm that TASK-1 underlies a proportion of this current by showing that it can be inhibited by the endocannabinoid anandamide, a selective inhibitor of TASK-1 when used at 1 $\mu\text{mol/L}$.¹⁸ However, we also found evidence for a pH-sensitive, anandamide-insensitive current component and, on the basis of expression studies in rat brain,²⁰ suggest that this is carried by TASK-3. In addition to these findings, we show that hypoxia can selectively inhibit native TASK-1. Such an inhibition of twin pore domain K⁺ channels has previously been shown for a TASK-like current in carotid body glomus cells¹³ and TASK-3 in a human neuroepithelial cell line.¹⁴ The findings that both anandamide and pH 6.4 occluded the inhibition by hypoxia (a characteristic of recombinant TASK-1¹⁵) provide compelling evidence that inhibition of TASK-1 accounts for the reduction of the standing outward current and cell depolarization of cerebellar granule neurons. This depolarization, which is accompanied by an increase of cell input resistance (Table), is consistent with the idea that acute hypoxia, by inhibiting a hyperpolarizing conductance active at resting membrane potential, would increase neuronal excitability. However, it should also be noted that more prolonged episodes of hypoxia are likely to lead to an accumulation of K⁺ extracellularly, an effect that would in itself depolarize neurons. In addition to increasing excitatory output from these neurons, this depolarization would also facilitate the glutamatergic excitatory input into these cells by relieving Mg²⁺-dependent blockage of N-methyl-D-aspartate receptors.²¹ However, and in common with other groups, we found it difficult to activate repetitive, all-or-none action potentials in these cultured neurons. Such poor excitability has been shown to be a consequence of the damping effect of the relatively large voltage-gated K⁺ channel current that these cells exhibit.²² This does not diminish the importance of our suggestion that the increased excitability observed in hypoxia/ischemia is likely due to inhibition of TASK-1.

There are potential pathological consequences arising from inhibition of TASK-1 in cerebellar granule neurons. The depolarization caused may lead to increased firing patterns, which in turn could cause excitotoxicity via excess glutamate release (this is especially so since the cell input resistance increases), a major determinant of ischemic cell death in central neurons.²³ Indeed, transient depolarizations during hypoxia have been demonstrated in more intact central neuronal preparations.²⁴ However, hyperpolarizations have also been reported, arising because of activation of ATP-dependent and Ca²⁺-sensitive K⁺ channels, although it should be noted that these studies examined the effects of anoxia, not hypoxia.²⁴ Clearly, neuronal responses to acute hypoxic/ischemic episodes are complex.^{2,23} However, since TASK-1 appears to be a major determinant of cell input resistance and membrane potential, its specific inhibition by acute hypoxia is likely to be a major contributory factor in the overall response of neurons during infarction; as such, it represents a potentially important therapeutic target for treatment of conditions characterized by ischemia/hypoxia, such as stroke.

Acknowledgments

This work was funded by the Wellcome Trust, the Medical Research Council, and the British Heart Foundation. Leigh D. Plant is a Medical Research Council scholar.

References

- Haddad GG, Jiang C. O₂-sensing mechanisms in excitable cells: role of plasma membrane K⁺ channels. *Annu Rev Physiol*. 1997;59:23–42.
- Lipton P. Ischemic cell death in brain neurons. *Physiol Rev*. 1999;79:1431–1568.
- Lesage F, Lazdunski M. Molecular and functional properties of two-pore-domain potassium channels. *Am J Physiol*. 2000;793:F793–F801.
- Duprat F, Lesage F, Fink M, Reyes R, Heurteaux C, Lazdunski M. TASK, a human background K⁺ channel to sense external pH variations near physiological pH. *EMBO J*. 1997;16:5464–5471.
- Reyes R, Duprat F, Lesage F, Fink M, Salinas M, Farman N, Lazdunski M. Cloning and expression of a novel pH-sensitive two pore domain K⁺ channel from human kidney. *J Biol Chem*. 1998;273:30863–30869.
- Kim Y, Bang H, Kim D. TASK-3, a new member of the tandem pore K⁺ channel family. *J Biol Chem*. 2000;275:9340–9347.
- Decher N, Maier M, Dittich W, Gassenhuber J, Bruggemann A, Busch AE, Steinmeyer K. Characterization of TASK-4, a novel member of the pH-sensitive, two-pore domain potassium channel family. *FEBS Lett*. 2001;492:84–89.
- Ashmole I, Goodwin PA, Stanfield PR. TASK-5, a novel member of the tandem pore K⁺ channel family. *Pflugers Arch*. 2001;442:828–833.
- Vega-Saenz DM, Lau DH, Zhadina M, Pountney D, Coetzee WA, Rudy B. KT3.2 and KT3.3, two novel human two-pore K⁺ channels closely related to TASK-1. *J Neurophysiol*. 2001;86:130–142.
- Millar JA, Barratt L, Southan AP, Page KM, Fyffe RE, Robertson B, Mathie A. A functional role for the two-pore domain potassium channel TASK-1 in cerebellar granule neurons. *Proc Natl Acad Sci U S A*. 2000;97:3614–3618.
- Brickley SG, Revilla V, Cull-Candy SG, Wisden W, Farrant M. Adaptive regulation of neuronal excitability by a voltage-independent potassium conductance. *Nature*. 2001;409:88–92.
- Lopez-Barneo J, Pardal R, Ortega-Saenz P. Cellular mechanism of oxygen sensing. *Annu Rev Physiol*. 2001;63:259–287.
- Buckler KJ, Williams BA, Honore E. An oxygen-, acid- and anaesthetic-sensitive TASK-like background potassium channel in rat arterial chemoreceptor cells. *J Physiol*. 2000;525:135–142.
- Hartness ME, Lewis A, Searle GJ, O'Kelly I, Peers C, Kemp PJ. Combined antisense and pharmacological approaches implicate hTASK as an airway O₂ sensing K⁺ channel. *J Biol Chem*. 2001;276:26499–26508.
- Lewis A, Hartness ME, Chapman CG, Fearon IM, Meadows HJ, Peers C, Kemp PJ. Recombinant hTASK-1 is an O₂-sensitive K⁺ channel. *Biochem Biophys Res Commun*. 2001;285:1290–1294.
- Held B, Pocock JM, Pearson HA. Endothelin-1 inhibits voltage-sensitive Ca²⁺ channels in cultured rat cerebellar granule neurones via the ET-A receptor. *Pflugers Arch*. 1998;436:766–775.
- Ramsden M, Plant LD, Webster NJ, Vaughan PFT, Henderson Z, Pearson HA. Differential effects of soluble and aggregated A β_{1-40} on K⁺ channel currents in primary cultures of rat cerebellar granule and cortical neurones. *J Neurochem*. 2001;79:699–712.
- Maingret F, Patel AJ, Lazdunski M, Honore E. The endocannabinoid anandamide is a direct and selective blocker of the background K⁺ channel TASK-1. *EMBO J*. 2001;20:47–54.
- Watkins CS, Mathie A. Effects on K⁺ currents in rat cerebellar granule neurones of a membrane-permeable analogue of the calcium chelator BAPTA. *Br J Pharmacol*. 1996;118:1772–1778.
- Talley EM, Solorzano G, Lei Q, Kim D, Bayliss DA. CNS distribution of members of the two-pore-domain (KCNK) potassium channel family. *J Neurosci*. 2001;21:7491–7505.
- Mayer ML, Westbrook GL, Guthrie PB. Voltage-dependent block by Mg²⁺ of NMDA responses in spinal cord neurones. *Nature*. 1984;309:261–263.
- Shibata R, Nakahira K, Shibasaki K, Wakazono Y, Imoto K, Ikenaka K. A-type K⁺ current mediated by the Kv4 channel regulates the generation of action potential in developing cerebellar granule cells. *J Neurosci*. 2000;20:4145–4155.
- Nicholls DG, Budd SL. Mitochondria and neuronal survival. *Physiol Rev*. 2000;80:315–360.
- Erdemli G, Xu YZ, Krnjevic K. Potassium conductance causing hyperpolarization of CA1 hippocampal neurons during hypoxia. *J Neurophysiol*. 1998;80:2378–2390.

David C. Warltier, M.D., Ph.D., Editor

Anesthesiology 2001; 95:1013-21

© 2001 American Society of Anesthesiologists, Inc. Lippincott Williams & Wilkins, Inc.

Anesthetic-sensitive 2P Domain K^+ Channels

Amanda J. Patel, Ph.D.,* Eric Honoré, Ph.D.†

VOLATILE anesthetics induce neuron hyperpolarization and consequent depression of the central nervous system.¹⁻¹⁰ In addition to the well-known potentiation of γ -aminobutyric acid type A and glycine chloride channels,^{2,3} evidence demonstrates that in both invertebrates and vertebrates, volatile anesthetics open background K^+ channels and thus increase the resting membrane potential.^{8,9,11,12} For instance, in the mollusk *Lymnaea*, halothane opens a class of baseline K^+ channels (IKAn) that hyperpolarize and silence pacemaker neurons (figs. 1A and B).^{9,11,13} In *Aplysia californica*, halothane-mediated neuronal hyperpolarization is caused by the opening of the background S-type (serotonin-sensitive) K^+ channel.¹² Similarly, opening of baseline acid-sensitive K^+ channels by volatile anesthetics produces rat hypoglossal and locus coeruleus neuron hyperpolarization.^{8,14}

Recent reports demonstrate that the volatile anesthetic-sensitive background K^+ channels belong to the family of mammalian K^+ channel subunits with four transmembrane segments and two P regions (fig. 2 and table 1).^{8,15-17} Interestingly, the yeast 2P domain K^+ channel, which is characterized by eight instead of four transmembrane segments, is also activated by volatile anesthetics, demonstrating the conservation of this pharmacology.^{18,19} The mammalian 2P domain K^+ channel subunits are characterized by diverse patterns of expression and functional properties.^{8,15,20-24} Volatile anesthetics selectively open human TREK-1, TREK-2, TASK-1, TASK-2, TASK-3, and TALK-2 channels.^{15-17,25,26} On the contrary, local anesthetics reversibly inhibit the 2P domain K^+ channels.²⁶⁻²⁹ In the current report, the expression and properties of these anesthetic-sensitive K^+ channels are reviewed, and their possible functional role in the mechanisms of anesthesia and analgesia is discussed.

Mammalian 2P Domain K^+ Channels

Mammalian K^+ channels belong to three main structural classes made of two, four, or six transmembrane segments (TMSs).^{30,31} The common feature of all K^+ channels is the presence of a conserved motif called the P domain (the K^+ channel signature sequence or putative pore-forming region), which is part of the K^+ conduction pathway.³² The two TMS and six TMS classes are characterized by the presence of a single P domain, whereas the most recently discovered class of four TMS subunits is characterized by the presence of a tandem of P domains (fig. 2A).^{30,31} Functional K^+ channels are tetramers of pore-forming subunits for the two and six TMS classes and possibly dimers in the case of the four TMS class.³³

The 2TMS-1P K^+ channels encode the inward rectifiers. These K^+ channels close with depolarization because of channel block by intracellular Mg^{2+} and polyamines (for review, see report by Ruppersberg³⁴). The conductance increases on hyperpolarization, and, consequently, the inward K^+ currents recorded at potentials below the equilibrium potential E_{K^+} (approximately -90 mV in a physiological K^+ gradient) are much larger than the outward K^+ currents recorded at depolarized potentials. Although the amplitude of the outward currents flowing through the inward rectifiers is limited, they will have a major influence on the resting membrane potential.³⁵ The voltage at which channel gating by intracellular Mg^{2+} and polyamines occurs will set the range in which the K^+ channel will influence the cell membrane potential. Because they are blocked at depolarized potentials, these channels will have a small but limited role in the repolarization of the action potential.

By contrast, the outward rectifiers encoded by the 6TMS-1P subunits open on depolarization (Kv channels) and after intracellular Ca^{2+} increase (BK and SK channels). Depolarization is sensed by the positively charged fourth TMS of Kv channels, which is coupled to activation gates. Opening of the voltage-gated K^+ channels is time-dependent (delayed rectifiers) and contributes to repolarize and terminate the action potential.³⁵ Several voltage-gated K^+ channels are also characterized by a fast (N-type) inactivation process. The inactivation gate is the positively charged amino terminus of these specific subunits (ball-and-chain mechanism).

* Senior Scientist, †Director of Research.

Received from the Institut de Pharmacologie Moléculaire et Cellulaire, Centre National de la Recherche Scientifique—Unité mixte de recherche 6097, Valbonne, France. Submitted for publication January 19, 2001. Accepted for publication May 21, 2001. Support was provided solely from institutional and/or departmental sources.

Address reprint requests to Dr. Honoré: Institut de Pharmacologie Moléculaire et Cellulaire, CNRS-UMR6097, 660 route des Lucioles, Sophia Antipolis, 06560 Valbonne, France. Address electronic mail to: honore@ipmc.cnrs.fr. Individual article reprints may be purchased through the Journal Web site, www.anesthesiology.org.

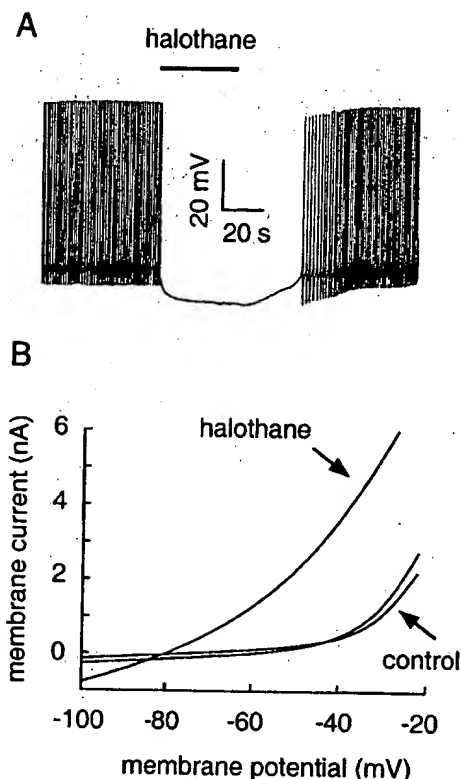


Fig. 1. Halothane opens background K^+ channels and hyperpolarizes specific neurons. (A) Anesthetic concentrations of halothane reversibly block the endogenous firing activity of a pacemaker neuron in *Lymnaea*. (Adapted with permission from Franks and Lieb.⁹) (B) Current-voltage relations for a typical *Lymnaea* isolated anesthetic-sensitive neuron in the presence of 1.4 mM halothane. The current-voltage relations in control (before the addition of halothane) and after washout are illustrated. (Adapted with permission from Lopes *et al.*¹¹)

The class of mammalian 4 TMS K^+ channel subunits has expanded to include 14 members (fig. 2B and table 1). These subunits share the same structural motif with 4TMS-2P, an extended M1P1 extracellular loop, and both amino and carboxy termini facing the cytosol. However, low sequence identity is found outside the pore domain.³⁰ The mammalian 2P domain K^+ channels are classified into five main structural subgroups: (1) TWIK-1, TWIK-2, and KCNK7³⁶⁻⁴⁰ (KCNK7 is not functional); (2) TASK-1, TASK-3, and KT 3-3 (Acc No.: NM 022358; expression has not been reported)^{21,23,28,41-43}; (3) TREK-1, TREK-2, and TRAAK^{17,20,44,45}; (4) TASK-2, TALK-1, and TALK-2 (also called TASK-4)^{16,25,46,47}; and (5) THIK-1 and THIK-2⁴⁸ (THIK-2 is not functional) (fig. 2B). 2P domain K^+ channels have also been identified in *Drosophila* and *Caenorhabditis elegans*.⁴⁹⁻⁵¹ In the nematode, approximately 50 of 80 K^+ channel subunits belong to the 2P domain family.^{49,52} In the *Drosophila*, 11 of 30 K^+ channel subunits belong to the 2P domain family.⁵³ Very little conservation (< 35%) is found between nematode, *Drosophila*, and human sequences.

TWIK-1, the first mammalian 2P domain K^+ channel to be identified, self-associates to form disulfide-bridged homodimers.³³ The extracellular M1P1 interdomain, predicted to form an amphipathic helix, promotes self-dimerization. A cysteine located in this domain appears to be important for the dimerization of some, but not all 2P domain K^+ channels, for instance, TASK-1.³³ A dimer contains 4P domains, which are essential in the formation of K^+ -selective pores. No evidence for heteromultimerization has yet been reported for the 2P domain K^+ channels.

Leak channels, which are opened pores in the membrane, have no voltage or time dependency by definition.³⁵ Activation is instantaneous on depolarization as the channels are always opened at rest. Because of an asymmetrical physiological K^+ gradient (approximately 150 mM intracellular and 5 mM extracellular), the current-to-voltage relation of a K^+ leak channel is predicted to be outwardly rectifying (Goldman, Hodgkin, and Katz constant-field theory, also called the open rectification) (fig. 2C).³⁵ In a symmetrical K^+ gradient, the current-to-voltage relation of the leak channel is expected to be linear, as observed for TASK-1, TRAAK, and TALK-1 (fig. 2C). These K^+ channels thus behave as open rectifiers. Because of this leak characteristic, the background 4TMS-2P K^+ channels are expected to influence both the resting membrane potential (along with the inward rectifiers) and the repolarization phase of the action potential (along with the voltage-gated and Ca^{2+} -activated outward rectifiers). Several 4TMS-2P background K^+ channels are, however, more than a simple open rectifier leak channel (figs. 2D and E). For instance, TREK-1 is a K^+ channel that displays a strong outward rectification in a symmetrical K^+ gradient (fig. 2D).^{20,29} This rectification is at least partly caused by a voltage-dependent gating.²⁹ Similar outward rectification has also been observed for TALK-2, TASK-2, TREK-2, and TASK-3.^{17,25,28,46} Moreover, the activation of TASK-2 and TREK-2 is time-dependent.^{16,17,46} On the contrary, TWIK-2 shows a mild inward rectification when recorded in a symmetrical K^+ gradient (fig. 2E).³⁷ Mild inward rectification is also typical to TWIK-1 and THIK-1.^{36,48} TWIK-2 is additionally characterized by a time-dependent inactivation.³⁷ The various 4TMS-2P channels will differentially tune the resting potential or the action potential duration because of these particular rectification-, time-, and voltage-dependent properties.

Mechano-gated TREK-1 and TREK-2 K^+ Channels are Opened by Inhalational Anesthetics

Human TREK-1 is highly expressed in brain and ovary and to a lesser extent in kidney and small intestine.^{15,17,54,55} In human brain, TREK-1 shows the greatest expression in the caudate nucleus, the putamen, the spinal cord, and the dorsal root ganglia (fig. 3).^{17,55} At the protein level, TREK-1 is present at both synaptic and

Table 1. Nomenclature of Mammalian 2P Domain K⁺ Channels

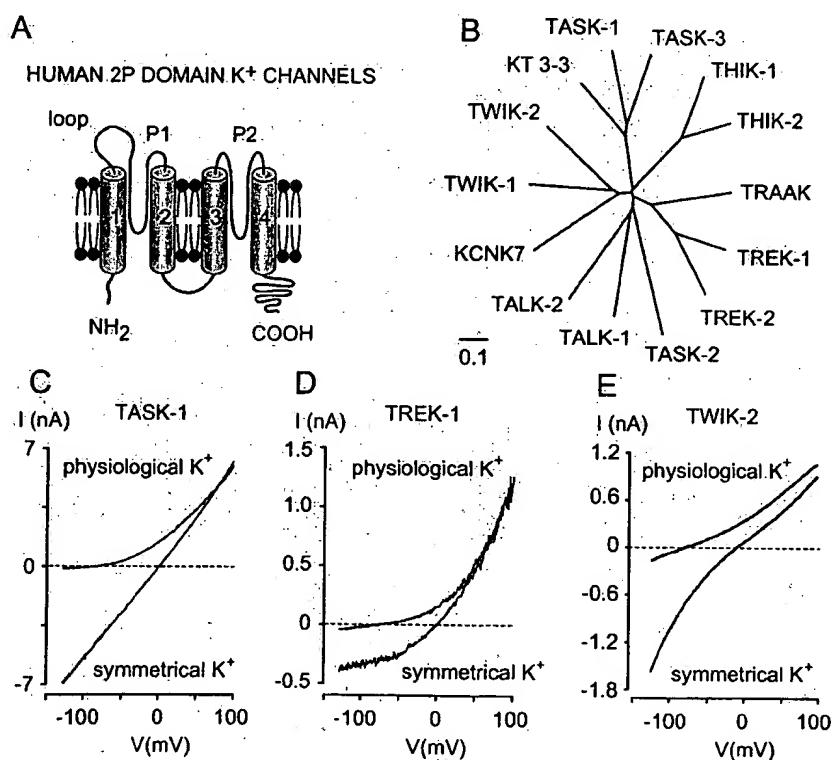
Original Abbreviations	Original Names	Hugo Nomenclature	Human Chromosomal Localization
TWIK-1	Tandem of P domains in a weak inward rectifying K ⁺ channel-1	KCNK1	1q42-q43
TWIK-2	Tandem of P domains in a weak inward rectifying K ⁺ channel-2	KCNK6	19q13.1
KCNK-7		KCNK7	11q13
TREK-1	TWIK-1-related K ⁺ channel-1	KCNK2	1q41
TREK-2	TWIK-1-related K ⁺ channel-2	KCNK10	14q31
TRAAK	TWIK-related arachidonic acid-stimulated K ⁺ channel	KCNK4	11q13
TASK-1	TWIK-related acid-sensitive K ⁺ channel-1	KCNK3	2p23
TASK-3	TWIK-related acid-sensitive K ⁺ channel-3	KCNK9	8q24.3
TASK-2	TWIK-related acid-sensitive K ⁺ channel-2	KCNK5	6p21
TALK-1	TWIK-related alkaline pH activated K ⁺ channel-1	KCNK16	6p21
TALK-2	TWIK-related alkaline pH activated K ⁺ channel-2	KCNK17	6p21
THIK-1	Tandem pore domain halothane inhibited K ⁺ channel-1	KCNK13	14q24.1-14q24.3
THIK-2	Tandem pore domain halothane inhibited K ⁺ channel-2	KCNK12	2p22-2p21

nonsynaptic sites in mouse brain.^{22,56,57} Significant expression is also detected in both small and medium sensory neurons of mouse dorsal root ganglia.²² Human TREK-2 (78% of homology with TREK-1) is abundantly expressed in kidney and pancreas and more moderately in testis, brain, colon, and small intestine.¹⁷ In human brain, TREK-2 shows the strongest expression in the caudate nucleus, the cerebellum, the corpus callosum, and the putamen (fig. 3).^{17,55} Some tissues only express TREK-1 (ovary) or TREK-2 (pancreas, colon).¹⁷ Other tissues do not express these channels or only to very modest levels (heart, skeletal muscle, lung, blood leuko-

cytes, and spleen). Finally, some tissues present overlapping expression (brain, kidney, small intestine).

TREK-1 and TREK-2 channels are mechano-gated K⁺ channels opened by membrane stretch.^{17,22,29,44} At the whole cell level, TREK-1 is modulated by cellular volume.^{22,29} Mechanical force is believed to be transmitted directly to the channel *via* the lipid bilayer.^{29,58} Lowering intracellular pH shifts the pressure-activation relation of TREK-1 and TREK-2 toward positive values and ultimately leads to channel opening at atmospheric pressure.^{17,59} Acidosis essentially converts a TREK mechano-gated channel into a constitutively active background

Fig. 2. The human 2P domain K⁺ channel subunits. (A) Membrane topology of a background K⁺ channel with four trans-membrane segments and two P domains. Both amino and carboxy termini are intracellular. (B) Phylogenetic tree of the human 2P domain K⁺ channels. (C) I-V curves of TASK-1, an open rectifier, constructed with voltage ramps of 600 ms in duration from -120 to 100 mV in a physiological (150 mM K⁺ intracellular and 5 mM K⁺ extracellular) and in a symmetrical K⁺ gradient (150 mM K⁺ intracellular and 150 mM K⁺ extracellular). (D) I-V curves of TREK-1, an outward rectifier. (E) I-V curves of TWIK-2, a mild inward rectifier.



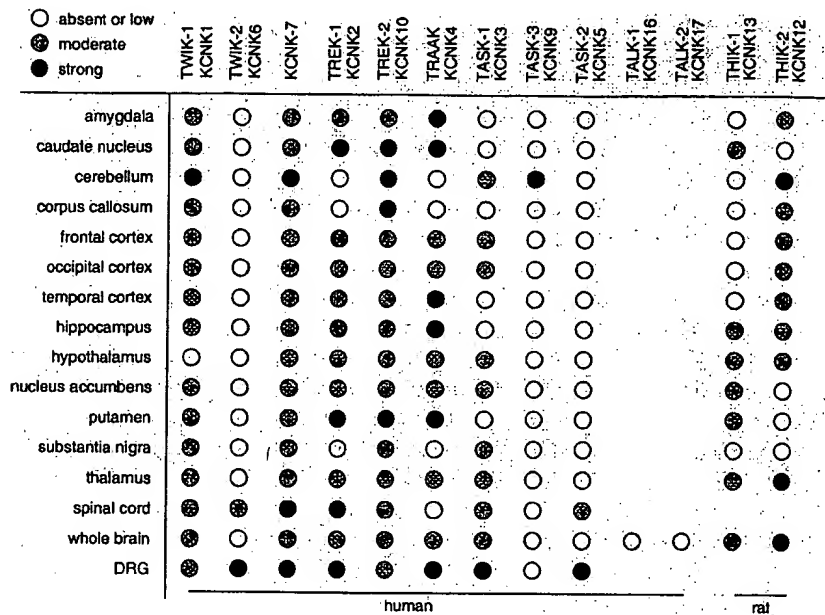


Fig. 3. Pattern of expression of 2P domain K^+ channels in the nervous system. In the absence of symbol, the expression has not been determined. Adapted from Girard *et al.*,²⁵ Rajan *et al.*,⁴⁸ and Medhurst *et al.*⁵⁵

K^+ channel.^{17,59} TREK-1 is also gradually and reversibly opened by heat. An increase in temperature of 10°C enhances TREK-1 current amplitude by approximately sevenfold.²² Finally, TREK-1, TREK-2, and TRAAK are reversibly opened by polyunsaturated fatty acids and lysophospholipids, including arachidonic acid and lysophosphatidylcholine (fig. 4).^{17,29,44,45,60} Deletional analysis demonstrates that the carboxy terminus, but not the amino terminus and the extracellular MIP1 loop, is critical for activation of TREK-1 by stretch, arachidonic acid, lysophospholipids, intracellular acidosis, and temperature.^{22,29,59} TREK-1 and TREK-2 activation are reversed by protein kinase A stimulation.^{17,20,22,29,60} Protein kinase A-mediated phosphorylation of Ser333 in the carboxy terminus mediates TREK-1 closing.²⁹ TREK-1 and TREK-2 are insensitive to most of the classical K^+ channel blockers, including tetraethylammonium (TEA^+ ; 10 mM), 4-aminopyridine (4-AP; 3 mM), Ba^{2+} (1 mM), glibenclamide (10 μ M), charybdotoxin (1 μ M), and apamin (10 μ M). TREK-1 is reversibly blocked by Gd^{3+} (30 μ M), amiloride (2 mM), and chlorpromazine (10 μ M).^{29,45,60}

TREK-1 and TREK-2 are opened by chloroform, diethyl ether, halothane, and isoflurane in transfected mammalian cells (figs. 4 and 5A).^{15,17,29} Opening of these channels by anesthetics induces cell hyperpolarization (fig. 5B). Interestingly, the other structurally and functionally related 2P domain K^+ channel, TRAAK, is insensitive to volatile anesthetics.¹⁵ Human TREK-1 is most sensitive to chloroform (2.3-fold increase in current amplitude at 1 mM), whereas halothane is the strongest opener of human TREK-2 (2.3-fold increase at 1 mM).^{15,17} In excised outside-out patches, the 48 pS TREK-1 channel is reversibly opened in a dose-dependent manner by chloroform and halothane (fig. 5C).¹⁵ No channel activity is observed in the absence of anesthetic, suggesting that it

converts inactive channels to active ones. Deletion of the amino terminus does not affect anesthetic-induced TREK-1 opening.¹⁵ In contrast, deletion of the carboxy terminus at Thr 322 completely suppresses responses to both chloroform and halothane.¹⁵ These results demonstrate that the carboxy terminus, but not the amino terminus, of TREK-1 is critical for anesthetic activation.

TREK-1 and TREK-2 share all the functional properties of the anesthetic-sensitive background K^+ channels in *Lymnaea* pacemaker neurons and the S channel in *Aplysia* sensory neurons (fig. 1B).^{9,11,12} Both endogenous

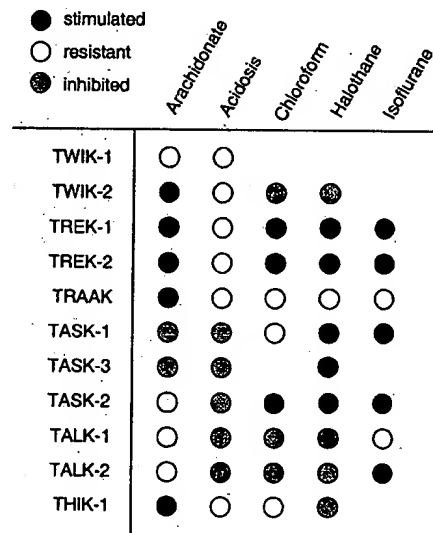
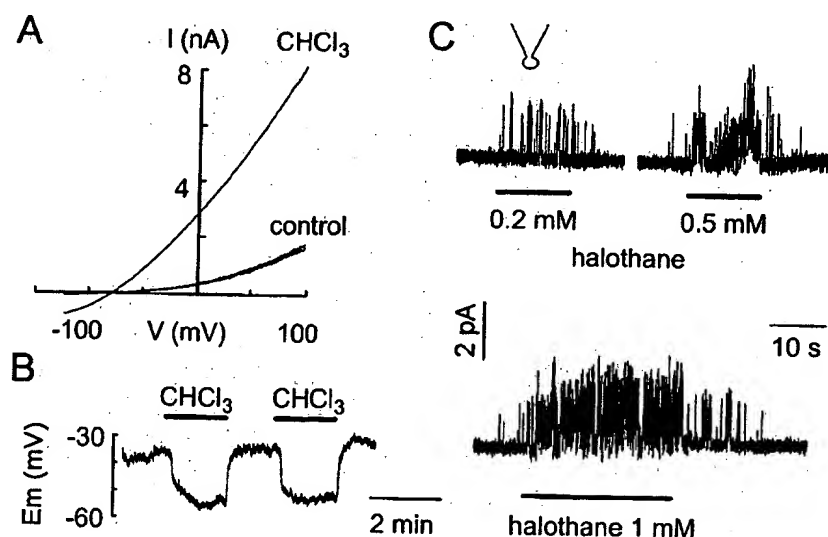


Fig. 4. Sensitivity of mammalian 2P domain K^+ channels to arachidonic acid, extracellular acidosis, chloroform, halothane, and isoflurane. In the absence of symbol, the properties of the channel have not been determined. Adapted from Patel *et al.*,¹⁵ Gray *et al.*,¹⁶ Girard *et al.*,²⁵ Patel *et al.*,³⁷ Kim *et al.*,⁴¹ and Rajan *et al.*⁴⁸

Fig. 5. TREK-1 is opened by general anesthetics. (A) Chloroform (0.8 mM) stimulates whole cell TREK-1 currents recorded in transfected epithelial cells. (B) Chloroform (0.8 mM) reversibly hyperpolarizes a cell expressing TREK-1. (C) Increasing concentrations of halothane reversibly open TREK-1 channels in an excised outside-out patch. (Adapted with permission from Patel *et al.*¹⁵)



and cloned background K⁺ channels are opened by volatile anesthetics in excised patches, suggesting a direct mechanism of action (fig. 5C).^{12,15} Moreover, the lack of effect of volatile anesthetics on TRAAK, another mechano-gated polyunsaturated fatty acid-sensitive 2P domain K⁺ subunit, suggests that an indirect membrane effect is unlikely.¹⁵ Pure optical isomers of the volatile anesthetic isoflurane show clear stereoselectivity in activating background K⁺ currents in pacemaker neurons of the *Lymnaea*.¹³ The + isomer is more potent than the - isomer in hyperpolarizing neurons, suggesting that volatile anesthetics act by direct binding to the protein rather than a nonspecific perturbation of lipids.¹³ Although the stimulation by inhalational anesthetics seems to be direct, one cannot fully rule out possible indirect effects.^{11,12,15} Indeed, it has been shown in *Lymnaea* neurons that, although the activation of IKAn by volatile anesthetics is independent of the lipoxygenase and cyclooxygenase pathways, it might involve the cytochrome P450 pathway.¹¹ Moreover, TREK-1 is not sensitive to volatile anesthetics when expressed in *Xenopus* oocytes.¹⁶ These negative results may indicate that either a specific membrane environment or critical cofactors, which are absent in *Xenopus* oocytes but present in mammalian cells, may be required.

Acid-sensitive Background K⁺ Channels TASK-1 and TASK-3 Are Opened by Volatile Anesthetics

Human TASK-1 is particularly abundant in the pancreas and the placenta.²¹ Lower levels of expression are found in brain, lung, prostate, heart, kidney, uterus, small intestine, and colon. High concentrations of TASK-1 are found in cerebellar and olfactory granule cells, olfactory tubercles, scattered neurons through all layers of cerebral cortex, intralaminar thalamic nuclei, pontine nuclei, and the locus coeruleus of the rat.^{8,21} Brainstem and spinal cord motoneurons display the strongest expression of TASK-1.⁸ Motor nuclei with high concentrations

of TASK-1 include facial, hypoglossal, ambigular, and motor trigeminal, as well as the vagal motor nucleus. TASK-1 is also particularly abundant in rat carotid body cells.⁶¹ In human brain, the strongest expression is found in the cerebellum, thalamus, and pituitary gland (fig. 3).⁵⁵ TASK-1 is also particularly abundant in human dorsal root ganglia.⁵⁵ Human TASK-3, which is 62% identical to TASK-1, is largely and selectively expressed in the cerebellum.^{42,55}

TASK-1 and TASK-3 K⁺ currents are instantaneous (or at least very rapidly activating^{28,62}) and non-inactivating.^{8,21,23,26,41,43} TASK-1 and TASK-3 are background K⁺ currents that are very sensitive to variations in extracellular pH (fig. 2C).^{8,21,23,26,28,41} Half of TASK-1 and TASK-3 channels are closed at pH values of 7.3 and 6.5, respectively.^{8,21,23,26,41,43} TASK-1 is inhibited by Zn²⁺, the local anesthetic bupivacaine, the anticonvulsant phenytoin, quinidine, and Ba²⁺.^{8,21,23,43} However, it is resistant to TEA⁺ and 4-AP. TASK-1 is inhibited by receptors coupled to Gq proteins, including the M3 muscarinic receptor.^{63,64} The second messenger involved in channel inhibition is still unknown. The endocannabinoid anandamide has recently been shown to be a direct and selective blocker of TASK-1.⁶⁵ It has been suggested that anandamide might be involved in receptor-induced down-modulation of TASK-1.⁶⁵ TASK-3 is blocked by lidocaine, bupivacaine, barium, and quinidine but resistant to tetraethylammonium.^{26,28,41}

TASK-1 is opened by halothane and isoflurane but is insensitive to chloroform and partially inhibited by diethylether (figs. 6A and B).^{8,15} Halothane opens TASK-1 in the excised patch configuration despite a strong run-down of channel activity on excision (fig. 6C).¹⁵ Deletion of the last 147 amino acids in the carboxy terminus of TASK does not alter halothane sensitivity, whereas further deletion kills channel activity. Fusing the carboxy terminus of TREK-1 restores basal but not anesthetic-stimulated activity, demonstrating that the region lo-

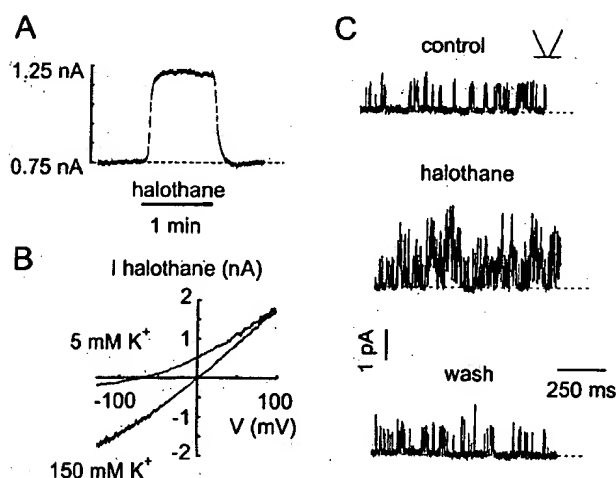


Fig. 6. TASK-1 is opened by halogenated inhalational anesthetics. (A) Halothane (1 mM) stimulates TASK-1 current in a transfected cell voltage clamped at 0 mV. (B) Halothane (1 mM)-stimulated I-V curves recorded in both physiological and symmetrical K⁺ gradients. (C) Halothane (1 mM) stimulates TASK-1 opening in an excised inside-out patch. (Adapted with permission from Patel *et al.*¹⁵)

cated between residues 242 and 248 (VLRFMF) is critical for anesthetic sensitivity.¹⁵

A background K⁺ current sets the resting membrane potential in type I carotid body chemoreceptor cells.^{61,66} Reversible inhibition of this background K⁺ current by hypoxia or acidosis induces membrane depolarization. Depolarization of type I cells leads to opening of voltage-gated Ca²⁺ channels, an increase in intracellular Ca²⁺, and release of neurotransmitters, including dopamine.⁶⁷ The released neurotransmitters stimulate sinus nerve endings and trigger the reflex increase in respiration. The endogenous background K⁺ channel in type I cells shares the biophysical and pharmacologic properties of TASK-1.⁶¹ It is reversibly inhibited by mild external acidosis, time- and voltage-independent, resistant to TEA⁺ and 4-AP, but blocked by Ba²⁺, Zn²⁺, bupivacaine, and quinidine. Moreover, the type I cell background K⁺ current is enhanced by halothane but is insensitive to chloroform.⁶¹ Opening of TASK-1-like background K⁺ channels in type I carotid body cells may be partially responsible for the suppression of hypoxic ventilatory drive during general anesthesia.

In rat somatic motoneurons, locus coeruleus neurons, and cerebellar granule neurons, inhalational anesthetics similarly activate a background TASK-1-like conductance, causing membrane hyperpolarization and suppressing action potential discharge (figs. 7A and B).^{8,65} These effects occur at clinically relevant anesthetic concentrations with the steep dose dependence expected for anesthetic effects of these compounds.⁸ External acidosis to pH 6.5 completely blocks the current activated by anesthetics (fig. 7B, inset).^{8,65} In motoneurons and cerebellar granule neurons, opening of TASK-1 channels may contribute to anesthetic-induced immobiliza-

tion, whereas in the locus coeruleus, it may support analgesic and hypnotic actions.⁸

Application of 1 mM halothane reversibly potentiates human TASK-3 current amplitude by 66%.²⁶ The onset of halothane stimulation in *Xenopus* oocyte is rapid (τ : 62 s), whereas full recovery takes as long as 5 min. By contrast, the neurosteroidal anesthetic alphaxalone inhibits TASK-3.²⁶ Pentobarbital and ketamine do not significantly affect TASK-3 at a concentration of 100 μ M.²⁶

Spinal Cord and Dorsal Root Ganglion Background K⁺ Channel TASK-2 Is Opened by Inhalational Anesthetics

Human TASK-2 is found in kidney, pancreas, lung, and placenta.⁴⁶ Although TASK-2 expression is weak in whole brain, it can be detected by polymerase chain reaction in rat spinal cord.¹⁶ TASK-2 is found throughout the spinal cord in both ventral and dorsal sections.¹⁶ Moreover, TASK-2 is expressed in high concentrations in

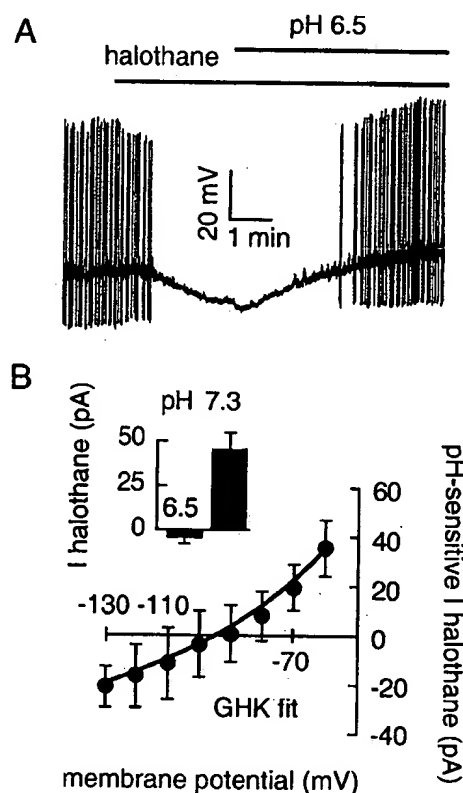


Fig. 7. (A) Halothane (0.3 mM) hyperpolarizes neurons of the rat locus coeruleus. These recordings were performed in the continued presence of bicuculline and strychnine to rule out the possible effects of γ -aminobutyric acid and glycine inhibition. In addition, ZD7288 was included in the pipette to block hyperpolarization-activated cationic current (I_h). The halothane-induced hyperpolarization is reversed by extracellular acidosis to pH 6.5. (B) pH sensitivity of the halothane-induced K⁺ current in locus coeruleus neurons. The I-V curve obtained from subtracting the halothane current in pH 6.5 from that in pH 7.3 follows the Goldman-Hodgkin-Katz equation. The histogram in the inset illustrates the current amplitude at -60 mV in control pH 7.3 and during acidosis at pH 6.5. (Adapted with permission from Sirois *et al.*⁸)

human spinal cord as well as in dorsal root ganglia (fig. 3).⁵⁵ TASK-2 produces non-inactivating, outwardly rectifying K⁺ currents with activation potential thresholds that closely follow the K⁺ equilibrium potential.^{16,46} TASK-2 activation is time-dependent with a fast time constant of approximately 60 ms at 0 mV. TASK-2 currents are blocked by quinine and quinidine but not by the classical K⁺ channel blockers TEA⁺, 4-AP, Cs⁺, and Ba²⁺.⁴⁶ TASK-2 is inhibited by external acidosis with a half-inhibition at pH 7.8.^{16,46} Application of volatile anesthetics causes a concentration-dependent increase in TASK-2 currents in a range overlapping minimum alveolar concentrations.¹⁶ TASK-2 is more sensitive to halothane than isoflurane.¹⁶ Unlike TASK-1, TASK-2 is also stimulated by chloroform (fig. 4). Site-directed mutagenesis has been used to delete the carboxy terminus of TASK-2.¹⁶ The truncated TASK-2 channel does not express a spontaneous or volatile anesthetic-evoked activity, further demonstrating the critical role of the carboxy terminus in the function of 2P domain K⁺ channels.^{15,16,29}

Volatile Anesthetic-inhibited 2P Domain K⁺ Channels

TWIK-2 is a background K⁺ channel that is highly expressed in both visceral and vascular smooth muscle.³⁷ Human TWIK-2 is absent in the brain and in the cerebellum (fig. 3).^{37-39,55} However, a moderate to strong expression is found in the human spinal cord and in the dorsal root ganglia.⁵⁵ Chloroform (300 μ M) and halothane (750 μ M) reversibly inhibit TWIK-2 by 32 and 27%, respectively.³⁷

THIK-1 expression is ubiquitous, with a substantial expression in some restricted areas of the rat brain (fig. 3).⁴⁸ The strongest concentrations are found in the olfactory bulb granule cell layer, the lateral septal nucleus dorsal, the ventromedial hypothalamic nucleus, the thalamus reticular and reunions nuclei, and, finally, the parabrachial nuclei.⁴⁸ THIK-1 is a weak inward rectifier that is stimulated by arachidonic acid but inhibited by halothane, with an IC₅₀ value of 2.83 mM (fig. 4).⁴⁸ Interestingly, 1 mM chloroform fails to affect THIK-1.⁴⁸

Human TALK-1 is exclusively expressed in the pancreas.²⁵ Human TALK-2 is similarly found in high concentrations in the pancreas but is also present in liver, placenta, heart, and lung.²⁵ TALK-1 and TALK-2 are background K⁺ currents that are activated by alkaline pH but are insensitive to arachidonic acid. Both channels are inhibited by 800 μ M chloroform (−21 and −44%, respectively) and 800 μ M halothane (−27 and −56%, respectively) (fig. 4).^{25,47} Interestingly, TALK-1 is not sensitive to 800 μ M isoflurane, whereas TALK-2 is stimulated (+58%).²⁵

Inhibition of Background K⁺ Channels by Local Anesthetics

Bupivacaine, tetracaine, and lidocaine inhibit several mammalian 2P domain K⁺ channels, including TASK-1, TASK-3, TREK-1, and TWIK-1.²⁶⁻²⁹ The presence of the uncharged form of the local anesthetic is important for channel inhibition. TASK-1 inhibition is greater at alkaline pH values (28% inhibition with 10 μ M bupivacaine at pH 8.4).²⁷ The potency of inhibition is directly correlated with the octanol:buffer distribution coefficient of the local anesthetic. The IC₅₀ values for TASK-1 are 709 μ M mepivacaine, 222 μ M lidocaine, 51 μ M R(+)-ropivacaine, 53 μ M S(−)-ropivacaine, 668 μ M tetracaine, 41 μ M bupivacaine, and 39 μ M etidocaine.²⁷ The Hill coefficient of the dose-effect curves is close to 1, suggesting that a single local anesthetic molecule binds to each 2P domain K⁺ channel. The stereoisomers of ropivacaine are equipotent, demonstrating that the inhibition is not stereoselective.²⁷ Local anesthetics significantly depolarize cells expressing TASK-1. The membrane depolarization may enhance the binding of local anesthetics to the open and inactivated states of the voltage-dependent Na⁺ channels.²⁷ Therefore, the inhibition of background 2P domain K⁺ channels by local anesthetics should contribute to enhance the conduction block of peripheral nerves.

Conclusions and Perspectives

These recent findings provide strong evidence that 2P domain K⁺ channels are sensitive molecular targets for volatile anesthetics. Together with the known modulation by neurotransmitter receptors,^{2,3} opening of these channels will contribute to the hyperpolarizing action of general anesthetics.¹⁵

Opening of the 2P domain K⁺ channels is agent-specific. For instance, TREK-1, TREK-2, and TASK-2 are opened by chloroform; TASK-1, THIK-1, and TRAAK are unaffected; and TWIK-2, TALK-1, and TALK-2 are inhibited.^{15-17,25,37,48} Interestingly, TALK-2 is inhibited by chloroform and halothane while it is stimulated by isoflurane.²⁵ The volatile anesthetic-inhibited 2P domain K⁺ channels, including TWIK-2, THIK-1, TALK-1, and TALK-2, are mostly nonneuronal (THIK-1 is restricted to some brain areas) and strongly expressed in peripheral organs.^{25,37,48} TREK-1, TREK-2, and TASK-1 are more sensitive to halothane than isoflurane.^{15,17} This difference in potency between the two volatile anesthetics indicates that opening of 2P domain K⁺ channels will probably be prevalent during halothane-induced anesthesia. Clearly, further work is necessary to map the putative anesthetic binding site and understand the role of the carboxy terminus in the mechanism of channel activation.¹⁵

Opening of 2P domain K⁺ channels will have profound hyperpolarizing effects at both presynaptic and

postsynaptic levels. Because of the leak behavior of the 2P domain K^+ channels, even moderate stimulation, as observed for clinical doses of volatile anesthetics, will have a major effect on the membrane potential.^{30,31} The discovery of this class of anesthetic-sensitive K^+ channels with distinct patterns of expression may provide a basis for how inhalational anesthetics depress the central nervous system.^{15-17,55} In the human brain, opening of TREK-1 and TREK-2 in the caudate nucleus and the putamen, opening of TREK-2 and TASK-3 in the cerebellum, and opening of TREK-2 in the corpus callosum may be functionally important during general anesthesia by volatile anesthetics (fig. 3).^{15,17,55} Opening of TREK-1, TASK-1, and TASK-2 in the sensory neurons of human dorsal root ganglia may block sensory inputs and contribute to loss of consciousness.^{15-17,55} Finally, opening of TREK-1 in motoneurons by inhalational anesthetics may depress mobility (fig. 3).^{15,55}

Local anesthetics inhibit background K^+ channels and induce cell depolarization.²⁷ These results suggest that closing of 2P domain K^+ channels by local anesthetics could contribute to peripheral analgesia by augmenting conduction blockade, whereas opening by volatile anesthetics may contribute to general anesthesia.^{15,27} These recent results contribute to the understanding of the molecular and cellular mechanisms of action of anesthetics.

The authors thank Michel Lazdunski, Ph.D. (Director, Institut de Pharmacologie Moléculaire et Cellulaire-Centre National de la Recherche Scientifique, Valbonne, France), for continual support; François Maingret, Ph.D. (Student, Institut de Pharmacologie Moléculaire et Cellulaire-Centre National de la Recherche Scientifique, Valbonne, France), for his contribution to the manuscript; and Martine Jodar, Valérie Lopez, and Franck Aguila (Technical Staff, Institut de Pharmacologie Moléculaire et Cellulaire-Centre National de la Recherche Scientifique, Valbonne, France) for excellent technical assistance.

References

1. Franks NP, Lieb WR: Molecular and cellular mechanisms of general anesthesia. *Nature* 1994; 367:607-14
2. Harris RA, Mihic SJ, Dildy-Mayfield JE, Machu TK: Actions of anesthetics on ligand-gated ion channels: Role of receptor subunit composition. *Faseb J* 1995; 9:1454-62
3. Belelli D, Pistis M, Peters JA, Lambert JL: General anaesthetics action at transmitter-gated inhibitory amino acid receptors. *TIPS* 1999; 20:496-502
4. Nicoll RA, Madison DV: General anaesthetics hyperpolarize neurons in the vertebrate central nervous system. *Science* 1982; 217:1055-7
5. Berg-Johnsen J, Langmoen IA: Isoflurane hyperpolarizes neurones in rat and human cerebral cortex. *Acta Physiol Scand* 1987; 130:679-85
6. Southan AP, Wann KT: Inhalation anaesthetics block accommodation of pyramidal cell discharge in the rat hippocampus. *Br J Anaesth* 1989; 63:581-6
7. Cl-Becheiry H, Puil E: Postsynaptic depression induced by isoflurane in neocortical neurons. *Exp Brain Res* 1989; 75:361-8
8. Sirois JE, Lei Q, Talley EM, Lynch C 3rd, Bayliss DA: The TASK-1 two-pore domain K^+ channel is a molecular substrate for neuronal effects of inhalational anesthetics. *J Neurosci* 2000; 20:6347-54
9. Franks NP, Lieb WR: Volatile general anaesthetics activate a novel neuronal K^+ current. *Nature* 1988; 333:662-4
10. MacIver MB, Kending JJ: Anesthetic effects on resting membrane potential are voltage-dependent and agent-specific. *ANESTHESIOLOGY* 1991; 74:83-8
11. Lopes CMB, Franks NP, Lieb WR: Actions of general anaesthetics and arachidonic acid pathway inhibitors on K^+ currents activated by volatile anaesthetics and FMRFamide in molluscan neurones. *Br J Pharmacol* 1998; 125:309-18
12. Winegar BD, Owen DF, Yost CS, Forsythe JR, Mayeri E: Volatile general anesthetics produce hyperpolarization of Aplysia neurons by activation of a discrete population of baseline potassium channels. *ANESTHESIOLOGY* 1996; 85: 889-900
13. Franks NP, Lieb WR: Stereospecific effects of inhalational general anesthetic optical isomers on nerve ion channels. *Science* 1991; 254:427-30
14. Sirois JE, Pancrazio JJ, Lynch C, Bayliss DA: Multiple ionic mechanisms mediate inhibition of rat motoneurons by inhalation anaesthetics. *J Physiol* 1998; 512:3:851-62
15. Patel AJ, Honoré E, Lesage F, Fink M, Romey G, Lazdunski M: Inhalational anaesthetics activate two-pore-domain background K^+ channels. *Nature Neurosci* 1999; 2:422-6
16. Gray AT, Zhao BB, Kindler CH, Winegar BD, Mazurek MJ, Xu J, Chavez RA, Forsythe JR, Yost CS: Volatile anesthetics activate the human tandem pore domain baseline K^+ channel KCNK5. *ANESTHESIOLOGY* 2000; 92:1722-30
17. Lesage F, Terrenoire C, Romey G, Lazdunski M: Human TREK2, a 2P domain mechano-sensitive K^+ channel with multiple regulations by polyunsaturated fatty acids, lysophospholipids, and Gs, Gi, and Gq protein-coupled receptors. *J Biol Chem* 2000; 275:28398-405
18. Gray AT, Winegar BD, Leonoudakis DJ, Forsythe JR, Yost CS: TOK1 is a volatile anesthetic stimulated K^+ channel. *ANESTHESIOLOGY* 1998; 88:1076-84
19. Ketchum KA, Joiner WJ, Sellers AJ, Kaczmarek LK, Goldstein SAN: A new family of outwardly rectifying potassium channel proteins with two pore domains in tandem. *Nature* 1995; 376:690-5
20. Fink M, Duprat F, Lesage F, Reyes R, Romey G, Heurteaux C, Lazdunski M: Cloning, functional expression and brain localization of a novel unconventional outward rectifier K^+ channel. *EMBO J* 1996; 15:6854-62
21. Duprat F, Lesage F, Fink M, Reyes R, Heurteaux C, Lazdunski M: TASK, a human background K^+ channel to sense external pH variations near physiological pH. *EMBO J* 1997; 16:5464-71
22. Maingret F, Lauritzen I, Patel A, Heurteaux C, Reyes R, Lesage F, Lazdunski M, Honoré E: TREK-1 is a heat-activated background K^+ channel. *EMBO J* 2000; 19:2483-91
23. Leonoudakis D, Gray AT, Winegar BD, Kindler CH, Harada M, Taylor DM, Chavez RA, Forsythe JR, Yost CS: An open rectifier potassium channel with two pore domains in tandem cloned from rat cerebellum. *J Neurosci* 1998; 18:868-77
24. Kim Y, Bang H, Kim D: TBK-1 and TASK-1, two-pore K^+ channel subunits: Kinetic properties and expression in rat heart. *Am J Physiol* 1999; 277:H1669-78
25. Girard C, Duprat F, Terrenoire C, Tinel N, Fosset M, Romey G, Lazdunski M, Lesage F: Genomic and functional characteristics of novel human pancreatic 2P domain potassium channels. *Biochem Biophys Res Commun* 2001; 282: 249-56
26. Meadows HJ, Randall AD: Functional characterisation of human TASK-3, an acid-sensitive two-pore domain potassium channel. *Neuropharmacology* 2001; 40:551-9
27. Kindler CH, Yost CS, Gray AT: Local anaesthetic inhibition of baseline potassium channels with two pore domains in tandem. *ANESTHESIOLOGY* 1999; 90:1092-102
28. Rajan S, Wischmeyer E, Liu GX, Preisig-Muller R, Daut J, Karschin A, Derst C: TASK-3, a novel tandem pore-domain acid-sensitive K^+ channel: An extracellular histidine as pH sensor. *J Biol Chem* 2000; 275:16650-7
29. Patel AJ, Honoré E, Maingret F, Lesage F, Fink M, Duprat F, Lazdunski M: A mammalian two pore domain mechano-gated Slike K^+ channel. *EMBO J* 1998; 17:4283-90
30. Lesage F, Lazdunski M: Molecular and functional properties of two-pore-domain potassium channels. *Am J Physiol Renal Physiol* 2000; 279:F793-801
31. Goldstein SAN, Bockenhauer D, O'Kelly I, Zilberg N: Potassium leak channels and the KCNK family of two-P-domain subunits. *Nature Rev Neurosci* 2001; 2:175-84
32. Doyle DA, Morais Cabral J, Pfuetzner RA, Kuo A, Gulbis JM, Cohen SL, Chait BT, MacKinnon R: The structure of the potassium channel: Molecular basis of K^+ conduction and selectivity. *Science* 1998; 280:69-77
33. Lesage F, Reyes R, Fink M, Duprat F, Guillemare E, Lazdunski M: Dimerization of TWIK-1 K^+ channel subunits via a disulfide bridge. *EMBO J* 1996; 15:6400-7
34. Ruppersberg JP: Intracellular regulation of inward rectifier K^+ channels. *Pflügers Arch* 2000; 441:1-11
35. Hille B: *Ionic Channels of Excitable Membranes*, 2nd edition. Edited by Hille B. Sunderland, MA, Sinauer Associates, 1992, pp 337-61
36. Lesage F, Guillemare E, Fink M, Duprat F, Lazdunski M, Romey G, Barhanin J: TWIK-1, a ubiquitous human weakly inward rectifying K^+ channel with a novel structure. *EMBO J* 1996; 15:1004-11
37. Patel AJ, Maingret F, Magnone V, Fosset M, Lazdunski M, Honoré E: TWIK-2, an inactivating 2P domain K^+ channel. *J Biol Chem* 2000; 275:28722-30
38. Pountney DJ, Gulkarov I, Vega-Saenz de Miera E, Holmes D, Saganich M, Rudy B, Artman M, Coetzee WA: Identification and cloning of TWIK-originated similarity sequence (TOSS): A novel human 2-pore K^+ channel principal subunit. *FEBS Lett* 1999; 450:191-6
39. Chavez RA, Gray AT, Zhao BB, Kindler CH, Mazurek MJ, Mehra Y, Forsythe JR, Yost CS: TWIK-2, a new weak inward rectifying member of the tandem pore domain potassium channel family. *J Biol Chem* 1999; 274:7887-92
40. Salinas M, Reyes R, Lesage F, Fosset M, Heurteaux C, Romey G, Lazdunski M: Cloning of a new mouse two-P domain channel subunit and a human homologue with a unique pore structure. *J Biol Chem* 1999; 274:11751-60
41. Kim Y, Bang H, Kim D: TASK-3, a new member of the tandem pore K^+ channel family. *J Biol Chem* 2000; 275:9340-7

42. Chapman CG, Meadows HJ, Godden RJ, Campbell DA, Duckworth M, Kelsell RE, Murdock PR, Randall AD, Rennie GI, Gloger IS: Cloning, localisation and functional expression of a novel human cerebellum specific, two pore domain potassium channel. *Brain Res Mol Brain Res* 2000; 82:74-83
43. Kim D, Fujita A, Horio Y, Kurachi Y: Cloning and functional expression of a novel cardiac two-pore background K⁺ channel (cTBK-1). *Circ Res* 1998; 82:513-8
44. Bang H, Kim Y, Kim D: TREK-2, a new member of the mechanosensitive tandem pore K⁺ channel family. *J Biol Chem* 2000; 275:17412-9
45. Fink M, Lesage F, Duprat F, Heurteaux C, Reyes R, Fosset M, Lazdunski M: A neuronal two P domain K⁺ channel activated by arachidonic acid and polyunsaturated fatty acid. *EMBO J* 1998; 17:3297-308
46. Reyes R, Duprat F, Lesage F, Fink M, Farman N, Lazdunski M: Cloning and expression of a novel pH-sensitive two pore domain potassium channel from human kidney. *J Biol Chem* 1998; 273:30863-9
47. Decher N, Maaier M, Dittrich W, Gassenhuber J, Bruggemann A, Busch AE, Steinmeyer K: Characterization of TASK-4, a novel member of the pH-sensitive, two-pore domain potassium channel family. *FEBS Lett* 2001; 24664:1-6
48. Rajan S, Wischmeyer E, Karschin C, Preisig-Muller R, Grzeschik KH, Daut J, Karschin A, Derst C: THIK-1 and THIK-2, a novel subfamily of tandem pore domain K⁺ channels. *J Biol Chem* 2000; 276:7302-11
49. Wei A, Jegla T, Salkoff L: Eight potassium channel families revealed by the *C. elegans* genome project. *Neuropharmacology* 1996; 35:805-29
50. Kunkel MT, Johnstone DB, Thomas JH, Salkoff L: Mutants of a temperature-sensitive two-P domain potassium channel. *J Neurosci* 2000; 20:7517-24
51. Goldstein SA, Price LA, Rosenthal DN, Pausch MH: ORK1, a potassium-selective leak channel with two pore domains cloned from *Drosophila melanogaster* by expression in *Saccharomyces cerevisiae*. *Proc Natl Acad Sci U S A* 1996; 93:13256-61
52. Bargmann C: Neurobiology of the *Caenorhabditis elegans* genome. *Science* 1998; 282:2028-33
53. Rubin GM, Yandell MD, Wortman JR: Comparative genomics of the eukaryotes. *Science* 2000; 287:2204-15
54. Meadows HJ, Benham CD, Cairns W, Gloger I, Jennings C, Medhurst AD, Murdock P, Chapman CG: Cloning, localisation and functional expression of the human orthologue of the TREK-1 potassium channel. *Pflugers Arch* 2000; 439:714-22
55. Medhurst AD, Rennie G, Chapman CG, Meadows H, Duckworth MD, Kelsell RE, Gloger I, Pangalos MN: Distribution analysis of human two pore domain potassium channels in tissues of the central nervous system and periphery. *Brain Res Mol Brain Res* 2001; 86:101-14
56. Reyes R, Lauritzen I, Lesage F, Ettaiche M, Fosset M, Lazdunski M: Immunolocalization of the arachidonic-acid and mechano-sensitive baseline TRAAK potassium channel in the nervous system. *Neurosci* 2000; 95:893-901
57. Lauritzen I, Blondeau N, Heurteaux C, Widmann C, Romey G, Lazdunski M: Polyunsaturated fatty acids are potent neuroprotectors. *EMBO J* 2000; 19:1784-93
58. Maingret F, Fosset M, Lesage F, Lazdunski M, Honoré E: TRAAK is a mammalian neuronal mechano-gated K⁺ channel. *J Biol Chem* 1999; 274:1381-7
59. Maingret F, Patel AJ, Lesage F, Lazdunski M, Honoré E: Mechano- or acid stimulation, two interactive modes of activation of the TREK-1 potassium channel. *J Biol Chem* 1999; 274:26691-6
60. Maingret F, Patel AJ, Lesage F, Lazdunski M, Honoré E: Lysophospholipids open the two P domain mechano-gated K⁺ channels TREK-1 and TRAAK. *J Biol Chem* 2000; 275:10128-33
61. Buckler K, Williams B, Honoré E: An oxygen-, acid- and anaesthetic-sensitive TASK-like background potassium channel in rat arterial chemoreceptor cells. *J Physiol* 2000; 525:135-42
62. Lopes CM, Gallagher PG, Buck ME, Butler MH, Goldstein SA: Proton block and voltage gating are potassium-dependent in the cardiac leak channel Kcnk3. *J Biol Chem* 2000; 275:16969-78
63. Millar JA, Barratt L, Southan AP, Page KM, Fyffe RE, Robertson B, Mathie A: A functional role for the two-pore domain potassium channel TASK-1 in cerebellar granule neurons. *Proc Natl Acad Sci U S A* 2000; 97:3614-8
64. Talley EM, Lei Q, Sirois JE, Bayliss DA: TASK-1, a two-pore domain K⁺ channel, is modulated by multiple neurotransmitters in motoneurons. *Neuron* 2000; 25:399-410
65. Maingret F, Patel A, Lazdunski M, Honoré E: The endocannabinoid anandamide is a direct and selective blocker of the background K⁺ channel TASK-1. *EMBO J* 2001; 20:47-54
66. Buckler KJ: A novel oxygen-sensitive potassium current in rat carotid body type I cells. *J Physiol* 1997; 498:649-62
67. Lopez-Barneo J: Oxygen-sensing by ion channels and the regulation of cellular functions. *Trends Neurosci* 1996; 19:435-40